Article

Current Biology

Tracing the evolution and diversity of human parvovirus B19 across human history

Graphical abstract

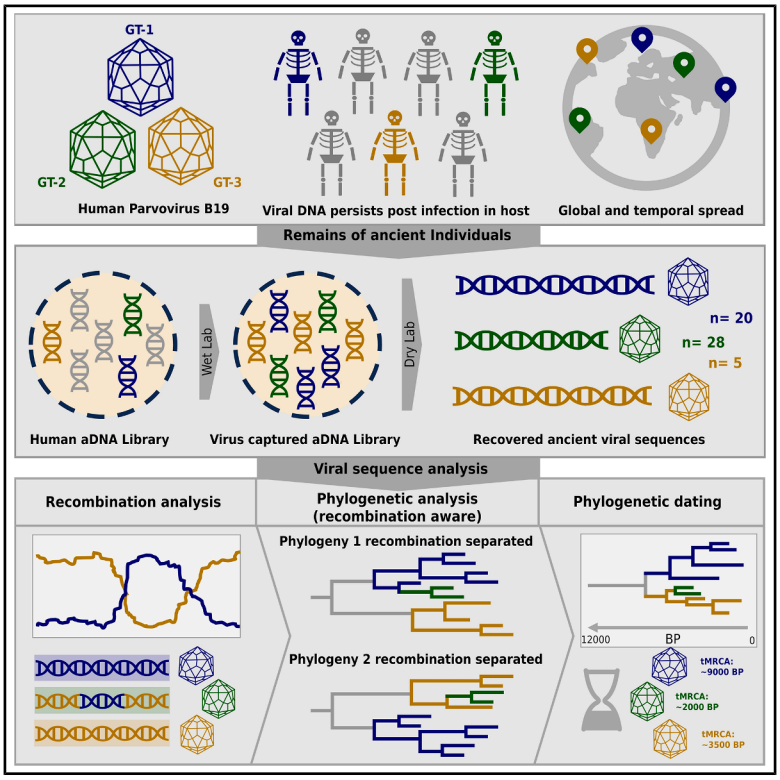

Highlights

- B19 infections spanned the Holocene with extensive extinct diversity
- Recombination to genotype 2 is dated to 3,000–1,800 years ago
- B19V spread along colonial routes, affected children, and caused epidemics
- Europeans introduced local and African B19V variants to the Americas

Authors

Teresa Zeibig, Maria A. Spyrou, Arthur Kocher, ..., Wolfgang Haak, Alexander Herbig, Johannes Krause

Correspondence

alexander_herbig@eva.mpg.de (A.H.), krause@eva.mpg.de (J.K.)

In brief

The emergence, evolution, and dispersal of human parvovirus B19V remain underexplored. Zeibig et al. demonstrate that B19V dispersed globally, participated in epidemics, and added to the disease burden of diverse populations, including children, as far back as the Late Mesolithic. These findings provide insight into this ubiquitous virus's evolutionary past.

Zeibig et al., 2026, Current Biology *36*, 4914–4929
October 5, 2026 © 2026 The Authors. Published by Elsevier Inc.
https://doi.org/10.1016/j.cub.2026.08.032

CellPress

CellPress
OPEN ACCESS

Current Biology

Article

Tracing the evolution and diversity of human parvovirus B19 across human history

Teresa Zeibig,[1,77] Maria A. Spyrou,[1,2,74,77] Arthur Kocher,[1,3] Emily Gaul,[2] Mark Aldenderfer,[4] Rodrigo Barquera,[1] Jessica F. Beckett,[5] Arman Beisenov,[6] Andrey B. Belinski,[7] Philip P. Betancourt,[8] Ruth Boersma,[1,3] Pablo Carrion,[1] Ainash Childebayeva,[1,9,10] Christine Cooper,[11,12] Francesco Cucca,[5] Rosaria Di Salvo,[13] Marko Dizdar,[14] Leyla Djansugurova,[10] Michal Ernée,[15] Susan C. Ferrence,[75] Lars Fehren-Schmitz,[16] Ayshin Ghalichi,[1,9] Karen L. Giffin,[1,26] Steven Gilbert,[17,18] Jorge A. Gómez-Valdés,[20] Joscha Gretzinger,[1] Leif Hansen,[21] Svend Hansen,[22] Diana Iraiz Hernandez-Zaragoza,[1] Rimantas Jankauskas,[23] Choongwon Jeong,[24,25] Marcel Keller,[26,27] Valery Khartanovich,[28] Daewook Kim,[29] Rebecca Kinaston,[30,31] Alexey Kovalev,[32]

(Author list continued on next page)

[1]Max Planck Institute for Evolutionary Anthropology, Deutscher Pl. 6, 04103 Leipzig, Germany
[2]Institute for Archaeological Sciences, Department of Geosciences, University of Tübingen, Geschwister-Scholl-Platz 7, 2074 Tübingen, Germany
[3]Transmission, Infection, Diversification and Evolution Group, Max Planck Institute of Geoanthropology, Kahlaische Straße 10, 07745 Jena, Germany
[4]Department of Anthropology and Heritage Studies, University of California, Merced, 5200 North Lake Rd., Merced, CA 95343, USA
[5]CNR-IRGB, Monserrato, Cittadella Universitaria, c/o S.S 554 bivio per Sestu Km 4, di Cagliari, 500, 09042 Monserrato, CA, Italy
[6]Institute of Archaeology by A.Kh. Margulan, Dostyk Ave 44, Almaty 050000, Kazakhstan
[7]Nasledie Cultural Heritage Unit, Prospekt Karla Marksa 56 355006 Stavropol, Russia
[8]Temple University, 1801 N Broad St, Philadelphia, PA 19122, USA
[9]Department of Anthropology, University of Texas at Austin, 2201 Speedway Stop C3200 (WCP 4.102), Austin, TX 78712, USA
[10]Center for Paleogenetics and Ethnogenomics, Institute of General Genetics and Cytology, Al-Farabi Avenue 93, Almaty 050060, Kazakhstan
[11]Office of Cultural Affairs, Archaeology Department, Peter-Kaiser-Platz 2, 9490 Vaduz, Liechtenstein
[12]Department of Physical Anthropology, Institute of Forensic Medicine, University of Bern, Murtenstrasse 2, 63008 Bern, Switzerland
[13]Museo Archeologico Regionale "Antonino Salinas,", Piazza Olivella, 1, 90133 Palermo, PA, Italy
[14]Archaeological Museum of Slavonia, Trg Svetog Trojstva 2, 31000 Osijek, Croatia
[15]Institute of Archaeology of the Czech Academy of Sciences Letenská 123/4, 118 00 Malá Strana, Prague, Czech Republic
[16]UCSC Paleogenomics, Department of Anthropology, University of California, Santa Cruz, Santa Cruz, CA, USA
[17]Tandy Institute for Archaeology, 4530 Stanley Ave, Fort Worth, TX 76115, USA
[18]Lanier Center for Archaeology, Lipscomb University, 1 University Park Drive, Nashville, TN 37204, USA
[19]UCL Institute of Archaeology, CAAL Project, 44 Avenue Dostyk/28 Shevchenko St, Almaty, Kazakhstan
[20]Instituto Nacional de Antropologia e Historia, Hamburgo 135, Colonia Juárez, Alcaldía Cuauhtémoc. C.P., Mexico City 06600, México
[21]Landesamt für Denkmalpflege im Regierungspräsidium Stuttgart, Berliner Straße 12, 73728 Esslingen am Neckar, Germany

(Affiliations continued on next page)

SUMMARY

Human parvovirus B19 (B19V) is an ubiquitously spread, exclusively human pathogen, mainly posing risks to children, as well as pregnant and immunocompromised individuals. Despite evidence of B19V infection of human populations as far back as 7,000 years, the evolutionary history of B19V remains poorly understood. In this study, we present B19V genomic data from the remains of 53 globally distributed individuals spanning more than 8,000 years, including 7 children. Our findings suggest that the most recent common ancestor of all present B19V lineages existed around 12,000 years ago, at the end of the last Ice Age. Additionally, we identified an extinct Eurasian clade that participated in the recombination event that led to the emergence of B19V genotype 2 (GT-2). We date this event to ~3,200–1,800 BP, potentially in the greater Mediterranean area. Our study shows aspects of how ancient parvovirus variants arose, disseminated, and impacted human health through time.

INTRODUCTION

Human parvovirus B19 (B19V) was first identified in 1975 by the Australian virologist Ivonne Cossart.[1] In children, B19V is the causative agent of *erythema infectiosum*, also known as fifth disease, and is characterized by a rash on the face and body.[2] Typically, infections fluctuate along a ~4-year[3–5] epidemic cycle, but following the SARS-CoV-2 (severe acute respiratory syndrome

This is an open access article under the CC BY license (http://creativecommons.org/licenses/by/4.0/).

CellPress
OPEN ACCESS

Justina Kozakaitė,[23] Dirk Krausse,[21] Siniša Krznar,[14] Mario Küßner,[33] Louise C. Langford,[76] Luca Lai,[34] Sandra Lösch,[35] Kerttu Majander,[26] Marcello A. Mannino,[36] Lourdes Márquez-Morfín,[37] Michael McCormick,[38] Photini J.P. McGeorge,[39] Megan Michel,[1] Vyacheslav Moiseyev,[28] Hyoungmin Moon,[24,25] Angela Mötsch,[1,68] Lyazzat Musralina,[10,40] Erdene Myagmar,[41] Elia Nakoro,[42] Rita E. Németh,[43] Gunnar U. Neumann,[1] Mario Novak,[44,45] Lauro Olmo Enciso,[46] Päivi Onkamo,[47] Luka Papac,[1] Sanni Peltola,[1,47,48] Cosimo Posth,[2,74] Adam Powell,[1] Chantal Radimilahy,[73] Dragana Rajković,[14] Jean-Aimé Rakotoarisoa,[73] Bako Nirina Rasoarifetra,[73] Sabine Reinhold,[22] Roberto Risch,[49] Zainolla Samashev,[50,51] Duncan Sayer,[52] Vittoria Schimmenti,[13] Felicitas Schmitt,[21] Elena Sintes,[53] Philip Slavin,[54] Denis Sorokin,[55] Thomas Terberger,[56,57] Rezeda Tukhbatova,[58] Åshild J. Vågene,[59,60] Katrien Van de Vijver,[61,62,63]

(Author list continued on next page)

[22]Eurasien-Abteilung Deutsches Archäologisches Institut, Im Dol 2-6, 14195 Berlin, Germany
[23]Translational Health Research Institute, Faculty of Medicine, Vilnius University, Žaliųjų Ežerų str. 2, LT-08406 Vilnius, Lithuania
[24]School of Biological Sciences, Seoul National University, Gwanakro 1, Gwanak-ku, 08826 Seoul, Republic of Korea
[25]Institute for Data Innovation in Science, Seoul National University, Gwanakro 1, Gwanak-ku, 08826 Seoul, Republic of Korea
[26]Department of Environmental Sciences, University of Basel, Bernoullistrasse 32, 4056 Basel, Switzerland
[27]Institute of Genomics, University of Tartu, Riia 23b, 51010 Tartu, Estonia
[28]Peter the Great Museum of Anthropology and Ethnography (Kunstkamera), RAS, University Embankment 3, St Petersburg, Russland 199034, Russian Federation
[29]The Yeungnam University Museum, Yeungnam University, 280 Daehak-ro, Gyeongsan, Gyeongbuk 38541, Republic of Korea
[30]BioArch South, P.O. Box 95, Waitati 9060, New Zealand
[31]Costal People Southern Skies National Centre for Research Excellence, University of Otago, 539 Castle Street, Dunedin 9016, New Zealand
[32]Institute of Archaeology Russian Academy of Sciences, Ulitsa Dmitriya Ul'yanova, 19, Moscow 117292, Russia
[33]Thuringian State Office for Heritage Conservation and Archeology, Petersberg 12, 99084 Erfurt, Germany
[34]University of North Carolina at Charlotte, 9201 University City Blvd, Charlotte, NC 28223, USA
[35]Institute of Archaeological Sciences, University of Bern, Mittelstrasse 43, 3012 Bern, Switzerland
[36]Department of Archaeology and Heritage Studies, Aarhus University, Moesgård Allé 20, 8270 Højbjerg, Denmark
[37]Escuela Nacional de Antropología e Historia, Instituto Nacional de Antropología e Historia, Periférico Sur y, C. Zapote S/N, Espacio Ecológico Cuicuilco, Tlalpan, 14030 Ciudad de México, CDMX, Mexico
[38]Initiative for the Science of the Human Past at Harvard, Department of History, Harvard University, 35 Quincy Street, Cambridge, MA 02138, USA
[39]British School at Athens, Souidias 52, Athina 106 76, Greece
[40]Kazakh National University by al-Farabi, Al-Farabi Avenue 71, Almaty 050040, Kazakhstan
[41]National University of Mongolia, Department of Archaeology, Anthropology and Demography, WWF9+6H6, Ulaanbaatar 14200, Mongolia
[42]Fiji Museum, VC2G+48R, 2 Cakobau Road, Suva, Fiji
[43]Mureș County Museum, Str. Mărăști 8a, Târgu Mureș, Romania
[44]Centre for Applied Bioanthropology, Institute for Anthropological Research, Gajeva ul. 32, 10000 Zagreb, Croatia
[45]Faculty of Humanities, University of Primorska, Praetorian Palace, Titov trg 5, 6000 Koper, Slovenia
[46]Department of History and Philosophy, University of Alcalá, Pza. San Diego, s/n, 28801 Alcalá de Henares, Madrid, Spain
[47]Department of Biology, University of Turku, Natura Building, Vesilinnantie 5, University of Turku, 20014 Turku, Finland
[48]Faculty of Biological and Environmental Sciences, University of Helsinki, Viikinkaari 1, Biocenter. 3, 00790 Helsinki, Finland
[49]Departament de Prehistòria, Universitat Autònoma de Barcelona, 08193 Cerdanyola del Vallès, Barcelona, Spain
[50]State Historical and Cultural Museum-Reserve "Berel," Katon-Karagay District (Katonkaragay District), East Kazakhstan Region, Kazakhstan
[51]Branch of Institute of Archaeology by A.Kh. Margulan, Beybitshilik Street 25, Room 405, Astana (Nur-Sultan), Kazakhstan
[52]School of Law and Policing, University of Lancashire, Adelphi Building, Preston, Lancashire PR1 2HE, UK
[53]Institut Menorquí d'Estudis, Camí des Castell, 28, 07702 Maó, Illes Balears, Spain
[54]University of Stirling, Stirling FK9 4LA Scotland, UK
[55]LLC "RUTRUM," Ulica Kazybek Bi, 185, KV 70 Almaty, Almalinsky District 050000 Kazakhstan
[56]State Agency for Cultural Heritage of Lower Saxony, Scharnhorststraße 13, 0175 Hannover, Germany
[57]Seminar for Prehistory, Göttingen University, Nikolausberger Weg 15, 37073 Göttingen, Germany
[58]Institute of Fundamental Medicine and Biology, Kazan Federal University, Kremlyovskaya St, 18, Kazan, Republic of Tatarstan 420008, Russia
[59]Max Planck Institute for the Science of Human History, Kahlaische Straße 10, 07745 Jena, Germany
[60]Section for Hologenomics, GLOBE Institute, University of Copenhagen, Øster Farimagsgade 5, Building 7, 1353 Copenhagen K, Denmark
[61]Royal Belgian Institute of Natural Sciences, Rue Vautier 29, 1000 Bruxelles, Belgium
[62]Center for Archaeological Sciences, University of Leuven, Celestijnenlaan 200E, 3001 Leuven, Belgium
[63]Dienst Archeologie - Stad Mechelen, Grote Markt 21, 2800 Mechelen, Belgium
[64]Complutense University of Madrid, Avenida de Séneca, 228040 Madrid, Spain
[65]Institute of Evolutionary Biology, CSIC-Universitat Pompeu Fabra, Pompeu Fabra University, Carrer de la Mercè, 12, Barcelona, Spain
[66]Department of History, Sejong University, 209 Neungdong-ro, Gwangjin-gu, Seoul 05006, Republic of Korea

(Affiliations continued on next page)

CellPress
OPEN ACCESS

Current Biology
Article

Alfonso Vigil-Escalera Guirado,[64] Vanessa Villalba-Mouco,[1,65] Dmitriy Voyakin,[19] Eun Jin Woo,[66] Teresa Ximenez,[67] Philipp Stockhammer,[1,68,72] Christina Warinner,[1,69,70,71] Kirsten Bos,[1] Stephan Schiffels,[1] Alissa Mittnik,[1] Wolfgang Haak,[1] Alexander Herbig,[1,*] and Johannes Krause[1,78,*]

[67]MARQ. Archaeological Museum of Alicante, Pl. Dr. Gómez Ulla, S/N, 03013 Alacant, Alicante, Spain
[68]Max Planck Harvard Research Center for the Archaeoscience of the Ancient Mediterranean, Deutscher Pl. 6, 04103 Leipzig, Germany
[69]Leibniz Institute for Natural Products Research and Infection Biology HKI, Beutenbergstraße 11A, 07745 Jena, Germany
[70]Department of Anthropology, Harvard University, 21 Divinity Avenue, Cambridge, MA 02138, USA
[71]Department of Human Evolutionary Biology, Harvard University, 11 Divinity Ave, Cambridge, MA 02138, USA
[72]Institute for Pre- and Protohistoric Archaeology and Archaeology of the Roman Provinces, Ludwig Maximilian University, Schellingstraße 12, 80799 München, Germany
[73]Institut de Civilisations Musée d'Art et d'Archéologie, Antananarivo University/Association Malgache d'Archéologie, 17 Rue Dok Villette, Antananarivo, Madagascar
[74]Senckenberg Centre for Human Evolution and Palaeoenvironment, University of Tübingen, Hölderlinstraße 12, 72074 Tübingen, Germany
[75]INSTAP Academic Press, 2133 Arch St., Ste. 301, Philadelphia, PA 19103 USA
[76]Independent Scholar, West Mt. Airy Avenue, Philadelphia, PA, 19119, USA
[77]These authors contributed equally
[78]Lead contact
*Correspondence: alexander_herbig@eva.mpg.de (A.H.), krause@eva.mpg.de (J.K.)
https://doi.org/10.1016/j.cub.2026.08.032

coronavirus 2) pandemic, there has been a stark increase in B19V cases in children, described as unusually high-frequency outbreaks.[4,6] B19V is a small, non-enveloped virus approximately 25 nm in diameter, containing a single-stranded DNA genome.[7] Ancient DNA suggests that B19V has been infecting humans since at least the Neolithic period.[8] Structurally, B19V is an icosahedral virus with an ultrasmall genome of roughly 5,500 nucleotides, comprising two open reading frames flanked by palindromic sequences capable of forming hairpin structures.[9–11] Based on sequence variation in a 994-nucleotide section of the NS1/VP1-unique region junction (Nonstructural protein 1/Viral protein 1),[12] B19V can be subdivided into three genotypes (GT-). The globally dominant GT-1, the recombinant GT-2, and the relatively rare GT-3, found primarily in sub-Saharan Africa but also in South America, France, and China.[12–14] It has been shown that GT-2 formed as a result of recombination between GT-1 and GT-3 viruses, wherein GT-1 accounts for approximately one-third and GT-3 two-thirds of the GT-2 genome. Prior to the 1950s, GT-2 was a circulating variant in Europe, and it progressively decreased in prevalence, potentially being displaced by GT-1, before being pronounced extinct from active circulation in 2025.[15,16]

Although commonly associated with childhood infections, B19V can infect individuals of all ages, with clinical outcomes largely influenced by the individual's immune and hematologic status.[17] Transmission of B19V occurs via multiple routes, with respiratory droplets being the most common, although bloodborne and intra-uterine transmission are also possible.[2,18–20] After primary infection, B19V DNA can persist lifelong in tissues[15,21] such as teeth,[22] bone,[23] bone marrow,[24–26] synovial tissue,[24,27] brain,[28,29] heart,[30] liver,[31] and sites in the oral cavity, such as the tonsils and the salivary glands.[16] The oral cavity-associated persistence appears dependent on tonsillar B cells, with up to ~70 B19V DNA copies per million cells. B cells are a preferential site for B19V DNA retention.[16] Studies of B19V seroprevalence indicate worldwide active circulation, with generally >50% of the adult population having been previously exposed to B19V. Typically, the infection spreads in children between 5 and 15 years, but previously unexposed individuals of all ages are also susceptible.[2,18] Among individuals of childbearing age, 1%–5% will experience a B19V infection during pregnancy, often without complications.[19,20,32] However, vertical transmission occurs in about half of maternal infections and can result in serious complications, such as spontaneous abortion or *hydrops fetalis*.[33,34]

Previous ancient DNA studies have reconstructed 13 B19V genomes,[8,35] representing all three genotypes, and shown the virus to have been present in adult individuals in Europe, Asia, and North America since at least ~6,900 BP. Within Eurasia, ancient GT-1 has only been found in Asia, and GT-2 was identified in Europe. While this suggests continental structuring of B19V genotypes in the recent past, the origins of the B19V genotypes and the process by which GT-2 arose and later dramatically declined remain unclear. Furthermore, the cases that geographically belong to the American continent occurred in Greenland and Mexico, and they are linked to Viking expeditions and colonial expansion because they were discovered in a Viking individual and first-generation enslaved Africans, respectively.[8,35] These cases are not evidence for new infections introduced to a new region, but more likely they are cases of persons with persistent infections moving into the region. Thus, we are still lacking a comprehensive overview of the genetic variability of ancient B19V in the Americas.

To address these questions, we present 53 globally distributed ancient B19V genomes spanning the past ~8,300 years and representing all three major viral genotypes. We show that B19V has infected European hunter-gatherer populations as early as ~8,300 BP, extending the known instances of the virus by more than 1,300 years. The dataset reveals that the recombination event that led to the formation of GT-2 was more recent than previously suggested, dating back to between ~3,200 and 1,800 BP. The broader Mediterranean area is identified as a potential geographical location for this recombination event. We also unveil the extinct diversity of GT-1 and GT-2 by showcasing GT-1's lost diversity before it rose to global dominance and that GT-2's diversity loss predates the known 1970s circulation reduction. Furthermore, we highlight the dispersion of GT-2 strains of European and Asian origin being found alongside colonial expansion routes. We present evidence for an outbreak event in colonial-era

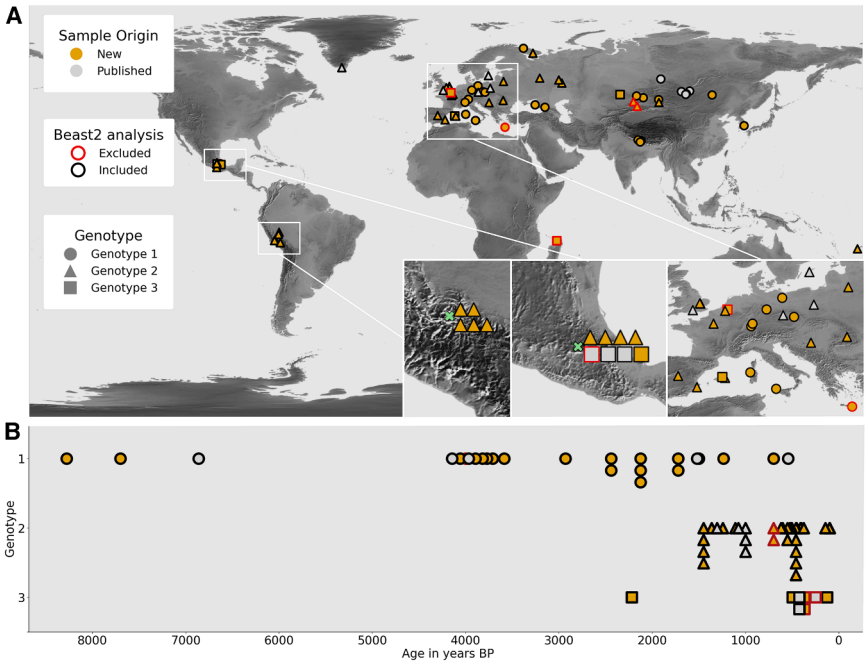

Figure 1. Global distribution of ancient B19 viruses by genotype and age

(A) Map indicating the geographical distribution of B19V genomes with their genotypes. Previously published B19V sequences are marked in gray. New B19V genomes are marked in orange. Red outlines indicate samples with insufficient genomic coverage, which were excluded from phylogenetic dating. Marker shapes indicate the assigned genotype: the circle denotes GT-1, the triangle denotes GT-2, and the square denotes GT-3. Samples from sites with multiple B19V genomes are jittered to aid visibility. Submaps containing green crosses indicate the locations of Machu Picchu and Mexico City, with the samples from these locations plotted next to the crosses.

(B) Age distribution of B19V samples separated by genotype. The color and shape scheme denoted in (A) applies.

Machu Picchu and two cases of co-infections with *Plasmodium* species, providing further insights into the ancient B19V health burden.

RESULTS

B19V detection and authentication

Shotgun-sequenced and human-enriched (1.24 million SNPs)[36–38] libraries from dental and skeletal remains of 16,546 ancient worldwide individuals were computationally screened using MALT[39] and HOPS.[40] Reads consistent with the presence of B19V were detected in 1,892 samples, with between 1 and 9,206 reads mapping per positive specimen. Among these, shotgun data from the individuals VOI007 (mean coverage 8.0×), SGA024 (7.6×), and SJN025 (14.3×) provided sufficient coverage for immediate genome reconstruction. Based on radiocarbon age, signal detection during screening, age at death, and geographic provenance, an additional 106 samples were selected for targeted B19V genome enrichment using an in-solution capture assay. This approach resulted in the recovery of 50 B19V genomes spanning all known genotypes (total: GT-1 $n = 20$, GT-2 $n = 28$, GT-3 $n = 5$), with mean coverage ranging from 1.6× to 82.1×. Sample ages range from ∼8,300 BP to 100 BP, with most specimens dating to within the last 4,000 years (Figure 1B). Adults account for ∼87% of B19V-positive individuals ($n = 46$), while infants and young children (1–6 years old) comprised the remaining ∼13% ($n = 7$; Table 1). All samples show deamination patterns consistent with ancient DNA molecules and their respective library type. In rooted nucleotide trees constructed using the maximum likelihood algorithm, ancient genomes usually fall outside of modern genotypes with tips closer to the root of the tree, which further supports their authenticity (Figures 2 and 3). Genotype assignment was based on sequence identity similarity to reference genomes of all three genotypes and validated by the recombination analysis for GT-2 samples (Figure 2).

Parvovirus infections span the Holocene

We observe a wide temporal and geographic distribution of B19V-positive individuals (Figure 1). Among these, we identify the oldest GT-1 virus in Sicily, Italy (8,370–8,190 cal BP), the earliest GT-2 virus in Great Britain and Spain (∼1,450 BP), and the oldest GT-3 instance in Menorca, Spain (∼2,310–2,115 cal BP). These represent the earliest known occurrences of each genotype, with the Italian GT-1 genome being the oldest B19 virus case identified to date. The distribution of genotypes follows a temporal pattern. The genomes associated with GT-1 ($n = 20$) span the widest chronological range and are observed from ∼8,275 BP onward. By contrast, the distribution of GT-2 ($n = 26$) is temporally more constrained, being found only in the past 1,500 years, despite being the most commonly detected genotype in the dataset (Figure 1). GT-3 was the least detected ($n = 5$), including the virus from an individual from Menorca, Spain (ABF006, ∼2,200 BP); an individual from Mexico, North America (SJN003, ∼490 BP); one from Kazakhstan, Central Asia (SRK002, ∼127 BP); as well as two additional individuals, one from Belgium in Europe and one from Madagascar in Africa, which did not meet the coverage depth necessary for inclusion in phylogenetic dating.

Ancient parvovirus genomes reveal extensive extinct diversity

We combined the newly sequenced B19V genomes with published data of ancient and modern sequences for phylogenetic analysis and molecular dating. As previously published ancient B19V genomes are limited to the coding sequence without the P6 promoter region, we generated two alignments: (1) one combining modern and newly recovered ancient sequences that includes the promoter region and (2) a second comprising the full set of ancient diversity, with all sequences trimmed to the coding region. To maximize inclusion of available ancient data, all phylogenetic and molecular dating analyses were performed on the coding sequence alignment only. With this dataset, all newly recovered GT-1 genomes branch ancestral to the split between GT-1a and GT-1b (Figure 2B), with the sole

Table 1. Overview of children with B19V infection

Individual	Osteo logical age in years	Geno type	Location	Date range	Sample type	Mean cov in X	≥ 1× in %	≥ 3× in %
NDR002	2–3	3	Madagascar	502–336 cal BP	Pars petrosa	1.6	65.2	24.3
CRO001	5–6	2	Spain, Menorca	670–565 cal BP	Pars petrosa	29.2	99.8	99.7
OAI017	1–3	2	Great Britain	1,524–1,409 cal BP	lower right incisor	8.9	94.9	76.7
ABF006	1–2	3	Spain, Menorca	2,310–2,125 cal BP	Pars petrosa	8.8	83.3	64.4
APG003	6–7	1	Germany	∼2,430–2,400 BP	lower right primary second molar	25.3	87.9	80.2
MIB039	4–5	1	Czech Republic	3,839–3,701 cal BP	Pars petrosa	12.5	84	72.7
YNK001	3	2	Fiji	270–1 cal BP	Pars petrosa	26.3	98	96.4

The sampled individuals' osteological age and location are presented alongside the viral genotype and sample age, either as ^{14}C or archeological date.

exception of the East Asian sample TSA002, which forms a clade with sister lineage GT-1a. In GT-2, seven ancient genomes from France, Spain, and Mexico fall basal to the radiation of all extant GT-2 sequences. The majority of the ancient diversity does not fall basal to the modern representatives but instead forms a separate, now-extinct sister clade to GT-2 spanning roughly 1,000 years, whose most recent representative is dated to 97 cal BP (∼260–1 cal BP; Fiji, YNK001). This subclade contains both newly uncovered and previously published genomes from Europe, Asia, the Americas, and Oceania (Figures 2B, 2C, and 3). Within GT-3, the majority of genomes (4 new, 3 published ancient) are phylogenetically placed into the existing subgenotypes 3a and 3b, with most ancient genomes (3 new, 2 published) grouping within subgenotype 3b. The B19V genome identified in African individual NDR002, although not sufficiently covered for phylogenetic dating analysis, can be assigned to a genotype and placed phylogenetically (Figure 2C) ancestral to the modern 3b strains detected in present-day Ghana. One notable exception is sample ABF006 from Menorca, dating to the late Iron Age, which occupies an intermediate position between GT-2 and GT-3. Importantly, this genome lacks the GT-1-derived recombination signature found in all GT-2 genomes, suggesting that it constitutes the closest representative of the GT-3-related lineage, which gave rise to GT-2, as further confirmed by subsequent recombination and phylogenetic analyses.

Earliest recombinant B19V genotype 2 identified across Europe

Recombination analyses were conducted using two complementary datasets. First, we analyzed an alignment of 162 B19V coding sequences (101 GT-1, 42 GT-2, 19 GT-3), encompassing both newly reported (n = 53) and published (n = 12) ancient genomes, together with modern representatives (n = 103). Second, we analyzed an alignment containing the same set of modern representatives and the newly recovered ancient B19V sequences, all of them containing the coding sequence and the P6 promoter region. The results for both analyses were consistent (Figures 2 and S1).

Using the RDP5 software,[41] all ancient and modern GT-2 genomes were identified as recombinants of GT-1 and GT-3. One GT-3 sample and two GT-1 samples showed the highest similarity to the inferred parental sequences: ABF006 from Menorca (GT-3; ∼2,310–2,115 cal BP), LEU007 from Germany (GT-1; 3,911–3,728 cal BP), and APG003 from Germany (GT-1; ∼2,400–2,430 BP). The inferred recombination breakpoints are consistent with previous estimates[42] (Figures 2 and S1).[8] The previously published date estimate was derived from 10 ancient coding sequences from two genotypes, GT-1 (n = 5) and GT-2 (n = 5), with no ancient GT-3 representatives. The viral coding sequence from ABF006 is the currently closest match to the expected sequence of the GT-3 originating sequence part of GT-2. In our dataset, we identified the earliest recombinant genotype at ∼1,500 BP and thereafter across various locations in Europe and Asia. We used the recombination analysis as the basis for generating the distributed alignments for the GT-2-separated phylogenetic dating. In this analysis, GT-2 is split into its GT-1- or GT-3-derived sequence parts, while the subsequent non-recombination parental parts are replaced with N. The identified parental sequences are further supported by the phylogeny of the recombination-separated trees. The identified parental matches, ABF006 and APG003, are sisters to the entire GT-2 clade derived from the partially masked coding sequence (Figures 2B and 2C).

Ancient B19V genotype-2 harbors extensive ancient diversity with no modern descendants

We reconstructed maximum likelihood phylogenies using both recombination-separated GT-2 sequences (Figures 2B, 2C, and S1) and the full GT-2 coding sequence alignment (Figure 3). Across all analyses, GT-2 genomes consistently separate into two subclades. One subclade contains the full spectrum of modern diversity, with a small number of ancient genomes occupying basal positions relative to modern diversity with high bootstrap support (Figures 2C and 3). By contrast, the majority of ancient GT-2 samples, both previously published and newly generated, cluster within a second, distinct subclade (green highlight, Figures 2B, 2C, and 3). Bootstrap support for the node connecting these two subclades is low in both the full coding sequence alignment and the masked alignment restricted to the GT-1-derived portion of GT-2. The placement of some basal genomes varies between these datasets; however, the second subclade clearly harbors substantial diversity. Notably, the most recent members of this subclade, YNK001 (Fiji) and CHV002 (Russia), date to ∼100 BP, indicating

CellPress
OPEN ACCESS

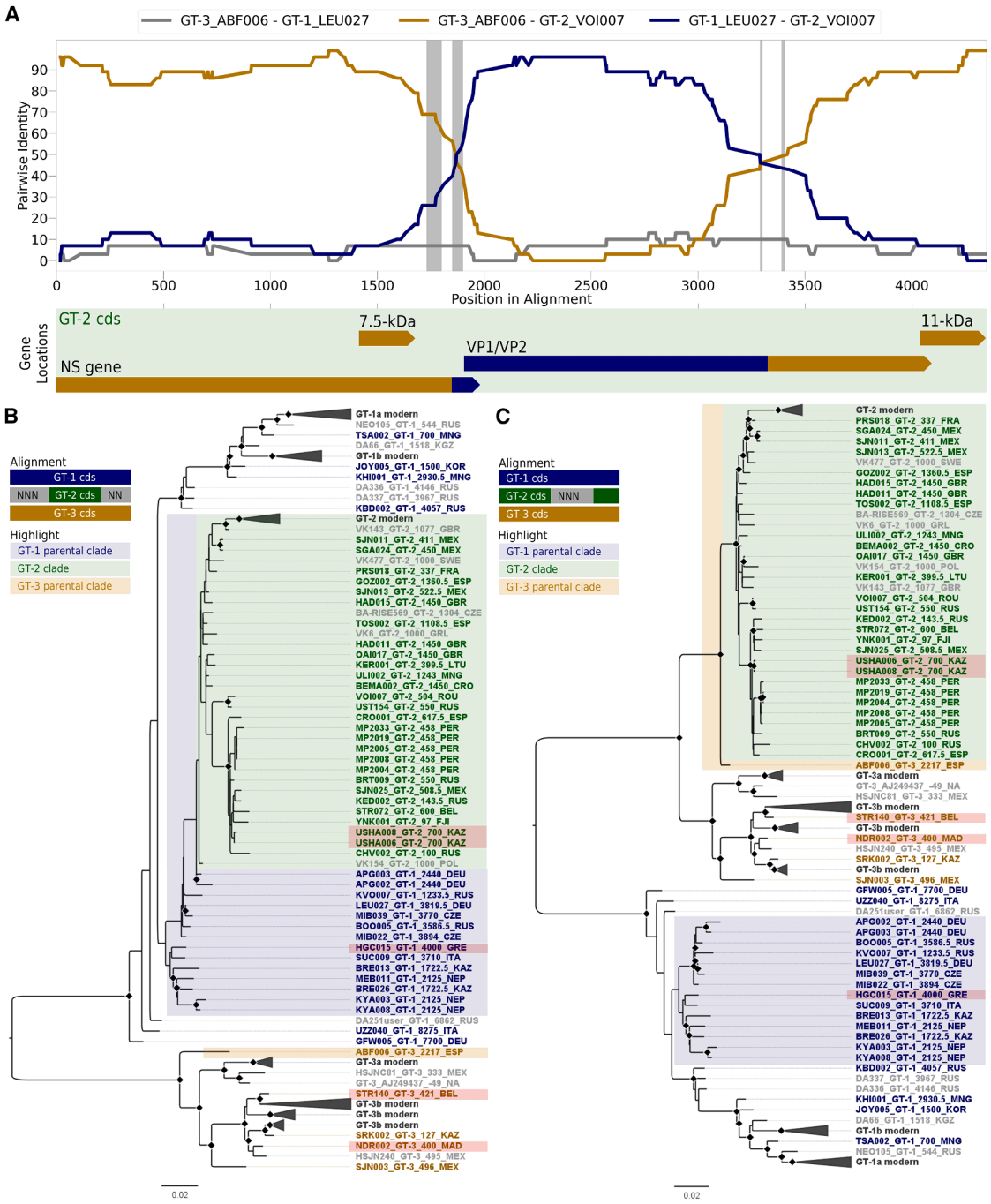

Figure 2. Recombination graph, an example for the sample VOI007 and the resulting recombination-separated maximum likelihood phylogeny

(A) Example graph for the recombination analysis: graph showcasing the RDP results obtained from analyzing VOI007 for evidence of recombination between GT-3 and GT-1. The pairwise sequence identity (*y* axis) is plotted against the nucleotide position in the alignment. The orange graph showcases the pairwise identity of the sample compared with the identified major parent GT-3 (ABF006). The blue graph showcases the pairwise identity of the sample compared with the identified minor parent GT-1 (LEU007). The gray graph showcases the pairwise sequence identity of both parental strains. The gray bars indicate the 95% confidence interval for the expected breakpoints. The location of the B19V genes within the GT-2 coding sequence is indicated schematically in the green square, separated by the parental sequence of origin denoted by color. Orange denotes a GT-3 origin, while blue denotes a GT-1 origin.

(B) The maximum likelihood phylogeny containing the GT-1 and GT-3 full coding sequence and partial GT-2 sequence. Newly added viral sequences are shown in blue (GT-1), green (GT-2), and orange (GT-3). The published diversity is represented in gray, and the modern diversity is collapsed. All trees were derived with 1,000 bootstrap replicates. Bootstrap values above 65 are indicated by a diamond symbol. Legends beside the symbols denote alignment components and highlights. Midpoint-rooted maximum likelihood tree of the distributed alignment containing the GT-1 originating sequence parts of GT-2. Highlights indicate the

(legend continued on next page)

that this lineage persisted at least into the 19th century. Contact-era GT-2 genomes from the site of Machu Picchu (MP2), Peru, are all closely related to each other and form a single clade nested within broader European and Asian diversity. By contrast, three GT-2 genomes from the early colonial site of Hospital Real de San José de los Naturales (SJN) in Mexico exhibit dispersed phylogenetic positions across the two subclades, suggesting that the individuals buried there were infected with B19V from diverse origins. They could either have been infected before arriving in the Americas (as suspected for SJN003, who was shown to be a first-generation enslaved African individual[43]) or contracted their infection as the result of B19V introduction by multiple sources. By contrast, infections recovered at Machu Picchu likely resulted from a single introduction, based on their uniform age and genotype and the high similarity between the viral genomes (Figure 3).

Revised genotype ages and recombination date

We included genomes for phylogenetic dating analysis only if $\geq$ 50% of their coding sequence was covered at $\geq 3\times$ depth and a ^{14}C date or strong archeological date was available, retaining a total of 48 genomes. Based on the recombination analyses, all GT-2 genomes were subsequently partitioned into two masked sequences per sample, each retaining either the GT-1-derived or the GT-3-derived genomic regions. Using these data, we generated new alignments containing all GT-1 and GT-3 sequences, as well as the aforementioned GT-1-originating or GT-3-originating sequence parts of GT-2. Only alignments with the partially masked GT-2 sequences were included in phylogenetic dating analyses in order to minimize recombination-based biases in estimates of node ages and evolutionary history.[44,45] Before inferring dated coalescent trees, we assessed the presence of a temporal signal using root-to-tip (RTT) regression and a date randomization test. To avoid bias in the temporal assessment introduced by the recombinant GT-2, we separated the GT-2 sequences into the GT-1- and the GT-3-derived regions, yielding two alignments with independent evolutionary histories. The GT-1 and GT-3 sequences are retained in full length in both alignments to maximize phylogenetic resolution. RTT regression was performed on both neighbor-joining and maximum likelihood trees. All tested trees show a strong temporal signal with an RTT correlation coefficient of 0.45–0.88 (Table S2). Date randomization tests performed with 10 replicates further supported the presence of a temporal signal in the data (Figure S2).

Dated coalescent trees were then inferred in BEAST 2 (Figure 4). Substitution-model tests and nested sampling guided the choice of clock model, leading to a relaxed lognormal clock with substitution-model averaging under a Bayesian skyline demographic prior. The mean rate prior at 1.0×10^{-5} substitutions per site per year, as previously estimated.[4,23] Monophyly of GT-1 and GT-3 was enforced based on support from the maximum-likelihood trees and the highest marginal likelihood analysis. For comparison, strict-clock analyses with model averaging and a skyline prior (without topological constraints) were also conducted on both alignments. All dating estimates were very consistent between the alignments. Ranges are presented over both alignments in brackets. The node age is given as the average between both alignment results, and the interval is set to cover the maximum interval. We inferred a root age for B19V of 12,656 BP (9,014–17,748 BP) and a median substitution rate of 1.58×10^{-5} s/s/y (1.97×10^{-5} to 1.24×10^{-5} s/s/y) under the relaxed lognormal clock setup, which are consistent with previous estimates.[8] The tMRCA (time to the most recent common ancestor) of genotype 1 is estimated to have existed 9,233 BP (8,543–10,269 BP). The GT-2 tMRCA is estimated to be 2,095 BP (1,771–2,370 BP), and the tMRCA of GT-3 is estimated to have existed 3,642 BP (2,500–5,189 BP).

DISCUSSION

Previous work had shown that full B19V genome recovery from skeletal remains was possible, but the limited number and geographic distribution of the ancient B19V genomes recovered thus far have provided only a glimpse into its past diversity. Here, we reconstructed 53 additional globally distributed ancient B19V genomes spanning more than 8,000 years, increasing the ancient sample size fourfold. Our dataset of ancient viral genomes contains representatives of all three present-day genotypes (GT-1, GT-2, and GT-3), including previously unknown subclades of GT-1 and GT-2. GT-3 is detectable in Europe, Asia, and Africa from ~2,200 years onward, with the oldest detection located in the Mediterranean. Utilizing the previously published and newly available ancient B19 virus sequences in combination with modern counterparts for dating its evolutionary history enables a more in-depth analysis. This allowed us to estimate the root age of B19V to 12,657 BP (9,079–17,748 HPD interval of both alignments), which is comparable to but older than previous estimates of ~10,000 BP (9,000–11,300 BP[8,35]). Besides the root age increasing somewhat, the ages of the distinct genotypes shifted strongly with a more robust signal. Our results suggest that genotypes 1 and 3 are older than previously estimated, while GT-2 is younger than previously thought.

The larger and more diverse dataset permits a more precise dating of the recombination event that gave rise to GT-2. On the one hand, this event is bound by the dates of divergence between GT-2 and its two parental lineages, GT-1 and GT-3. These dates mark the appearance of the two unsampled lineages, which, later on, contributed to the formation of GT-2 diversity. Hence, the recombination event cannot be older than either of these nodes, which are both confidently dated to less than ~3,200 BP. On the other hand, all GT-2 genomes descending from this recombination event must have occurred after the tMRCA of GT-2, which we confidently date to at least ~1,800 BP in both phylogenetic reconstructions. Following these principles, our analyses place the recombination event between ~3,200 and ~1,800 BP. The putative geographic origin of the recombination event that has given rise to GT-2 has not been

recombinant clade and the parental subclades of the respective genotypes. Red highlights denote samples excluded from phylogenetic dating. Tip labels consist of the *Sample-ID_Genotype_Age_Country 3-letter code*.

(C) Midpoint-rooted maximum likelihood tree of the distributed alignment containing the GT-3 originating sequence parts of GT-2.

See also Figure S1 for the recombination analysis with the P6 promoter region included.

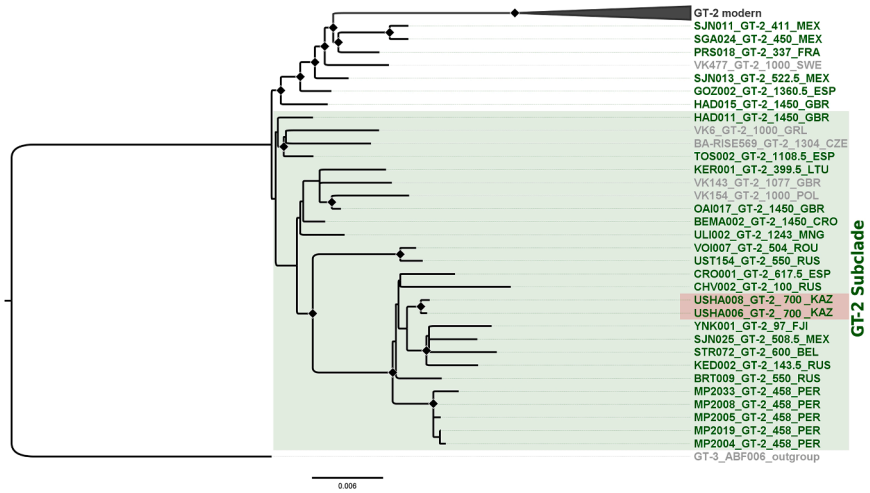

Figure 3. Maximum likelihood tree of the full coding sequence alignment of all available ancient sequences and modern representatives of B19V genotype 2

Bootstrap values were created with 1,000 replicates, and they are represented by diamond shapes when >65. Modern diversity is shown collapsed. Newly added ancient samples are represented in color. Published ancient samples are shown in gray. Viruses excluded from phylogenetic dating are highlighted in a red box. The subclade with no modern descendants is highlighted with a green box.

explored yet. Here, we propose the broader Mediterranean region as a plausible location for this event. Indeed, while GT-3 nowadays has a strong presence on the African continent, our results unveil the presence of this genotype on the Mediterranean island of Menorca ~2,200 BP (ABF006). This GT-3 genome is not only the closest sequence match to the recombination parent of the GT-3-derived portion of GT-2 but also derives from a community with strong African connections at a place that functioned as a contact and exchange point between Europe and Africa.[43,46–48] Together with the established presence of GT-1 on the Eurasian continent, prior to the GT-2 emergence, this suggests the broader Mediterranean region as a good candidate for the place where GT-1 and GT-3 hybridized. This exchange may have been made possible due to the high degree of connectivity in the 1st millennium BCE Mediterranean, whereby the large-scale mobility of humans also facilitated the spread of pathogens.[49]

These findings on the timing and geographic context of recombination are particularly interesting in the light of the recent suggestion that GT-2 is now extinct.[17] Our analysis of the temporal and geographic distribution of B19V genomes indicates that GT-2 was widespread in Europe from at least ~1,500 BP and likely persisted until the 1950s, when its prevalence appears to have declined. However, the extensive extinct diversity identified here suggests that GT-2 underwent a major population bottleneck much earlier than the 20th century CE, as most of its past diversity appears to have gone extinct by then. Taken together, our study captures an essential, albeit relatively brief, part of B19V history, showcasing the emergence, rise, and decline of the recombinant genotype 2 within no more than ~2,000 years.

Interpreting our B19V detections with respect to their impact on the health of past populations is complicated by the fact that, beyond acute infections, individuals may harbor B19V DNA in various tissues for decades, regardless of symptoms or immune status.[21] This persistence, found in bone marrow as well as hard tissues like bone[50,51] and teeth,[23] explains the frequent recovery of ancient B19V genomes. However, it complicates interpretation, as viral traces may represent an active infection at death or a much older persistent one. The eight B19V genomes recovered from co-infected individuals and from young and very young children are most likely to derive from active infections, providing a potential starting point for developing approaches to distinguish active from persistent infections in ancient individuals. Moreover, the detection of B19V in children offers direct evidence that this pathogen, today primarily associated with pediatric populations, also affected children in premodern contexts, suggesting a long-standing association with this age group.

As mentioned, detected viral genomes may result from either a persistent or active infection. Yet, with both scenarios, the genetic data offer insights into past distribution through time, cross-continental viral dispersals, and long-term viral evolutionary history. By integrating our results with social and archeological context, our study reveals three key insights into the health burden that B19V posed to humans through time.

First, the detection of B19V in hunter-gatherer individuals from central Europe (6,980–6,750 cal BP) and the Mediterranean (Sicily: 8,370–8,190 cal BP) demonstrates that the virus was circulating prior to the widespread establishment of farming communities and animal husbandry in these regions. Notably, the Sicilian hunter-gatherer individual dates to the final phase of the Mesolithic, several centuries before the introduction of farming in Sicily, although contemporaneous with evidence for farming practices in other regions of the Mediterranean.[52,53] Interactions between incoming farmers and local foragers may therefore have contributed to the spread of the virus during the Neolithic transition. It remains challenging to interpret whether B19V was transferred from mobile foraging communities onto the arising agriculturalists, or in the opposite direction, or through reciprocal exchanges within contact zones. This uncertainty aligns within the framework of the first epidemiological transition,[54,55] which proposes that many human-adapted pathogens emerged or expanded during the shift to sedentary lifestyles and agriculture as a result of increased exposure to domesticated animals, higher population density, and increased group exchange. Phylogenetic dating indicates that the coevolution of B19V with humans predates the Neolithic and was already present in earlier foraging societies. This pattern parallels observations from other viral pathogens, such as HBV (hepatitis B virus), whose evolutionary history with humans also predates the Neolithic period. Rather than functioning as a persistent, highly epidemic "crowd" disease, B19V was likely maintained at low levels within dispersed communities of both early farmers and hunter-gatherers.

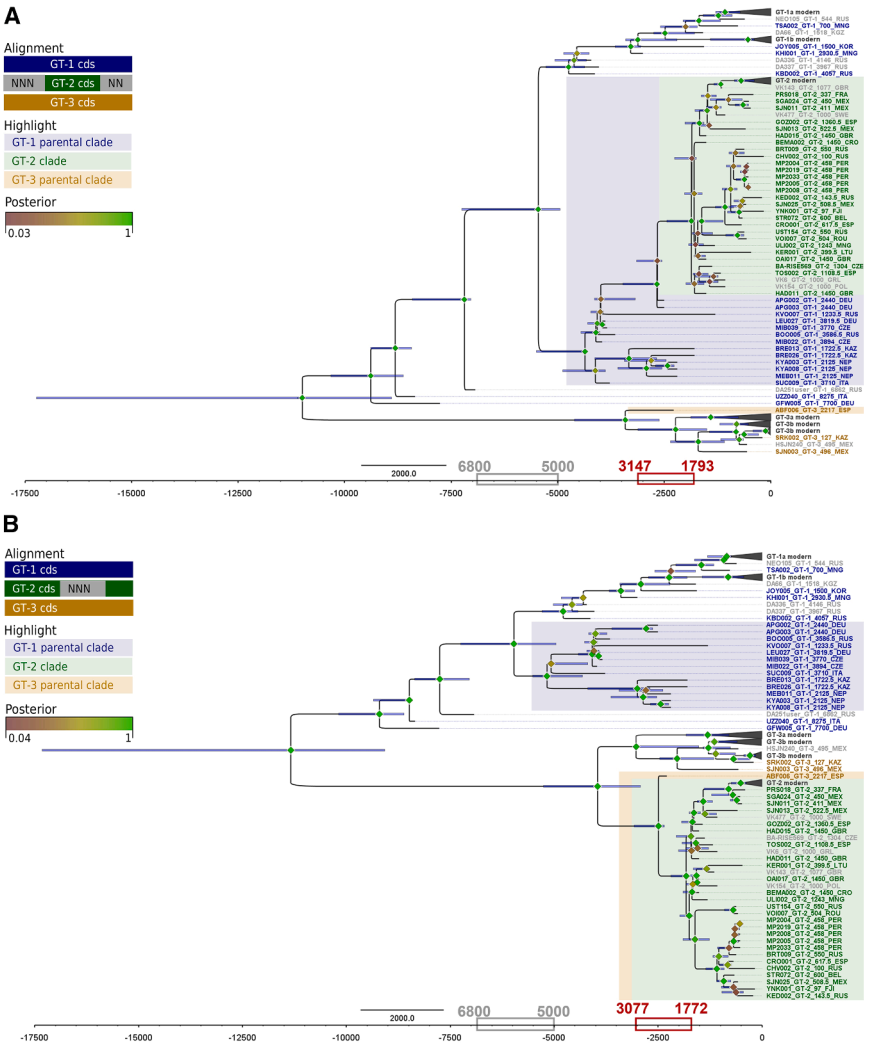

Figure 4. Phylogenetic dating of modern and ancient B19V diversity

Maximum clade credibility trees of the masked GT-2 alignments were inferred using BEAST 2 under a lognormal relaxed clock model and a coalescent Bayesian skyline population prior.

(A) The alignment contains unaltered GT-1 and GT-3 sequences and masked GT-2 sequences to contain only the GT-1 originating sequence parts located from nucleotide 1881–3351.

(B) The alignment contains unaltered GT-1 and GT-3 sequences and masked GT-2 sequences to contain only the GT-3 originating sequence parts, all nucleotides except 1881–3351. The mean substitution rate was provided as the default gamma prior with the starting point set to 1.0×10^{-5}. The horizontal blue bars mark the 95% highest posterior density (HPD) of each node, and the node circles indicate the posterior strength by color. Genotype clades are indicated by color: GT-1 is represented in blue with the extinct subclade in teal, GT-2 is indicated in green, and GT-3 is indicated in yellow. The alignment scheme in the top left corners showcases the sequence alignment by genotype, indicating the masked sections of GT-2 in the respective alignments. Sequence parts present in the alignment are indicated by color in the legend, while gray represents masked areas. The 95% HPD span of the GT-2 tMRCA and the node above are highlighted with a red box on the time axis. The previous recombination date estimate is shown in a gray box.

See also Figure S2 for the temporal signal testing and Figure S3 for the strict clock results.

See also Table S1 for the result of the nested sampling.

Second, a Romanian individual yielded the B19V GT-2 genome VOI007 and was previously found to have suffered from a malaria infection caused by *Plasmodium vivax*.[56] Active co-infection of *Plasmodium* species and B19V has substantial adverse impacts on health and is well documented today.[57,58] Individual VOI007 appears to be an ancient instance of this co-infection. Sample STR140, although yielding only a low-coverage GT-3 B19V genome (Figure 2), was co-infected with *Plasmodium malariae*, which causes a less virulent form of malaria. These instances highlight the potential synergistic impact of B19V and other pathogens on morbidity and mortality in the past, as is observed today.[57,58] However, because ancient viral sequences cannot distinguish persistent forms from active infection, definitive evidence of an active co-infection remains elusive.

Third, the peri-Contact Inca site of Machu Picchu—inhabited from the 1420s to 1540s and showing no evidence of European admixture[59]—yielded multiple B19V sequences highly similar to Eurasian-derived lineages, with a tMRCA dated to 659 BP (582–734 BP). The estimated tMRCA places the diversity of B19V observed in Machu Picchu prior to European arrival in the Americas, with substantial overlap between inferred ages of Machu Picchu lineages and contemporary European diversity. This finding further supports the hypothesis that European-derived B19V variants introduced to the Americas caused the first major B19V epidemic and that the virus was absent from the Americas prior to European contact. The modeled time of death estimates for each of the positively tested individuals fall within the window of ~480–440 BP,[60] which would allow for a period of not more than 17 years to reach the subtropical eastern flanks of the Central Andes after Columbus's first expedition reached the Caribbean in 1493. As a majority of B19V infections are asymptomatic, most people are unaware they are infected by the virus. B19V spreads mainly via saliva and droplets, but transmission is enhanced by the virus' environmental stability, which also allows it to spread via surface contamination.[61,62] Today, parvovirus shows clear seasonal variation, being most frequent in late winter and spring. In combination with a short epidemic period of ~4 years,[3–5] this enables high transmission rates inside a potentially naive human population.[5,63] The similarity of the Machu Picchu B19V genomes indicates a possible outbreak event caused by the introduction of a B19V GT-2 strain during the Contact Period. Combined with the highly diverse viral instances observed in colonial Mexico, these findings suggest that the virus reached the Americas in either one of two forms, carried as

a persistent infection by some individuals (SJN003) and as an active infection, which enabled viral spread. These active infections disseminated rapidly, possibly outpacing the speed of humans. The colonial introduction of B19V to the Americas is a remarkable example of how viral infections can leap across populations through informal networks ahead of major migration events. These observations mirror the pattern of other pathogens, such as *Plasmodium*, reaching the Americas via both the European colonizers (*P. vivax*) and the transatlantic slave trade (*P. falciparum*).[56]

Taken together, our findings reshape our understanding of B19V's place in history and underscore the role of cross-cultural contacts in the dissemination of infectious disease. Although B19V today is a ubiquitous pathogen typically associated with mild childhood illness, its impact in the past may have been considerably greater. By rapidly spreading through immunologically naive populations, e.g., Native Americans post contact, and interacting with other endemic diseases, B19V likely exacerbated the health outcomes among vulnerable groups. While infection is usually mild in healthy people, B19V can cause severe disease immunocompromised individuals as well as pregnant women, where vertical transmission poses a substantial risk for fetal mortality (5%–10%).[64,65] Infected fetuses are at risk to develop hydrops fetalis or suffering fetal death, complications that could also endanger maternal survival in the absence of medical interventions. During epidemic outbreaks, the incidence of acute B19V infections in pregnancy has been reported to exceed 10%,[66] further increasing the risk of adverse pregnancy outcomes. While this study cannot assess the clinical manifestations of past infections, it contributes to a more comprehensive understanding of the evolutionary trajectory of B19V and its close entanglement with human populations through time. Currently available ancient B19V genomes largely originate from Europe and Asia, and despite the successful recovery of an ancient B19V GT-3 genome from Madagascar, ancient African B19V diversity remains largely unknown and unexplored. Today, GT-3 is associated with west Africa, besides being detected in Europe and Asia. All ancient B19V genomes recovered from individuals of African origin (SJN003 - 496 BP and NDR002 - 400 BP) have been identified as GT-3 infected, suggesting a long-standing presence of this genotype on the continent. The newly identified ancient GT-3 genomes from Europe, Asia, and the Americas demonstrate that GT-3 has been spread throughout these three continents by at least the late 19th century, reaching Europe at least 400 years ago (STR140, Belgium) and Asia at least a hundred years ago (SRK002, Kazakhstan). Although current evidence suggests that all extant B19V diversity descends from a lineage that existed around the end of the last Ice Age, a broader representation of its ancient diversity will be necessary to disentangle the phylogeographic origins of this virus more confidently. In particular, future research should prioritize the recovery and analysis of ancient B19V genomes from African populations to illuminate the early history of this pathogen.

RESOURCE AVAILABILITY

Lead contact

Requests for further information and resources should be directed to and will be fulfilled by the lead contact, Johannes Krause (krause@eva.mpg.de).

Materials availability

This study did not generate any new, unique materials or reagents.

Data and code availability

- The data of this study are available as a standardized dataset. The partial genomes of B19V with their associated metadata are available as FASTA files.
- The nucleic acid sequences have been deposited at figshare under 10.6084/m9.figshare.30786167. The data for this study have been deposited in the European Nucleotide Archive (ENA) at EMBL-EBI under accession number PRJEB123221, and are publicly available, free of cost, as of the date of this publication.
- Any additional information required to reanalyze the data reported in this paper is available from the lead contact upon request.

ACKNOWLEDGMENTS

This research was supported by the United States National Science Foundation (grant no. BCS-1528698); the National Geographic Society; the Science Committee of the Ministry of Science and Higher Education of the Republic of Kazakhstan (grant no. AP23489627); the Praemium Academiae Award of the Czech Academy of Sciences (M.E.); the Ministry of Education, Culture, Science, and Sport of Mongolia (grant no. 2018/25); the National University of Mongolia (grant no. P2020-3955); the European Research Council under the European Union's Horizon 2020 research and innovation program (grant agreement no. 851511 for S.S.); the ERC (grant no. 804884 – DAIRYCULTURES) for C.W.; the ERC Initiative grant agreement number 834616-ARCHCAUCASUS; S.H.(KVO) DFG- RE2688/3; and S.R. (KBD). Additional support was received from the American School of Prehistoric Research, the Werner Siemens Foundation (Paleobiotechnology), and the Deutsche Forschungsgemeinschaft (German Research Foundation) under Germany's Excellence Strategy EXC 2051 (project no. 390713860, "Balance of the Microverse"). We also acknowledge funding provided by the Ministerio de Ciencia, Innovación y Universidades through the projects "La genómica antigua de Al-Andalus: Cambios demográficos y sociales en la Edad Media de Iberia" (PID2023-148718NA-I00) and "Ayudas para contratos Ramón y Cajal" (RYC2022-035700-I). We thank the Croatian Science Foundation (grant IP-2022-10-8558). We thank the Institute for Field Research for supporting the Oakington excavation and the Deutsche Forschungsgemeinschaft (DFG grant no. 497783672). This work was supported by the Eliteprogramm for postdocs of the Baden-Württemberg Stiftung (M.A.S.). This work was additionally supported by the National Research Foundation of Korea (NRF grant no. RS-2023-00212640), funded by the Korean Government (Ministry of Science and ICT). We also thank the Max Planck- Harvard Research Center for the Archaeoscience of the Ancient Mediterranean, the Institute for Aegean Prehistory, and Temple University. The funding bodies did not participate in the designing of the study, sample collection, analysis, data interpretation, and creating the manuscript. We express our sincere gratitude to archaeologist D. Khatanbaatar for providing access to anthropological materials from his excavations. We thank Gabriele Arenz, Guido Schreurs, Vincent Serneels, Nikolaj Makarov, Maria Dobrovolskaya, Claudia Pätzold, and Joana Gual for their contributions. We sincerely thank Alfonso Vigil-Escalera Guirado, Darlene Weston, Charlotte Roberts, Terry Brown, Terry L. Hunt, David Burley, Katerina Harvati, Hannes Rathmann, and colleagues at the Max Planck Institute for the Science of Human History in Jena for generously providing access to samples and contributing to the success of this research. We thank the staff of the archaeogenetics laboratory at the Max Planck Institute for Evolutionary Anthropology for performing sampling and for ssDNA and dsDNA library production as well as pathogen DNA capture. Data were produced by the Ancient DNA Core Unit of the Max Planck Institute for Evolutionary Anthropology, which is funded by the Max Planck Society.

AUTHOR CONTRIBUTIONS

A.H. and J. Krause initiated and supervised the study. M.A.S. supervised the initial phase of the study. M.A.S., A. Kocher, R. Barquera, R. Boersma, P.C., A.C., A.G., J.G., D.I.H.-Z., M. Michel., A. Mötsch, G.U.N., L.P., S.P., C.P., A.P., Å.J.V., V.V.-M., C.W., K.B., S.S., A. Mittnik, W.H., P. Slavin., J. Krause,

and A.H. coordinated the collection of samples for genetic analysis. E.G., M.A., J.F.B., A.B., A.B.B., P.P.B., S.C.F., L.C.L., C.C., F.C., L.D., M.E., L.F.-S., J.A.G.-V., A.V.-E.G., L.H., S.H., R.J., V.K., D. Kim, R.K., J. Kozakaitė, J. Krause, D. Krausse, M. Keller., M. Küßner., L.L., S.L., M. McCormick., M.A.M., L.M.-M., P.J.P.M., V.V.-M., H.M., L.M., E.M., R.E.N., L.O.E., R.D.S., Z.S., D. Sayer, V.S., F.S., E.S., T.T., R.T., K.V.d.V., E.J.W., T.X., M. McCormick, R.R., S.R., C.J., P.O., J.-A.R., C.R., K.M., A.K., S.K., M.D., D.R., M.N., D.V., S.G., E.N., P. Slavin., P. Stockhammer., B.N.R., S.C.F., L.C.L., and D. Sorokin participated in archeological excavation, provided anthropological assessment and/or contributed to the curation of skeletal materials, managed samples and metadata and/or conducted laboratory work. A. Kocher and T.Z. conducted metagenomic screening of ancient sequencing datasets. T.Z. and R.B. performed bioinformatic analysis. M.A.S., E.G., and T.Z. curated the ancient parvovirus datasets. All coauthors compiled archeological metadata and edited site descriptions. All authors contributed to the interpretation of the data. T.Z. drafted the manuscript with contributions from all co-authors.

DECLARATION OF INTERESTS

The authors declare no competing interests.

DECLARATION OF GENERATIVE AI AND AI-ASSISTED TECHNOLOGIES IN THE WRITING PROCESS

During the preparation of this work, the author(s) used Grammarly services throughout the writing in order to catch and highlight spelling errors. After using this tool or service, the authors reviewed and edited the content as needed and take full responsibility for the content of the publication.

STAR★METHODS

Detailed methods are provided in the online version of this paper and include the following:

- KEY RESOURCES TABLE
- EXPERIMENTAL MODEL AND STUDY PARTICIPANT DETAILS
  - Sampled ancient individuals
  - African archeological sites
  - European archeological sites
  - Asian archeological sites
  - Oceanian archeological sites
  - American archeological sites
- METHOD DETAILS
  - Sampling of skeletal material and DNA extraction
  - DNA Library generation and sequencing
- QUANTIFICATION AND STATISTICAL ANALYSIS
  - Screening for Human Parvovirus B19
  - Human Parvovirus B19 Capture Design
  - Capture data processing with the nfcore/eager pipeline
  - Genotyping, sequence recovery and alignment curation
  - Recombination analysis
  - Phylogenetic Analysis
  - Phylogenetic dating Analysis

SUPPLEMENTAL INFORMATION

Supplemental information can be found online at https://doi.org/10.1016/j.cub.2026.08.032.

Received: December 4, 2025
Revised: May 22, 2026
Accepted: August 12, 2026
Published: September 8, 2026

REFERENCES

1. Cossart, Y.E., Field, A.M., Cant, B., and Widdows, D. (1975). PARVOVIRUS-LIKE PARTICLES IN HUMAN SERA. Lancet *1*, 72–73. https://doi.org/10.1016/S0140-6736(75)91074-0.
2. Anderson, M.J., Jones, S.E., Fisher-Hoch, S.P., Lewis, E., Hall, S.M., Bartlett, C.L.R., Cohen, B.J., Mortimer, P.P., and Pereira, M.S. (1983). HUMAN PARVOVIRUS, THE CAUSE OF ERYTHEMA INFECTIOSUM (FIFTH DISEASE)? Lancet *1*, 1378. https://doi.org/10.1016/S0140-6736(83)92152-9.
3. Enders, M., Weidner, A., and Enders, G. (2007). Current epidemiological aspects of human parvovirus B19 infection during pregnancy and childhood in the western part of Germany. Epidemiol. Infect. *135*, 563–569. https://doi.org/10.1017/S095026880600731X.
4. Russcher, A., van Boven, M., Benincà, E., Verweij, E.J.T.J., Molenaar-de Backer, M.W.A., Zaaijer, H.L., Vossen, A.C.T.M., and Kroes, A.C.M. (2024). Changing epidemiology of parvovirus B19 in the Netherlands since 1990, including its re-emergence after the COVID-19 pandemic. Sci. Rep. *14*, 9630. https://doi.org/10.1038/s41598-024-59582-7.
5. Fourgeaud, J., Allali, S., Toubiana, J., Pinhas, Y., Frange, P., Leruez-Ville, M., and Cohen, J.F. (2023). Post-COVID-19 pandemic outbreak of severe Parvovirus B19 primary infections in Paris, France: 10-year interrupted time-series analysis (2012–2023). J. Clin. Virol. *167*, 105576. https://doi.org/10.1016/j.jcv.2023.105576.
6. d'Humières, C., Fouillet, A., Verdurme, L., Lakoussan, S.B., Gallien, Y., Coignard, C., Hervo, M., Ebel, A., Soares, A., Visseaux, B., et al. (2024). An unusual outbreak of parvovirus B19 infections, France, 2023 to 2024. Euro Surveill. *29*, 2400339. https://doi.org/10.2807/1560-7917.ES.2024.29.25.2400339.
7. Qiu, J., Söderlund-Venermo, M., and Young, N.S. (2017). Human parvoviruses. American Society for Microbiology. Clin. Microbiol. Rev. *30*, 43–113. https://doi.org/10.1128/CMR.00040-16.
8. Mühlemann, B., Margaryan, A., Damgaard, P.B., Allentoft, M.E., Vinner, L., Hansen, A.J., Weber, A., Bazaliiskii, V.I., Molak, M., Arneborg, J., et al. (2018). Ancient human parvovirus B19 in Eurasia reveals its long-term association with humans. Proc. Natl. Acad. Sci. USA *115*, 7557–7562. https://doi.org/10.1073/pnas.1804921115.
9. Cotmore, S.F., Agbandje-McKenna, M., Chiorini, J.A., Mukha, D.V., Pintel, D.J., Qiu, J., Soderlund-Venermo, M., Tattersall, P., Tijssen, P., Gatherer, D., et al. (2014). The family Parvoviridae. Arch. Virol. *159*, 1239–1247. https://doi.org/10.1007/s00705-013-1914-1.
10. Shade, R.O., Blundell, M.C., Cotmore, S.F., Tattersall, P., and Astell, C.R. (1986). Nucleotide Sequence and Genome Organization of Human Parvovirus B19 Isolated from the Serum of a Child during Aplastic Crisis. J. Virol. *58*, 921–936. https://doi.org/10.1128/jvi.58.3.921-936.1986.
11. Deiss, V., Tratschin, J.D., Weitz, M., and Siegl, G. (1990). Cloning of the human parvovirus B19 genome and structural analysis of its palindromic termini. Virology *175*, 247–254. https://doi.org/10.1016/0042-6822(90)90205-6.
12. Servant, A., Laperche, S., Lallemand, F., Marinho, V., De Saint Maur, G., Meritet, J.F., and Garbarg-Chenon, A. (2002). Genetic Diversity within Human Erythroviruses: Identification of Three Genotypes. J. Virol. *76*, 9124–9134. https://doi.org/10.1128/jvi.76.18.9124-9134.2002.
13. Parsyan, A., Szmaragd, C., Allain, J.P., and Candotti, D. (2007). Identification and genetic diversity of two human parvovirus B19 genotype 3 subtypes. J. Gen. Virol. *88*, 428–431. https://doi.org/10.1099/vir.0.82496-0.
14. Jia, J., Ma, Y., Zhao, X., Huangfu, C., Zhong, Y., Fang, C., Fan, R., Lv, M., and Zhang, J. (2016). Existence of various human parvovirus B19 genotypes in Chinese plasma pools: Genotype 1, genotype 3, putative inter-genotypic recombinant variants and new genotypes. Virol. J. *13*, 155. https://doi.org/10.1186/s12985-016-0611-6.
15. Ivi Norja, P., Hokynar, K., Aaltonen, L.-M., Chen, R., Ranki, A., Partio, E.K., Kiviluoto, O., Davidkin, I., and Leivo, T. (2006). Maria Eis-Hü binger,

A., et al. In Bioportfolio: Lifelong Persistence of Variant and Prototypic Erythrovirus DNA Genomes in Human Tissue, *103* (PNAS), pp. 7450–7453. https://doi.org/10.1073/pnas.0602259103.

16. Pyöriä, L., Toppinen, M., Mäntylä, E., Hedman, L., Aaltonen, L.M., Vihinen-Ranta, M., Ilmarinen, T., Söderlund-Venermo, M., Hedman, K., and Perdomo, M.F. (2017). Extinct type of human parvovirus B19 persists in tonsillar B cells. Nat. Commun. *8*, 14930. https://doi.org/10.1038/ncomms14930.
17. Heegaard, E.D., and Brown, K.E. (2002). Human parvovirus B19. Clin. Microbiol. Rev. *15*, 485–505. https://doi.org/10.1128/CMR.15.3.485-505.2002.
18. Mossong, J., Hens, N., Friederichs, V., Davidkin, I., Broman, M., Litwinska, B., Siennicka, J., Trzcinska, A., Van Damme, P., Beutels, P., et al. (2008). Parvovirus B19 infection in five European countries: Seroepidemiology, force of infection and maternal risk of infection. Epidemiol. Infect. *136*, 1059–1068. https://doi.org/10.1017/S0950268807009661.
19. Bouraddane, M., Warda, K., and Zouhair, S. (2021). Parvovirus B19 and Pregnant Women: A Bibliographic Review. Open J. Obstet. Gynecol. *11*, 1543–1564. https://doi.org/10.4236/ojog.2021.1111145.
20. Colazo Salbetti, M.B., Boggio, G., Dicuatro, N., Gudiño, A.P., Olivera, N., Pedranti, M., Isa, M.B., Bertoldi, A., Miranda, M.J., Rodriguez Lombardi, G., et al. (2024). Parvovirus B19 remains an underestimated pathogen among infections during gestation in Argentina: Insights through the study of symptomatic and asymptomatic pregnant patients and newborns from Córdoba. J. Clin. Virol. *175*, 105739. https://doi.org/10.1016/j.jcv.2024.105739.
21. Corcioli, F., Zakrzewska, K., Rinieri, A., Fanci, R., Innocenti, M., Civinini, R., De Giorgi, V., Di Lollo, S., and Azzi, A. (2008). Tissue persistence of parvovirus B19 genotypes in asymptomatic persons. J. Med. Virol. *80*, 2005–2011. https://doi.org/10.1002/jmv.21289.
22. Mielonen, O.I., Hänninen, S., Willberg, J., Salo, T., and Mauramo, M. (2025). DNA virus tropism in healthy dental pulp: an in-situ reservoir site for torque teno virus and parvovirus B19. J. Oral Microbiol. *17*, 2499924. https://doi.org/10.1080/20002297.2025.2499924.
23. Toppinen, M., Pratas, D., Väisänen, E., Söderlund-Venermo, M., Hedman, K., Perdomo, M.F., and Sajantila, A. (2020). The landscape of persistent human DNA viruses in femoral bone. Forensic Sci. Int. Genet. *48*, 102353. https://doi.org/10.1016/j.fsigen.2020.102353.
24. Nikkari, S., Roivainen, A., Hannonen, P., Mottonen, T., Luukkainen, R., Yli-Jama, T., Toivanen, P., and Nikkari, S. (1995). Persistence of Parvovirus B 19 in Synovial Fluid and Bone Marrow. Ann Rheum Dis *54*, 597–600.
25. Brown, K.E., and Young, N.S. (1996). Parvoviruses and bone marrow failure. Stem Cellsn *14*, 151–163. https://doi.org/10.1002/stem.140151.
26. Cassinotti, P., Burtonboy, G., Fopp, M., and Siegl, G. (1997). Evidence for persistence of human parvovirus B19 DNA in bone marrow. J. Med. Virol. *53*, 229–232. https://doi.org/10.1002/(SICI)1096-9071(199711)53:3<229::AID-JMV8>3.0.CO;2-A.
27. Söderlund, M., von Essen, R., Haapasaari, J., Kiistala, U., Kiviluoto, O., and Hedman, K. (1997). Persistence of parvovirus B19 DNA in synovial membranes of young patients with and without chronic arthropathy. Lancet *349*, 1063–1065. https://doi.org/10.1016/S0140-6736(96)09110-6.
28. Manning, A., Willey, S.J., Bell, J.E., and Simmonds, P. (2007). Comparison of tissue distribution, persistence, and molecular epidemiology of parvovirus B19 and novel human parvoviruses PARV4 and human bocavirus. J. Infect. Dis. *195*, 1345–1352. https://doi.org/10.1086/513280.
29. Grant, J.K., Yin, N.C., Zaytoun, A.M., Waseem, H., and Hobbs, J.A. (2009). Persistent adeno-associated virus 2 and parvovirus B19 sequences in post-mortem human cerebellum. Cerebellum *8*, 490–498. https://doi.org/10.1007/s12311-009-0126-4.
30. Stewart, G.C., Lopez-Molina, J., Gottumukkala, R.V.S.R.K., Rosner, G.F., Anello, M.S., Hecht, J.L., Winters, G.L., Padera, R.F., Baughman, K.L., and Lipes, M.A. (2011). Myocardial Parvovirus B19 Persistence: Lack of Association With Clinicopathologic Phenotype in Adults With Heart failure. Circ., Heart Fail. *4*, 71–78. https://doi.org/10.1161/CIRCHEARTFAILURE.110.958249.
31. Alves, A.D.R., Melgaço, J.G., Cássia Nc Garcia, R. De, Raposo, J.V., De Paula, V.S., Araújo, C.C.V., Pinto, M.A., and Amado, L.A. (2020). Persistence of Parvovirus B19 in liver from transplanted patients with acute liver failure. Future Microbiol. *15*, 307–317. https://doi.org/10.2217/fmb-2019-0224.
32. Moosazadeh, M., Alimohammadi, M., and Mousavi, T. (2023). Seroprevalence and geographical distribution of parvovirus B19 antibodies in pregnant women: A-meta analysis. J. Immunoassay Immunochem. *44*, 103–116. https://doi.org/10.1080/15321819.2023.2167520.
33. Gigi, C.E., and Anumba, D.O.C. (2021). Parvovirus b19 infection in pregnancy – A review. Eur. J. Obstet. Gynecol. Reprod. Biol. *264*, 358–362. https://doi.org/10.1016/j.ejogrb.2021.07.046.
34. Brown, T., Anand, A., Ritchie, L.D., Clewley, J.P., and Reid, T.M.S. (1984). INTRAUTERINE PARVOVIRUS INFECTION ASSOCIATED WITH HYDROPS FETALIS. Lancet *2*, 1033–1034. https://doi.org/10.1016/S0140-6736(84)91126-7.
35. Guzmán-Solís, A.A., Villa-Islas, V., Bravo-López, M.J., Sandoval-Velasco, M., Wesp, J.K., Gómez-Valdés, J.A., de la Luz Moreno-Cabrera, M., Meraz, A., Solís-Pichardo, G., Schaaf, P., et al. (2016). Ancient Viral Genomes Reveal Introduction of Human Pathogenic Viruses into Mexico during the Transatlantic Slave Trade. eLIFE *10*, e68612. https://doi.org/10.7554/eLife.
36. Fu, Q., Hajdinjak, M., Moldovan, O.T., Constantin, S., Mallick, S., Skoglund, P., Patterson, N., Rohland, N., Lazaridis, I., Nickel, B., et al. (2015). An early modern human from Romania with a recent Neanderthal ancestor. Nature *524*, 216–219. https://doi.org/10.1038/nature14558.
37. Haak, W., Lazaridis, I., Patterson, N., Rohland, N., Mallick, S., Llamas, B., Brandt, G., Nordenfelt, S., Harney, E., Stewardson, K., et al. (2015). Massive migration from the steppe was a source for Indo-European languages in Europe. Nature *522*, 207–211. https://doi.org/10.1038/nature14317.
38. Mathieson, I., Lazaridis, I., Rohland, N., Mallick, S., Patterson, N., Roodenberg, S.A., Harney, E., Stewardson, K., Fernandes, D., Novak, M., et al. (2015). Genome-wide patterns of selection in 230 ancient Eurasians. Nature *528*, 499–503. https://doi.org/10.1038/nature16152.
39. Herbig, A., Maixner, F., Bos, K.I., Zink, A., Krause, J., and Huson, D.H. (2016). MALT: Fast alignment and analysis of metagenomic DNA sequence data applied to the Tyrolean Iceman. Preprint at bioRxiv. https://doi.org/10.1101/050559.
40. Hübler, R., Key, F.M., Warinner, C., Bos, K.I., Krause, J., and Herbig, A. (2019). HOPS: automated detection and authentication of pathogen DNA in archaeological remains. Genome Biol. *20*, 280. https://doi.org/10.1186/s13059-019-1903-0.
41. Martin, D.P., Varsani, A., Roumagnac, P., Botha, G., Maslamoney, S., Schwab, T., Kelz, Z., Kumar, V., and Murrell, B. (2021). RDP5: A computer program for analyzing recombination in, and removing signals of recombination from, nucleotide sequence datasets. Virus Evol. *7*, veaa087. https://doi.org/10.1093/ve/veaa087.
42. Shen, H., Zhang, W., Wang, H., and Shao, S. (2016). Identification of recombination in the NS1 and VPs genes of parvovirus B19. J. Med. Virol. *88*, 1457–1461. https://doi.org/10.1002/jmv.24471.
43. Ringbauer, H., Salman-Minkov, A., Regev, D., Olalde, I., Peled, T., Sineo, L., Falsone, G., van Dommelen, P., Mittnik, A., Lazaridis, I., et al. (2025). Punic people were genetically diverse with almost no Levantine ancestors. Nature *643*, 139–147. https://doi.org/10.1038/s41586-025-08913-3.
44. Posada, D., and Crandall, K.A. (2002). The effect of recombination on the accuracy of phylogeny estimation. J. Mol. Evol. *54*, 396–402. https://doi.org/10.1007/s00239-001-0034-9.

45. Murray, G.G.R., Wang, F., Harrison, E.M., Paterson, G.K., Mather, A.E., Harris, S.R., Holmes, M.A., Rambaut, A., and Welch, J.J. (2016). The effect of genetic structure on molecular dating and tests for temporal signal. Methods Ecol. Evol. *7*, 80–89. https://doi.org/10.1111/2041-210X.12466.

46. Gili, S., Lull, V., Micó, R., Rihuete, C., and Risch, R. (2006). An island decides: Megalithic burial rites on Menorca. Antiquity *80*, 829–842. https://doi.org/10.1017/S0003598X0009445X.

47. Docter, R., and Gubel, E. (2022). AMPHORAE IN THE Phoenician-PUNIC WORLD the State of the Art (Amphorae in the Phoenician-Punic World).

48. Pons, G. (2018). The Talaiotic Culture of the Balearic Islands. Preprint at Institut d'Estudis Catalans. https://doi.org/10.2436/20.1000.01.143.

49. Broodbank, C. (2014). The Making of the Middle Sea: a History of the Mediterranean from the Beginning to the Emergence of the Classical World (Thames & Hudson).

50. Toppinen, M., Perdomo, M.F., Palo, J.U., Simmonds, P., Lycett, S.J., Söderlund-Venermo, M., Sajantila, A., and Hedman, K. (2015). Bones hold the key to DNA virus history and epidemiology. Sci. Rep. *5*, 17226. https://doi.org/10.1038/srep17226.

51. Toppinen, M. (2021). Parvoviral Genomes in Human Soft Tissues and Bones Over Decades. Haartman Institute Lecture Hall (Helsingin yliopisto).

52. González-Fortes, G., Jones, E.R., Lightfoot, E., Bonsall, C., Lazar, C., Grandal-d'Anglade, A., Garralda, M.D., Drak, L., Siska, V., Simalcsik, A., et al. (2017). Paleogenomic Evidence for Multi-generational Mixing between Neolithic Farmers and Mesolithic Hunter-Gatherers in the Lower Danube Basin. Curr. Biol. *27*, 1801–1810.e10. https://doi.org/10.1016/j.cub.2017.05.023.

53. Posth, C., Yu, H., Ghalichi, A., Rougier, H., Crevecoeur, I., Huang, Y., Ringbauer, H., Rohrlach, A.B., Nägele, K., Villalba-Mouco, V., et al. (2023). Palaeogenomics of Upper Palaeolithic to Neolithic European hunter-gatherers. Nature *615*, 117–126. https://doi.org/10.1038/s41586-023-05726-0.

54. Barrett, R., Kuzawa, C.W., McDade, T., and Armelagos, G.J. (1998). EMERGING AND RE-EMERGING INFECTIOUS DISEASES: The Third Epidemiologic Transition. Annu. Rev. Anthropol. *27*, 247–271. https://doi.org/10.1146/annurev.anthro.27.1.247.

55. Diamond, J. (2002). Evolution, consequences and future of plant and animal domestication. Nature *418*, 700–707. https://doi.org/10.1038/nature01019.

56. Michel, M., Skourtanioti, E., Pierini, F., Guevara, E.K., Mötsch, A., Kocher, A., Barquera, R., Bianco, R.A., Carlhoff, S., Coppola Bove, L., et al. (2024). Ancient Plasmodium genomes shed light on the history of human malaria. Nature *631*, 125–133. https://doi.org/10.1038/s41586-024-07546-2.

57. Motta, E.D.S., Alves, A.D.R., Leon, L.A.A., Silva, J.R.S., Cerilo-Filho, M., Gomes, M.D.S.M., Menezes, R.A. de O., Machado, R.L.D., and Cubel Garcia, R. de C.N. (2025). Human parvovirus B19 infection in a Plasmodium vivax endemic area on the Brazil-French Guiana border. Acta Trop. *263*, 107542. https://doi.org/10.1016/j.actatropica.2025.107542.

58. Toan, N.L., Sy, B.T., Song, L.H., Luong, H.V., Binh, N.T., Binh, V.Q., Kandolf, R., Velavan, T.P., Kremsner, P.G., and Bock, C.T. (2013). Co-infection of human parvovirus B19 with Plasmodium falciparum contributes to malaria disease severity in Gabonese patients. BMC Infect. Dis. *13*, 375. https://doi.org/10.1186/1471-2334-13-375.

59. Salazar, L., Burger, R., Forst, J., Barquera, R., Nesbitt, J., Calero, J., Washburn, E., Verano, J., Zhu, K., Sop, K., et al. (2023). Insights into the genetic histories and lifeways of Machu Picchu's occupants. Sci. Adv. *9*, eadg3377. https://doi.org/10.1126/sciadv.adg3377.

60. Lane, K., and Marsh, E.J. (2024). Absolute Chronology revisited: Integrating precise Bayesian models from Machu Picchu with Inca ethnohistoric praise narratives. Quat. Int. *703*, 21–31. https://doi.org/10.1016/j.quaint.2023.11.006.

61. Eggers, M., Hübner, N.-O., Helber-Soszynski, U., Blümel, J., Exner, M., Gebel, J., Ilschner, C., Rabenau, H.F., Schwebke, I., and Enders, M. (2025). Hygiene and Disinfection Measures for Parvovirus B19 Infections Hygiene-Und Desinfektionsmaßnahmen bei Parvovirus B19-Infektionen. GMS Hygiene and Infection Control *20*.

62. (2010). Parvovirus B19. Stellungnahmen des Arbeitskreises Blut des Bundesministeriums für Gesundheit. Bundesgesundheitsblatt Gesundheitsforschung Gesundheitsschutz *53*, 944–956. https://doi.org/10.1007/s00103-010-1109-9.

63. Oliveira, S.A., Camacho, L.A.B., Pereira, A.C.M., Faillace, T.F., Setúbal, S., and Nascimento, J.P. (2002). Clinical and Epidemiological Aspects of Human Parvovirus B19 Infection in an Urban Area in Brazil (Niterói City Area, State of Rio de Janeiro, Brazil). Mem. Inst. Oswaldo Cruz *97*, 965–970. https://doi.org/10.1590/S0074-02762002000700007.

64. Ergaz, Z., and Ornoy, A. (2006). Parvovirus B19 in pregnancy. Reprod. Toxicol. *21*, 421–435. https://doi.org/10.1016/j.reprotox.2005.01.006.

65. Boissiere, J., Watkins, V., Kuller, J.A., and Dotters-Katz, S.K. (2024). Parvovirus B19 in Pregnancy. Obstet. Gynecol. Surv. *79*, 281–289. https://doi.org/10.1097/OGX.0000000000001263.

66. Lamont, R.F., Sobel, J.D., Vaisbuch, E., Kusanovic, J.P., Mazaki-Tovi, S., Kim, S.K., Uldbjerg, N., and Romero, R. (2011). Parvovirus B19 infection in human pregnancy. BJOG *118*, 175–186. https://doi.org/10.1111/j.1471-0528.2010.02749.x.

67. Serneels, V., Morel, M., Nitsche, C., Radimilahy, C., Rakotoarisoa, J.-A., Rasoarifetra, B., and Schreurs, G. (2017). Pierre et Fer à Madagascar (1) – Vestiges Sidérurgiques de Bénavony et de la Rivière Matavy (Jahresberciht SLSA).

68. Acsádi, G., and Nemeskéri, J. (1970). History of Human Life Span and Mortality (Akadémiai Kiadó).

69. Byers, S.N. (2016). Introduction to Forensic Anthropology: a Textbook, Fifth Edition (Routledge).

70. Ferembach, D., Schwidetzky, I., and Stloukal, M. (1980). Recommendations for age and sex diagnoses of skeletons. J. Hum. Evol. *9*, 517–549. https://doi.org/10.1016/0047-2484(80)90061-5.

71. Trotter, M., and Gleser, G.C. (1958). A re-evaluation of estimation of stature based on measurements of stature taken during life and of long bones after death. Am. J. Phys. Anthropol. *16*, 79–123. https://doi.org/10.1002/ajpa.1330160106.

72. Trotter, M., and Gleser, G.C. (1952). Estimation of stature from long bones of American Whites and Negroes. Am. J. Phys. Anthropol. *10*, 463–514. https://doi.org/10.1002/ajpa.1330100407.

73. Gretzinger, J., Schmitt, F., Mötsch, A., Carlhoff, S., Lamnidis, T.C., Huang, Y., Ringbauer, H., Knipper, C., Francken, M., Mandt, F., et al. (2024). Evidence for dynastic succession among early Celtic elites in Central Europe. Nat. Hum. Behav. *8*, 1467–1480. https://doi.org/10.1038/s41562-024-01888-7.

74. Kolpakov, E., Murashkin, A., Khartanovich, V., and Shumkin, V. (2019). Kola Oleneostrovsky Cemetery (1925–2013) (Institute for the History of Material Culture Russian Academy Sciences). https://doi.org/10.31600/978-5-93061-149-6.

75. Moiseyev, V.G., and Khartanovich, V.I. (2012). Early Metal Age crania from Bolshoy Oleniy Island, Barents Sea. Archaeol. Ethnol. Anthropol. Eurasia *40*, 145–154. https://doi.org/10.1016/j.aeae.2012.05.018.

76. Der Sarkissian, C., Balanovsky, O., Brandt, G., Khartanovich, V., Buzhilova, A., Koshel, S., Zaporozhchenko, V., Gronenborn, D., Moiseyev, V., Kolpakov, E., et al. (2013). Ancient DNA Reveals Prehistoric Gene-Flow from Siberia in the Complex Human Population History of North East Europe. PLoS Genet. *9*, e1003296. https://doi.org/10.1371/journal.pgen.1003296.

77. Lamnidis, T.C., Majander, K., Jeong, C., Salmela, E., Wessman, A., Moiseyev, V., Khartanovich, V., Balanovsky, O., Ongyerth, M., Weihmann, A., et al. (2018). Ancient Fennoscandian genomes reveal origin and spread of Siberian ancestry in Europe. Nat. Commun. *9*, 5018. https://doi.org/10.1038/s41467-018-07483-5.

78. Mustonen, T. (2022). Indigenous knowledge, mercury, and a remote Russian Indigenous river basin—Ponoi River. In Indigenous Water and Drought Management in a Changing World (Elsevier), pp. 299–307. https://doi.org/10.1016/B978-0-12-824538-5.00015-7.

79. Shakhnovitch, M.M., and Kolivatov, E.B. (2024). Chapel of the Nativity of the Lovozersky Sami Churchyard. Finno-Ugric World *16*, 361–372. https://doi.org/10.15507/2076-2577.016.2024.03.361-372.

80. Kotula, A., Piezonka, H., and Terberger, T. (2020). The Mesolithic cemetery of Groß Fredenwalde (north-eastern Germany) and its cultural affiliations. Lietuvos Archeologija *46*, 65–84. https://doi.org/10.33918/25386514-046002.

81. Terberger, T., Kotula, A., Lorenz, S., Schult, M., Burger, J., and Jungklaus, B. (2015). Standing upright to all eternity – The Mesolithic burial site at Groß Fredenwalde, Brandenburg (NE Germany). Quartar *62*, 133–154. https://doi.org/10.7485/QU62_6.

82. Groß, D., and Rothstein, M. (2023). Changing Identity in a Changing World. Current Studies on the Stone Age around 4000 BCE (Sidestone Press). https://doi.org/10.59641/pfm7c6gh.

83. Gretzinger, J., Sayer, D., Justeau, P., Altena, E., Pala, M., Dulias, K., Edwards, C.J., Jodoin, S., Lacher, L., Sabin, S., et al. (2022). The Anglo-Saxon migration and the formation of the early English gene pool. Nature *610*, 112–119. https://doi.org/10.1038/s41586-022-05247-2.

84. Betancourt, P.P. (2014). Hagios Charalambos: A Minoan Burial Cave in Crete (Institute for Aegean Prehistory Academic Press (Institute for Aegean Prehistory)). https://doi.org/10.2307/j.ctt13x0mn3.

85. Betancourt, P.P., Davaras, C., Dierckx, H.M.C., Ferrence, S.C., Hickman, J., Karkanas, P., McGeorge, P.J.P., Muhly, J.D., Reese, D.S., Stravopodi, E., et al. (2008). Excavations in the Hagios Charalambos Cave: A Preliminary Report. Hesperia *77*, 539–605. https://doi.org/10.2972/hesp.77.4.539.

86. Langford-Verstegen, L.C. (2016). Hagios Charalambos: A Minoan Burial Cave in Crete (Institute for Aegean Prehistory Academic Press (Institute for Aegean Prehistory)). https://doi.org/10.2307/j.ctt1g69zr0.

87. Skourtanioti, E., Ringbauer, H., Gnecchi Ruscone, G.A., Bianco, R.A., Burri, M., Freund, C., Furtwängler, A., Gomes Martins, N.F., Knolle, F., Neumann, G.U., et al. (2023). Ancient DNA reveals admixture history and endogamy in the prehistoric Aegean. Nat. Ecol. Evol. *7*, 290–303. https://doi.org/10.1038/s41559-022-01952-3.

88. Lazaridis, I., Mittnik, A., Patterson, N., Mallick, S., Rohland, N., Pfrengle, S., Furtwängler, A., Peltzer, A., Posth, C., Vasilakis, A., et al. (2017). Genetic origins of the Minoans and Mycenaeans. Nature *548*, 214–218. https://doi.org/10.1038/nature23310.

89. Neumann, G.U., Skourtanioti, E., Burri, M., Nelson, E.A., Michel, M., Hiss, A.N., McGeorge, P.J.P., Betancourt, P.P., Spyrou, M.A., Krause, J., et al. (2022). Ancient Yersinia pestis and Salmonella enterica genomes from Bronze Age Crete. Curr. Biol. *32*, 3641–3649.e8. https://doi.org/10.1016/j.cub.2022.06.094.

90. Küßner, M. (2015). Leubingen und Dermsdorf, Lkr. Sömmerda-"Fürstengrab", Großbau und Schatzdepot der Frühen Bronzezeit. Erfurt und Umgebung. Archäologische Denkmale in Thüringen *3*, 194–197.

91. Penske, S., Küßner, M., Rohrlach, A.B., Knipper, C., Nováček, J., Childebayeva, A., Krause, J., and Haak, W. (2024). Kinship practices at the early bronze age site of Leubingen in Central Germany. Sci. Rep. *14*, 3871. https://doi.org/10.1038/s41598-024-54462-6.

92. Ernée, M., and Langová, M. Památky archeologické, Supplementum 21 Pohřebiště starší doby bronzové na Jantarové stezce Early Bronze Age Cemetery on the Amber Road.

93. Papac, L., Ernée, M., Dobeš, M., Langová, M., Rohrlach, A.B., Aron, F., Neumann, G.U., Spyrou, M.A., Rohland, N., Velemínský, P., et al. (2021). Dynamic changes in genomic and social structures in third millennium BCE central Europe. Sci. Adv. *7*, eabi6941. https://doi.org/10.1126/sciadv.abi6941.

94. Abadie, I. (2021). L'évolution des pratiques funéraires religieuses des Parisiens. Hist. Urbaine *60*, 97–126. https://doi.org/10.3917/rhu.060.0099.

95. Demartis, G.M. (1998). Tomba v di Montalè (Betagamma: Necropoli di Su Crucifissu Mannu (Ss)).

96. Marcus, J.H., Posth, C., Ringbauer, H., Lai, L., Skeates, R., Sidore, C., Beckett, J., Furtwängler, A., Olivieri, A., Chiang, C., et al. (2019). Population history from the Neolithic to present on the Mediterranean island of Sardinia: An ancient DNA perspective. Preprint at BioRxiv. https://doi.org/10.1101/583104.

97. Olcina Doménech, M., Tendero Porras, E., and Guilabert Mas, A. (2008). La maqbara del Tossal de Manises (Alicante). Lucentum *27*, 213–227. https://doi.org/10.14198/LVCENTVM2008.27.17.

98. Tagliacozzo, A. (1995). Archeozoologia della Grotta dell'Uzzo, Sicilia. Da un'Economia di Caccia ad un'Economia di Pesca Ed Allevavamento. Arheologia Moldovei *18*. https://doi.org/10.11588/amold.1995.1.91246.

99. Conte, L., and Tusa, S. (2012). Approfondimento stratigrafico alla Grotta dell'Uzzo. In Istituto Italiano di Preistoria e Protostoria, pp. 437–445.

100. Mannino, M.A., Talamo, S., Tagliacozzo, A., Fiore, I., Nehlich, O., Piperno, M., Tusa, S., Collina, C., Di Salvo, R., Schimmenti, V., et al. (2015). Climate-driven environmental changes around 8,200 years ago favoured increases in cetacean strandings and Mediterranean hunter-gatherers exploited them. Sci. Rep. *5*, 16288. https://doi.org/10.1038/srep16288.

101. Yu, H., van de Loosdrecht, M.S., Mannino, M.A., Talamo, S., Rohrlach, A.B., Childebayeva, A., Villalba-Mouco, V., Aron, F., Brandt, G., Burri, M., et al. (2022). Genomic and dietary discontinuities during the Mesolithic and Neolithic in Sicily. iScience *25*, 104244. https://doi.org/10.1016/j.isci.2022.104244.

102. Gogaltan, F. (2015). Bronze Age Chronology in the Carpathian Basin. In Proceedings of the International Colloquium from Târgu Mureş, 2–4 October 2014, E.,R. Németh, and B. Rezi, eds. (Mega Publishing House), pp. 53–95.

103. Baimukhanov, N., and Besetayev, B. (2021). Weapons and horse equipment of the medieval nomads of the East Kazakhstan (Based on materials from the Ayan burial ground). Ulken Altai Elem – The World of the Great Altai – World of Great. Altay *6* (2), 2020.

104. Samashev, Z. (2011). Berel (Taimas Publishing House). http://kronk.spb.ru/library/samashev-zs-2011.htm.

105. Samashev, Z., Kariyev, E.M., and Erbolatov, C.E. (2019). Hun-Syanbian cultural and chronological horizon of Berel. In Materials of the International Archaeological Conferences, L.N. Gumilyov Eurasian National University, 2019, pp. 385–394.

106. Musralina, L.Z., Altynova, N.K., Khussainova, E.M., Zhaniyazov, Z.A., Nurzhibek, K., Samashev, Z.S., Bekmanov, B.O., and Djansugirova, L.B. (2021). Paleogenetic analysis of ancient pathogenic microorganisms from human bone remains found in the Berel region. J. Problem Evol. Open Syst. *23*. https://peos.kaznu.kz/index.php/peos/en/article/view/301/267.

107. Kocher, A., Papac, L., Barquera, R., Key, F.M., Spyrou, M.A., Hübler, R., Rohrlach, A.B., A.B., Aron, F., Stahl, R., Wissgott, A., et al. (2021). Ten millennia of hepatitis B virus evolution. Science *374*, 182–188. https://doi.org/10.1126/science.abi5658.

108. Gnecchi-Ruscone, G.A., Khussainova, E., Kahbatkyzy, N., Musralina, L., Spyrou, M.A., Bianco, R.A., Radzeviciute, R., Martins, N.F.G., Freund, C., Iksan, O., et al. (2021). Ancient genomic time transect from the Central Asian Steppe unravels the history of the Scythians. Sci. Adv. *7*, eabe4414. https://doi.org/10.1126/sciadv.abe4414.

109. Spyrou, M.A., Tukhbatova, R.I., Feldman, M., Drath, J., Kacki, S., Beltrán de Heredia, J., Arnold, S., Sitdikov, A.G., Castex, D., Wahl, J., et al. (2016). Historical Y. pestis Genomes Reveal the European Black Death as the Source of Ancient and Modern Plague Pandemics. Cell Host Microbe *19*, 874–881. https://doi.org/10.1016/j.chom.2016.05.012.

110. Human Skeletal Remains from the Imdang Site in Gyeongsan, Housed in the Yeungnam University Museum.

111. Kim, D. (2015). A study on The characteristics of buried person and The culture of sacrificial burial of Ancient tombs in Im-dang. Soc. Stud. Early Kor. His. *20*, 145–181. https://doi.org/10.35160/sjekh.2015.08.20.147.

112. Gyeongsan Imdang Burial Mounds IV – Joyeong CI and II Tombs.

113. Knipper, C., Reinhold, S., Gresky, J., Berezina, N., Gerling, C., Pichler, S.L., Buzhilova, A.P., Kantorovich, A.R., Maslov, V.E., Petrenko, V.G., et al. (2020). Diet and subsistence in Bronze Age pastoral communities from the southern Russian steppes and the North Caucasus. PLOS One *15*, e0239861. https://doi.org/10.1371/journal.pone.0239861.

114. Wang, C.-C., Reinhold, S., Kalmykov, A., Wissgott, A., Brandt, G., Jeong, C., Cheronet, O., Ferry, M., Harney, E., Keating, D., et al. (2019). Ancient human genome-wide data from a 3000-year interval in the Caucasus corresponds with eco-geographic regions. Nat. Commun. *10*, 590. https://doi.org/10.1038/s41467-018-08220-8.

115. Peltola, S., Majander, K., Makarov, N., Dobrovolskaya, M., Nordqvist, K., Salmela, E., and Onkamo, P. (2023). Genetic admixture and language shift in the medieval Volga-Oka interfluve. Curr. Biol. *33*, 174–182.e10. https://doi.org/10.1016/j.cub.2022.11.036.

116. Beisenov, A.Z. (2016). Monuments of the early stage of the Tasmola culture. History *1*, 119–126. https://doi.org/10.17223/19988613/39/17.

117. Beisenov A.Z. (2018) Tasmola Culture of Central Kazakhstan in Studies of the Beginning of the XXI Century.Archaeology and Early History of Ukraine. 27. 10.37445/adiu.2018.02.28.

118. Beisenov A.Z. (2015) Sak culture of Saryarka in the context of the study of ethnic and sociocultural processes of Steppe Eurasia. The collection of scientific articles, dedicated to the memory archaeologist Kemal Akishev. ISBN 978-601-7312-03-9.

119. Alarcón Tinajero, E., Hadden, C.S., and Cherkinsky, A. (2024). Comparing Bioapatite and Collagen Radiocarbon Dates from a 16th century Cemetery Context — El Japón, Xochimilco, Mexico City. Radiocarbon *66*, 1481–1492. https://doi.org/10.1017/RDC.2023.60.

120. Zamora, A., Menéndez Garmendia, A., Ruiz-Velazco, F., Sánchez-Mejorada, G., Márquez-Morfín, L., and Gómez-Valdés, J.A. (2022). Sex estimation using humeral and femoral head diameters in contemporary and prehispanic mexican populations. Rev. Argent. Antropol. Biol. *24*, 044. https://doi.org/10.24215/18536387e044.

121. Bullock, M., Márquez, L., Hernández, P., and Ruíz, F. (2013). Paleodemographic age-at-death distributions of two Mexican skeletal collections: A comparison of transition analysis and traditional aging methods. Am. J. Phys. Anthropol. *152*, 67–78. https://doi.org/10.1002/ajpa.22329.

122. González, C.J. (1996). Investigaciones arqueológicas en "El Japón": sitio chinampero en Xochimilco. Arqueología *16*, 81–93.

123. Hernández Espinoza, P.O. (2006). Entre flores y chinampas: La salud de los antiguos habitantes de Xochimilco. In Sociedad y Salud en el México Prehispánico y Colonial, L, M. Morfín, and P. Hernández Espinoza, eds. (CONACULTA-INAH/Promep), pp. 327–366.

124. Lechuga, M.G. (1977). Análisis de un Elemento de la Estructura Económica Azteca: la Chinampa (Mexico, DF: UAM Azcapotzalco).

125. Hernández Espinoza, P.O. (2006). La Regulación del Crecimiento de la Población en el México Prehispánico (Instituto Nacional de Antropología e Historia (INAH)).

126. Dabney, J., Meyer, M., and Pääbo, S. (2013). Ancient DNA Damage. Cold Spring Harb.. Perspect. Biol. *5*, a012567. https://doi.org/10.1101/cshperspect.a012567.

127. Aron, F., U Neumann, G., and Brandt, G. (2020). Half-UDG treated double-stranded ancient DNA library preparation for Illumina sequencing v1. protocols.io. https://doi.org/10.17504/protocols.io.bmh6k39e.

128. Aron, F., U Neumann, G., and Brandt, G. Non-UDG treated double-stranded ancient DNA library preparation for Illumina sequencing v1. https://doi.org/10.17504/protocols.io.bakricv6.

129. Gansauge, M.-T., Aximu-Petri, A., Nagel, S., and Meyer, M. (2020). Manual and automated preparation of single-stranded DNA libraries for the sequencing of DNA from ancient biological remains and other sources of highly degraded DNA. Nat. Protoc. *15*, 2279–2300. https://doi.org/10.1038/s41596-020-0338-0.

130. Gansauge, M.-T., Gerber, T., Glocke, I., Korlević, P., Lippik, L., Nagel, S., Riehl, L.M., Schmidt, A., and Meyer, M. (2017). Single-stranded DNA library preparation from highly degraded DNA using *T4* DNA ligase. Nucleic Acids Res. *45*, e79. https://doi.org/10.1093/nar/gkx033.

131. Fu, Q., Meyer, M., Gao, X., Stenzel, U., Burbano, H.A., Kelso, J., and Pääbo, S. (2013). DNA analysis of an early modern human from Tianyuan Cave, China. Proc. Natl. Acad. Sci. USA *110*, 2223–2227. https://doi.org/10.1073/pnas.1221359110.

132. Nickel, B., Patova, A., and Meyer, M. (2024). SPRI beads, variable PEG concentration v1. protocols.io. https://doi.org/10.17504/protocols.io.rm7vzj5n4lx1/v1.

133. Aron, F., and Brandt, G. (2020). Library Adapter Preparation for Dual-Index Double Stranded DNA Illumina Sequencing v1. Protocols.io. https://doi.org/10.17504/protocols.io.bem5jc86.

134. Martin, D., and Rybicki, E. (2000). RDP: detection of recombination amongst aligned sequences. Bioinformatics *16*, 562–563. https://doi.org/10.1093/bioinformatics/16.6.562.

135. Padidam, M., Sawyer, S., and Fauquet, C.M. (1999). Possible Emergence of New Geminiviruses by Frequent Recombination. Virology *265*, 218–225. https://doi.org/10.1006/viro.1999.0056.

136. Martin, D.P., Posada, D., Crandall, K.A., and Williamson, C. (2005). A modified bootscan algorithm for automated identification of recombinant sequences and recombination Bbreakpoints. AIDS Res Hum Retroviruses *21*, 98–102. https://doi.org/10.1089/aid.2005.21.98.

137. Smith, J.M. (1992). Analyzing the Mosaic Structure of Genes. J. Mol. Evol. *34*, 126–129. https://doi.org/10.1007/BF00182389.

138. Posada, D., and Crandall, K.A. (2001). Evaluation of methods for detecting recombination from DNA sequences: Computer simulations. Proc. Natl. Acad. Sci. USA *98*, 13757–13762. https://doi.org/10.1073/pnas.241370698.

139. Gibbs, M.J., Armstrong, J.S., and Gibbs, A.J. (2000). Sister-Scanning: a Monte Carlo procedure for assessing signals in recombinant sequences. Bioinformatics *16*, 573–582. https://doi.org/10.1093/bioinformatics/16.7.573.

140. Boni, M.F., Posada, D., and Feldman, M.W. (2007). An Exact Nonparametric Method for Inferring Mosaic Structure in Sequence Triplets. Genetics *176*, 1035–1047. https://doi.org/10.1534/genetics.106.068874.

141. Rambaut, A., Lam, T.T., Max Carvalho, L., and Pybus, O.G. (2016). Exploring the temporal structure of heterochronous sequences using TempEst (formerly Path-O-Gen). Virus Evol. *2*, vew007. https://doi.org/10.1093/ve/vew007.

142. Bouckaert, R., Vaughan, T.G., Barido-Sottani, J., Duchêne, S., Fourment, M., Gavryushkina, A., Heled, J., Jones, G., Kühnert, D., De Maio, N., et al. (2019). BEAST 2.5: An advanced software platform for Bayesian evolutionary analysis. PLOS Comput. Biol. *15*, e1006650. https://doi.org/10.1371/journal.pcbi.1006650.

143. Lartillot, N., and Philippe, H. (2006). Computing Bayes factors using thermodynamic integration. Syst. Biol. *55*, 195–207. https://doi.org/10.1080/10635150500433722.

144. Fan, Y., Wu, R., Chen, M.-H., Kuo, L., and Lewis, P.O. (2011). Choosing among partition models in Bayesian phylogenetics. Mol. Biol. Evol. *28*, 523–532. https://doi.org/10.1093/molbev/msq224.

145. Skilling, J. (2006). Nested sampling for general Bayesian computation. Bayesian Anal. *1*, 833–860. https://doi.org/10.1214/06-BA127.

146. Russel, P.M., Brewer, B.J., Klaere, S., and Bouckaert, R.R. (2019). Model selection and parameter inference in phylogenetics using Nested Sampling. Syst. Biol. *68*, 219–233. https://doi.org/10.1093/sysbio/syy050.

147. Xie, W., Lewis, P.O., Fan, Y., Kuo, L., and Chen, M.-H. (2011). Improving marginal likelihood estimation for Bayesian phylogenetic model selection. Syst. Biol. *60*, 150–160. https://doi.org/10.1093/sysbio/syq085.

148. Drummond, A.J., Ho, S.Y.W., Phillips, M.J., and Rambaut, A. (2006). Relaxed phylogenetics and dating with confidence. PLoS Biol. *4*, e88. https://doi.org/10.1371/journal.pbio.0040088.

149. Bouckaert, R.R., and Drummond, A.J. (2017). bModelTest: Bayesian phylogenetic site model averaging and model comparison. BMC Evol. Biol. *17*, 42. https://doi.org/10.1186/s12862-017-0890-6.

150. Drummond, A.J., Rambaut, A., Shapiro, B., and Pybus, O.G. (2005). Bayesian coalescent inference of past population dynamics from molecular sequences. Mol. Biol. Evol. *22*, 1185–1192. https://doi.org/10.1093/molbev/msi103.

STAR★METHODS

KEY RESOURCES TABLE

REAGENT or RESOURCE	SOURCE	IDENTIFIER
Biological samples		
ancient human Pars petrosa	Consell Insular de Menorca	IndID: ABF006
ancient human tooth 27	Landesamt für Denkmalpflege Baden-Württemberg	IndID: APG002
ancient human tooth 85	Landesamt für Denkmalpflege Baden-Württemberg	IndID: APG003
ancient human Tooth unspecified	Institute of Archaeology, Zagreb, Croatia	IndID: BEMA002
ancient human Tooth unspecified	Kunstkameramuseum St.Petersburg	IndID: BOO005
ancient human Pars petrosa	Regional Museum of Local History, State Historical and Cultural Museum-Reserve	IndID: BRE013
ancient human Tooth unspecified	Institute of archaeology by A. Kh. Margulan, Almaty, Kazakhstan	IndID: BRE026
ancient human Permanent molar	Institute of Archaeology, Tatarstan, Russia	IndID: BRT009
ancient human Tooth unspecified	Peter the Great Museum of Anthropology and Ethnography (Kunstkamera), RAS. Saint-Petersburg, Russia	IndID: CHV002
ancient human Pars petrosa	Museu de Menorca	IndID: CRO001
ancient human Pars petrosa	State Agency for Cultural Heritage of Lower Saxony	IndID: GFW005
ancient human Permanent molar	Museo Arqueologico regional Alcala de Henares	IndID: GOZ002
ancient human Pars petrosa	University of Central Lancashire	IndID: HAD011
ancient human Pars petrosa	University of Central Lancashire	IndID: HAD015
ancient human Permanent molar	Ephorate of Paleoanthropology, Speleolog	IndID: HGC015
ancient human Pars petrosa	Museum of Yeungnam University	IndID: JOY005
ancient human Pars petrosa	Deutsches Archäologisches Institut	IndID: KBD002
ancient human Permanent molar	Nikolaj Makarov	IndID: KED002
ancient human Rib	Durham University	IndID: KER001
ancient human Permanent molar	National University of Mongolia	IndID: KHI001
ancient human Permanent incisor	Deutsches Archäologisches Institut	IndID: KVO007
ancient human Tooth unspecified	UC Merced	IndID: KYA003
ancient human Tooth unspecified	UC Merced	IndID: KYA008
ancient human Pars petrosa	Landesamt für Denkmalpflege und Archäologie Freistaat Thüringen	IndID: LEU027
ancient human Tooth unspecified	Mark Aldenderfer	IndID: MEB011
ancient human Pars petrosa	National Museum Prague	IndID: MIB022
ancient human Pars petrosa	National Museum Prague	IndID: MIB039
ancient human Tooth unspecified	UCSC Paleogenomics, Department of Anthropology, University of California, Santa Cruz, 95064, CA, USA	IndID: MP2004
ancient human Tooth unspecified	UCSC Paleogenomics, Department of Anthropology, University of California, Santa Cruz, 95064, CA, USA	IndID: MP2005
ancient human Tooth unspecified	UCSC Paleogenomics, Department of Anthropology, University of California, Santa Cruz, 95064, CA, USA	IndID: MP2008

(*Continued on next page*)

Continued

REAGENT or RESOURCE	SOURCE	IDENTIFIER
ancient human Tooth unspecified	UCSC Paleogenomics, Department of Anthropology, University of California, Santa Cruz, 95064, CA, USA	IndID: MP2019
ancient human Tooth unspecified	UCSC Paleogenomics, Department of Anthropology, University of California, Santa Cruz, 95064, CA, USA	IndID: MP2033
ancient human Pars petrosa	Universität Bern	IndID: NDR002
ancient human tooth 26	University of Central Lancashire	IndID: OAI017
ancient human tooth 33	Department of Environmental Sciences	IndID: PRS018
ancient human Permanent premolar	Escuela Nacional de Antropología e Historia, Instituto Nacional de Antropología e Historia, México	IndID: SGA024
ancient human Permanent molar	Escuela Nacional de Antropología e Historia, Instituto Nacional de Antropología e Historia, México	IndID: SJN003
ancient human tooth 47	Escuela Nacional de Antropología e Historia, Instituto Nacional de Antropología e Historia, México	IndID: SJN011
ancient human tooth 47	Escuela Nacional de Antropología e Historia, Instituto Nacional de Antropología e Historia, México	IndID: SJN013
ancient human tooth 47	Escuela Nacional de Antropología e Historia, Instituto Nacional de Antropología e Historia, México	IndID: SJN025
ancient human Deciduous molar	Institute of archaeology by A. Kh. Margulan, Almaty, Kazakhstan	IndID: SRK002
ancient human Tooth unspecified	City of Mechelen	IndID: STR072
ancient human Tooth unspecified	City of Mechelen	IndID: STR140
ancient human Pars petrosa	Mansarda ex Genio civile, Porto Torres	IndID: SUC009
ancient human Permanent premolar	Museo Arqueológico de Alicante (MARQ)	IndID: TOS002
ancient human Permanent molar	National University of Mongolia	IndID: TSA002
ancient human tooth 27	National University of Mongolia	IndID: ULI002
ancient human Permanent molar	Institute of Archaeology, Tatarstan, Russia	IndID: UST154
ancient human Permanent molar	MPI for Evolutionary Anthropology	IndID: UZZ040
ancient human Indeterminate Molar	Tandy Institute for Archaeology, Ft. Worth, T	IndID: USHA006
ancient human Permanent Premolar	Tandy Institute for Archaeology, Ft. Worth, T	IndID: USHA008
ancient human Tooth unspecified	Mureş County Museum, Târgu Mureş, Romania.	IndID: VOI007
ancient human Pars petrosa	Fiji Museum	IndID: YNK001
Chemicals, peptides, and recombinant proteins		
Weighing tray	Roth	Cat# 2159.2
Buffer PE	Qiagen	Cat# 19065
Buffer PB	Qiagen	Cat# 19066
MinElute PCR Purification Kit	Qiagen	Cat# 28006
QIAquick Nucleotide Removal Kit	Qiagen	Cat# 28304
20% SDS Solution	Serva	Cat# 39575.01
Dynabeads MyOne Streptavidin C1	Life Technologies	Cat# 65002
Dynabeads MyOne Streptavidin T1	Life Technologies	Cat# 65601
Weighing paper	Macherey-Nagel	Cat# 186002
15 ml Falcon Tube	Greiner Bio-one	Cat# 188271

(*Continued on next page*)

Continued

REAGENT or RESOURCE	SOURCE	IDENTIFIER
50 ml Falcon Tube, skirted	Greiner Bio-one	Cat# 210261
96 Nunc deep well	VWR	Cat# 260251
Strip caps	Agilent Technologie	Cat# 401425
Optical tube strips	Agilent Technologie	Cat# 401428
Adhesive clear qPCR seal sheets	Biozym	Cat# 600238
Pfu Turbo Cx Hotstart DNA Polymerase	Agilent Technologie	Cat# 600412
Herculase II Fusion DNA Polymerase	Agilent Technologie	Cat# 600679
Pipettes 10ml	Greiner Bio-one	Cat# 607160
Tips 100µl	Greiner Bio-one	Cat# 737261
Tips 300µl	Greiner Bio-one	Cat# 738261
Parafilm	Biozym	Cat# 743311
Tips 1250µl	Greiner Bio-one	Cat# 750261
Pipettes 25ml	Greiner Bio-one	Cat# 760160
Pipettes 50ml	Greiner Bio-one	Cat# 768160
Tips 10µl	Greiner Bio-one	Cat# 771261
2x TBE-Urea Sample Buffer	BioRad	Cat# 1610768
Saw blade	Zeus	Cat# 1744894
Paper wipes	Igefa	Cat# 2117602
96 deep well PP Sqr well	Thermo Scientific	Cat# 3154740
10% Criterion™ TBE-Urea Polyacrylamide Gel, 18 well, 30 µl	BioRad	Cat# 3450089
10x GeneAmp PCR Gold Buffer	Life Technologies	Cat# 4379874
Sodiumhydroxide Pellets	Fisher Scientific	Cat# 10306200
AccuPrime Pfx Pfu Polymerase	Thermo Scientific	Cat# 12344024
Human Cot-1 DNA	Life Technologies	Cat# 15279011
1M Tris-HCl, pH 8.0	Life Technologies	Cat# 15568025
UltraPure™ TBE Buffer, 10X	Life Technologies	Cat# 15581044
UltraPure™ Salmon Sperm DNA Solution	Life Technologies	Cat# 15632011
Tips 10µl Eppendorf	Eppendorf	Cat# 30073746
Tips 5000µl	Eppendorf	Cat# 30077580
Dualfilter epTIPS G 0.1–20ul, PCR Clean, Sterile, 384 tips	Eppendorf	Cat# 30078403
Combitip Adv Biop 1.0mL	Eppendorf	Cat# 30089642
Combitip Adv Biop 5.0mL	Eppendorf	Cat# 30089669
Combitips® advanced Biopur®	Eppendorf	Cat# 30089677
Combitip Adv Biop 10.0mL	Eppendorf	Cat# 30089677
1.5 ml LoBind	Eppendorf	Cat# 30108051
2 ml LoBind	Eppendorf	Cat# 30108078
5 ml LoBind	Eppendorf	Cat# 30119460
5 ml Biopur	Eppendorf	Cat# 30119479
1.5 ml Biopur	Eppendorf	Cat# 30121589
2 ml Biopur	Eppendorf	Cat# 30121597
0.2 ml PCR strips	Eppendorf	Cat# 30124839
Cap Strips	Eppendorf	Cat# 30124839
twin.tec PCR Plate 96	Eppendorf	Cat# 30128575
Ethanol	Merck	Cat# 1009832511
Isopropanol	Merck	Cat# 1070222511
LightCycler 480 Multiwell Plate 384, white – 5 x 10 plates	Roche	Cat# 4729749001

(*Continued on next page*)

Continued

REAGENT or RESOURCE	SOURCE	IDENTIFIER
LightCycler 480 Sealing Foil – 50 foils	Fisher Scientific	Cat# 4729757001
High Pure Viral Nucleic Acid Large Volume Kit	Roche	Cat# 5114403001
Sera-Mag Speed CM	GE Healthcare Lifesc	Cat# 65152100000000
dsLibrary Adapter	homemade	See capture design
qPCR-Standard	homemade	See capture design
TL181	IDT	N/A
TL159	IDT	N/A
CL53	IDT	N/A
TL178	IDT	N/A
CL128	IDT	N/A
60N	Sigma-Aldrich	N/A
SPRI Beads	homemade	See capture design
Probes	homemade	See capture design
BO4.P7.part1.R (500µM)	Sigma-Aldrich	N/A
BO6.P7.part2.R (500µM)	Sigma-Aldrich	N/A
BO8.P5.part1.R (500µM)	Sigma-Aldrich	N/A
BO10.P5.part2.R (500µM)	Sigma-Aldrich	N/A
Overall Tyvek Classic Xpert	VWR	Cat# 113-6061
Bravo tips	Agilent Technologie	Cat# 19477-022
Water Chromasolv Plus	Sigma-Aldrich	Cat# 34877-2.5L
FrameStar® 480 PCR plate 96, semi-skirted	4titude	Cat# 4ti-0951
D1000 ScreenTapes	Agilent Technologie	Cat# 5067-5582
D1000 Reagents	Agilent Technologie	Cat# 5067-5583
HS D1000 ScreenTapes	Agilent Technologie	Cat# 5067-5584
HS D1000 Reagents	Agilent Technologie	Cat# 5067-5585
Oligo Length Standards 20/100 Ladder	IDT	Cat# 51-05-15-02
Oligo aCGH/Chip-on-Chip Hybridization Kit	Agilent Technologie	Cat# 5188-5220
Combitips 0,2ml	Eppendorf	Cat# 613-2077
Combitips 0,5ml	Eppendorf	Cat# 613-2078
Combitips 5ml	Eppendorf	Cat# 613-2081
96 Matrix open reservoir	Thermo Scientific	Cat# 613-2099
1.0 mL External Thread Jacket Tube with 2D Code on tube base & linear barcode on side	Brooks	Cat# 66-51020
Silica Magnetic Beads	G-Bioscience	Cat# 786-915
Diamond saw blade	NTI Kahla	Cat# 806 104 358 514 220
1x Tris-EDTA pH 8.0	AppliChem	Cat# A8569, Cat# 0500
Aluminium foil	Roth	Cat# AA76.1
0.5 M EDTA pH 8.0	Life Technologies	Cat# AM9261
20x SCC Buffer	Life Technologies	Cat# AM9770
T4 RNA ligation Buffer	NEB	Cat# B0216L
NEBuffer 2 10x	NEB	Cat# B7002 S
BSA 20mg/ml	NEB	Cat# B9000 S
Buffer Tango	Life Technologies	Cat# BY5
Polyethyleneglycol 8000 50%	Jena Bioscience	Cat# CSS-256
Denhardt's solution	Sigma-Aldrich	Cat# D9905-5Ml
FastAP Thermosensitive Alkaline Phosphatase	Thermo Scientific	Cat# EF0652
T4 DNA-Ligase	Thermo Scientific	Cat# EL0013

(*Continued on next page*)

Continued

REAGENT or RESOURCE	SOURCE	IDENTIFIER
Klenow fragment	Thermo Scientific	Cat# EP0052
DyNAmo Flash SYBR Green qPCR Kit	Life Technologies	Cat# F-415L
Guanidine hydrochloride	Sigma-Aldrich	Cat# G3272-500G
Drill bit	NTI Kahla	Cat# H1-016-HP
Reservoir	Roth	Cat# HT65.1
DanKlorix	VWR	Cat# KAMM2113534
Sekuroka®-Ärmelschoner Standard	Roth	Cat# KP24.1
Hairnet	Roth	Cat# L092.1
T4 Polynucleotide Kinase	NEB	Cat# M0201 L
T4 DNA Polymerase	NEB	Cat# M0203 L
Bst 2.0 DNA Polymerase	NEB	Cat# M0537 S
Quick Ligation Kit	NEB	Cat# M2200 L
User Enzyme	NEB	Cat# M5505 L
ATP	NEB	Cat# P0756 S
Proteinase K	Sigma-Aldrich	Cat# P2308-100MG
Sample bags	Roth	Cat# P281.2
Tween 20	Sigma-Aldrich	Cat# P9416-50ML
ATP 100 mM	Thermo Scientific	Cat# R0441
dNTPs 25 mM	Thermo Scientific	Cat# R1121
SYBR® Gold Nucleic Acid Gel Stain (10,000X Concentrate in DMSO)	Life Technologies	Cat# S11494
5 M Sodium chloride solution	Sigma-Aldrich	Cat# S5150-1L
3M Sodium Acetate pH 5,2	Sigma-Aldrich	Cat# S7899-500ML
StarGuard Touch Nitril	StarLab	Cat# SG-P-S, Cat# SG-P-M, Cat# SG-P-L
StarGuard Touch Latex	StarLab	Cat# SG-T-S, Cat# SG-T-M, Cat# SG-T-L
Tips 200µl Liquidator	Steinbrenner	Cat# SL-LT-LSR200
Face mask Visma® ear-loop	Roth	Cat# X458.1
DNA-Away	Roth	Cat# X996.2
Critical commercial assays		
MinElute PCR Purification Kit	QIAGEN	Cat# 28006
QIAquick PCR Purification Kit	QIAGEN	Cat# 28104
Qubit dsDNA HS Assay Kit, 500 assays	Thermo Fisher Scientific	Cat# Q32854
High Pure Extender Assembly from the Roche High Pure Viral Nucleic Acid Large Volume Kit,40 reactions	Roche	Cat# 5114403001
QIAquick Nucleotide Removal Kit	Quiagen	Cat# 28304
MiSeq Reagent Kit v3 (150 cycle)	Illumina	Cat# MS-102-3001
NextSeq 500/550 High Output Kit v2.5	Illumina	Cat# 20024906
Deposited data		
Genomes of 53 ancient Parvoviruses	This study	10.6084/m9.figshare.30786167
Sequencing dataset from the newly reported individuals	This study	ENA: PRJEB123221
Software and algorithms		
nf-core/eager	version 2.4.7	https://nf-co.re/eager/2.5.3/parameters
MultiVCFAnalyzer	version 0.85.2	https://github.com/alexherbig/multivcfanalyzer
Mafft	version 7.467	https://mafft.cbrc.jp/alignment/server/index.html
RDP5	Beta 5.84	https://web.cbio.uct.ac.za/~darren/rdp.html

(*Continued on next page*)

Continued

REAGENT or RESOURCE	SOURCE	IDENTIFIER
RAxML	version 8.2.12	https://cme.h-its.org/exelixis/web/software/raxml/
TempEST	version 1.5.3	https://tree.bio.ed.ac.uk/software/tempest/
BEAST2	version 2.7.7	https://www.beast2.org/
LogCombiner	version 2.7.7	https://www.beast2.org/programs/
TreeAnnotator	version 1.6.2	https://www.beast2.org/treeannotator/
MALT	version 0.6.1	https://software-ab.cs.uni-tuebingen.de/download/malt/welcome.html
HOPS	version 0.2	https://github.com/rhuebler/HOPS
AdapterRemoval	version 2.3.2	https://github.com/MikkelSchubert/adapterremoval
bwaaln	version 0.7.17	https://mybiosoftware.com/bwa-burrows-wheeler-aligner-short-long-reads.html
samtools	version 1.12	https://www.htslib.org/
GATK unified Genotyper	version 3.5	https://gatk.broadinstitute.org/hc/en-us/community/posts/34026498169243-GATK-UnifiedGenotyper
Qualimap	version 1.14	http://qualimap.conesalab.org/

EXPERIMENTAL MODEL AND STUDY PARTICIPANT DETAILS

Sampled ancient individuals

All ancient individuals featured within this study originate from diverse archeological excavations. Each individuals remains have been sampled with approval from the custodians and the relevant local Ministries/Museums/Institutions. The sampling was performed following both local and international guidelines including restriction placed on individual samples. All demographic information as well as the information on the relevant permits are available below and ordered by continent of origin. Each site entry contains the three-letter site code, the relevant site information, information on the individuals remains containing the viral genomes and the permits associated with the site and the sample. When applicable previous publications on the site and or the human library are cited.

African archeological sites

NDR

Andrangana, Madagascar; 15th century, radiocarbon 1448–1614 cal CE.

The necropolis in Andrangana (northeastern Madagascar) was discovered during research on chloritoschistes and metallurgy at a quarry nearby and was thought to belong to the Rasikajy civilization.[67] Human remains from this civilization had so far only been found in Vohemar, approx. 50 km away. Three graves of the Andrangana necropolis were excavated in an exploratory campaign in 2019 to determine the cultural affiliation and the dating as well as the state of preservation of the human remains. The anthropological subproject was conducted under the direction of the Department of Physical Anthropology (University of Bern) and was carried out by Dr. Christine Cooper. The preservation of the undisturbed human burials was generally good, except for root damage in some parts, and it was sufficient for a comprehensive osteological analysis, which took place on site by means of conventional morphological methods.[68–72] The human remains belonged to two adult males and a 23-year-old child. Burial positions of all skeletons indicated that the bodies were wrapped in a shroud and buried directly in the sand without a coffin or any other container. The male from grave 350 was buried on his right side facing north with the head in the east and the feet in the west. The individuals from graves 356 (infant) and 863 were placed on their back and also with the head in the east and the feet in the west. Two sets of samples (pars petrosa and one intact tooth per set) were taken from each individual for radiocarbon dating, analysis of stable light isotopes and paleogenetic investigations before their reburial and the restoration of the graves' original appearance. The extracted collagen that we used for stable isotope ratios as well as radiocarbon dating had good quality. Calibrated radiocarbon dates revealed that all three burials date to the 15th century CE. While the three individuals from Andrangana may not be representative of the entire population buried there, their cranial and postcranial traits are suggestive of sub-Saharan African ancestry.

NDR002 – The infant was aged 2–3 years at death and exhibited pathological alterations in several bones. There was porous new bone formation in both orbits. The endocranial aspects of both parietals exhibited patches of pronounced vascularization. Active new bone formation was observed in the distal third of the right ulna as well as the proximal medial portion of the left tibia. Individually, these changes may be caused by scurvy, anemia, infection or trauma. This infant yielded a Parvovirus B19V genome belonging to Genotype 3. It is the oldest African parvovirus infection known, and it is evidence of ancient Parvovirus infecting children. The infant

was ^{14}C dated to 1448–1614 cal CE. The midpoint was chosen, and the sample age for phylogenetic dating and was set to 400 years BP.

An excavation survey of the necropolis at Andrangana was conducted in 2019 under official authorization (no. 218/2017/MCPASP) issued by the Ministry of Culture and Heritage of Madagascar. From the outset, the project was designed as a collaborative initiative involving Malagasy scholars (co-authors of the present paper) and the local community of Andrangana. Prior to the excavation, the aims, methods and potential outcomes of the research were discussed with community representatives. The excavation of the human remains was undertaken with the knowledge, consent and ceremonial blessing of the village community, in accordance with local customs and expectations. Continuous dialogue was maintained throughout the fieldwork to ensure transparency and mutual understanding. Permission to export selected skeletal samples for bioarcheological analyses abroad was granted by both the relevant authorities and the local community. All sampling procedures were kept to the minimum necessary to address the research questions. Following the completion of the analyses, the human remains were respectfully reburied in consultation with the community.

European archeological sites

ABF

Ciutadella de Menorca, s'Albufera, Menorca, Spain; 300 BCE–700 CE, radiocarbon most individuals 300–200 cal BCE.

The site was excavated in 2013 and 2014 by Elena Sintes. This complex funerary site is located in the modern city of Ciutadella, to the north of the bay (over 1 km long x only 15–100 m wide), which served as a natural harbor at least since the late Iron Age. Ciutadella was one of the three Roman cities of Menorca, and it continued to be an important political and religious centre throughout the Middle Ages. Two different burial areas were identified, one presenting rock-cut tombs, and another with single graves. Both partially preserved rock-cut tombs (hypogea) consisted of a chamber, where most of the human remains and grave goods had originally been deposited, and an entrance court that could be accessed from the outside by a rock-cut stair. The post-Talayotic deposit included both cremated and inhumated remains, as well as abundant pottery. However, next to the base of the broken central column of the burial chamber and covering the prehistoric deposit, two later burials were found. The human remains of AR-2 (ABF002) were found in a highly altered state, but individual AR-1 (ABF001) was undoubtedly on its right side. Absolute dating of both adults, likely male, confirmed their Early Medieval date. In the same field, a few meters southwest, two single tombs were discovered in pits, roughly cut in the limestone bedrock. One of them contained a well-preserved skeleton of an adult woman (ABF020). The coin from the time of Augustus dates the burial around or shortly after 9–14 CE. A charcoal fragment obtained from one of the cremated remains (ABF015/CIU-03-22-OC5) provided a date around 400–200 cal BCE, confirming the post-Talayotic identification of the hypogea (RICH-22036/C5_I1: 2273±32 BP).

ABF006 - We recovered Parvovirus B19V DNA from the Pars petrosa of this 2-year-old, genetically female individual. The virus we isolated belonged to Genotype 3. The individual is ^{14}C dated to 360–175 BCE, the median value, 2217 was used as the individual age for phylogenetic dating. It is associated with the post-Talayotic period.

Three samples from Spain—ABF006 (Ciutadella de Menorca, s'Albufera, Menorca), CRO001 (Costa de Ronda, Menorca), and TOS002 (Tossal de Manises, Alicante)—were all exported under a framework agreement between Max Planck Institute for the Science of Human History, where the Department of Archaeogenetics of the Max Planck Institute for Evolutionary Anthropology was formerly housed, and the Universitat Autònoma de Barcelona, signed 2020-09-16 (no document number). Samples within this framework agreement are documented in specific sample lists mentioning the owning institutions, responsible collaboration partners and the obligation of returning samples after analysis. Analysis of aDNA is explicitly permitted within this framework.

BEMA

Beli Manastir, Baranja, Croatia; Late Antiquity, radiocarbon graves 200–400 CE, calibrated.

The site of AN 2 Beli Manastir/Staro selo is located on the route of the bypass of the town Beli Manastir within Osijek-Baranja County. The excavated area is 16.205 m^2, and it contained finds spanning from prehistory to the Roman period, the Middle Ages, and the early modern period. The remains of a settlement and a neighboring cemetery date to Late Antiquity. Within the settlement, a large number of rectangular semi-dugouts indicated that the settlement was family organized and occupied from the middle of the 3rd until the end of the 4th/early 5th century CE. The cemetery, located west of the settlement, held 26 graves dated to the 4th century CE. The majority of burials were rectangular inhumations, the sole exception being a cremation burial with brick architecture. The burials associated with women were distinguishable by items of costume as well as jewelry. Coins and votive deposits (ceramic and glass vessels) were found in the graves of both sexes and confirmed the dating of the cemetery.

BEMA002 - The indeterminate molar yields a parvovirus B19 genome belonging to GT-2. The rectangular burial pit (Grave 24) contained a skeleton oriented east-west with slightly crossed arms, which were placed on the pelvis, and the legs were crossed. The very poorly preserved bones indicated a total skeleton length of 1.48 m. No recorded finds in the grave.

BEMA009 - The indeterminate molar yields a parvovirus B19 genome belonging to GT-2. The rectangular burial pit (Grave 11) contained a skeleton oriented east-west with the cranium missing. The rest of the skeleton is completely preserved, excluding small bones of both hands and feet. The skeleton has arms slightly outstretched while on its back. The length of the preserved skeleton is 1.32 m, and it is accompanied by several finds such as bracelets and coins.

Excavation at this site during 2020 was conducted by Dragana Rajković, Marko Dizdar and colleagues of the Archaeological Museum of Osijek and the Institute of Archaeology in Zagreb. It was a protective archeological excavation undertaken by the Institute of Archaeology and the Archaeological Museum of Osijek. In direct communication with the directors of the Archaeological Museum

CellPress
OPEN ACCESS

of Osijek and the Institute of Archaeology in Zagreb in June 2022, they both granted their oral permission for ancient DNA (pathogen) analyses. Communication (November 2021) with a colleague from the Institute for Anhropological Research, Zagreb (Dr. Mario Novak), granted permission for human analyses.

APG

Asperg "Grafenbühl", Baden-Württemberg, Germany; 500–400 BCE, end of late Hallstatt period (Hallstatt D) and early La Tène period (no radiocarbon).

About 650 m southeast of the Celtic centre of power on the Hohenasperg, a burial mound—measuring approximately 40 m in diameter and still preserved to a height of about 2.2 m (reconstructed at approximately 4 m)—was located on a flat ridge. Due to viticulture during the 16th century and the later establishment of an orchard, the mound had already been severely disturbed. Today the area is located in the middle of the town of Asperg, and it has been almost completely built over. After the State Office for Cultural Heritage had been notified following the discovery of a skeleton and an accompanying arrowhead, Hartwig Zürn investigated the tumulus in 1964–65. During this excavation, the central grave chamber—measuring approximately 4.5 by 4.5 m—was uncovered. It had been dug about 0.8 m into the existing soil but had already been extensively looted in antiquity. In the southwestern corner of the chamber, the disarticulated skeleton of a mature male was found. The deceased's personal equipment included a gold-plated belt hook and two gold covered bronze fibulae. In addition, the remains of a sumptuous textile adorned with gold lamé were documented, scattered around the chamber. Further burial goods included the remains of a four-wheeled wagon, two lion feet of a probably bronze tripod imported from Greece, parts of two bronze cauldrons, a drinking horn, as well as fittings and inlays of amber, bone, and ivory from a seating device and other pieces of Mediterranean furniture. Particularly noteworthy are a Phoenician-Syrian ivory disc, likely part of a mirror or fan handle, and a rattle with an ivory handle.

Despite the looting, it appears that the central grave from Grafenbühl had once been the most opulent grave in the vicinity of the Hohenasperg. New DNA analyses of selected Celtic elite burials in southern Germany have confirmed what archaeology had long assumed: the central burial of the tumulus of Eberdingen-Hochdorf (district Ludwigsburg) and the central burial at Grafenbühl were biologically closely related. A second-degree genetic relationship on the maternal side was established, allowing only one plausible scenario: the sister of the deceased from Hochdorf must have been the mother of the deceased from Grafenbühl—they were uncle and nephew.

In the area of the mound, 33 secondary burials, including several double graves, were uncovered, dating as late as the Early La Tène period. All of them represent relatively simply furnished inhumations, some of which were heavily disturbed. The individuals relevant to this study are the secondary burials from Graves 17 (APG002) and 18 (APG003), which represent a double grave. The adult female (APG002) and the male child (APG003) were buried less than 2 m east and stratigraphically above the central burial chamber. Their grave pit was covered with a layer of stones measuring 2.5 m in length and 1.1 m in width. Grave goods consisted mainly of bronze fibulae, as well as arm and finger rings. Both individuals were genetically proven to be unrelated.[73]

APG002 - The individual from Grave 17 was osteologically aged at approximately 40 years and was determined to be female both osteologically and genetically. Parvovirus B19 genotype 1 was recovered from her tooth. Based on the archaeological context of the site, the individual is dated to 480–450 BCE, which is set to the midpoint of 2415 BP for phylogenetic dating. She is currently housed in the Osteological Collection of the University of Tübingen, inv. no. OSUT 5310.

APG003 - The individual from Grave 18 was osteologically estimated to be approximately 6–7 years old and was genetically determined to be male. We recovered Parvovirus B19V genotype 1 from his tooth 85. Based on the archaeological context of the site, the individual is dated to 480–450 BCE, which is set to the midpoint of 2415 BP. He is currently housed in the Osteological Collection of the University of Tübingen, inv. no. OSUT 5370.

The samples from this site were exported in the framework of a cooperation agreement among Max Planck Institute for the Science of Human History (where the Department of Archaeogenetics of the Max Planck Institute for Evolutionary Anthropology was formerly housed), the Landesamt für Denkmalpflege im Regierungspräsidium Stuttgart, and the Freie Universität Berlin, signed 15th, 17th, and 30th November 2018 (no document number). Samples within this framework agreement are documented in specific sample lists. Analysis of aDNA is explicitly permitted within this framework.

BOO

Bol'shoy Oleni Ostrov, Murmansk, Russian Federation; 2000–1500 BCE (no radiocarbon).

The Bronze Age burial ground (BOO) also called Kola Oleneostrovsky Cemetery[74] is situated on Bol'shoy Oleny (Big Deer) Island in the Kola Bay of the Barents Sea, 2.4 km north-northeast of Polyarnyi (69.078, 36.343). It occupies a sand bar (saddle) bordered by the lake and a steeply rising rock in the north, by the sea terrace slope in the south, and an easy grade in the west. The width of the saddle is 70–100 m north to south; the length is 190 m east to west. The height is 11–15 m according to the Baltic elevation system. The site was discovered in 1925. The first archaeological excavations started in 1928 by A.V. Schmidt, continued in 1947–1948 by N.N. Gurina, and in the early 2000s by V.Y. Shumkin.

A total of 31 single, double and collective burials were excavated. Most skeletons lay in anatomical order stretched on their back in the shallow grave pits up to 0.6 m in depth with their heads turned to the northeast. The burial pits were covered with boulders. The burials were made in boats (boat-kerezhka), which are very characteristic of the BOO burial ground. One burial with cremation and one cenotaph was excavated as well. The remains of 42 individuals of different preservation were found. The grave inventory includes different stone and bone tools, including harpoons, arrowheads, daggers, needles, fishhooks and several rods with a finial in the form of an elk or deer head. Fragments of ceramics with asbestos additives were found in Burial X and possibly 1. They were decorated with a "waffle" ornament similar to that of the Yamyakhtakh East Siberian Neolithic culture.[74].

Cranial metric and dental studies suggest double structure of the BOO population, which resulted from admixture of Eastern (Ymyakhtakh) groups and groups related to ancient Western Siberian[75] and modern Uralic speaking peoples.[74] The analysis of mtDNA[76] and full genome analysis[77] reaffirmed the Siberian origin of BOO people indicating a genetic connection with modern Uralic-speaking populations.

BOO005 - A morphologically mature female (skeleton 2) about 50 years old, in anatomical order, was found buried in a boat-like construction in a collective burial 16, which contained 4 individuals. The burial inventory set includes a number of stone and bone artifacts: bone dagger-shaped pins, needle and fragments of needles; a quartz flake; a bone rod with a finial in the form of an elk or deer head; and others. No pathological lesions on the skull are visible. We isolated Parvovirus B19 genotype 1 from her tooth. She is dated based on the site date and one other individual of this site being ^{14}C dated to 3586.5 years BP.[74–77]

The skeletal collection of the Bol'shoy Oleny Ostrov cemetery was obtained during archaeological excavations in 1928, 1935 and 2001–2004 by a number of researchers. The studies were undertaken according to the decision and under the supervision of the Scientific Counsel of field archaeological excavations of the USSR and Russian Academy of Science, respectively. All the materials were transferred to the Peter the Great Museum of Anthropology and Ethnography of the Russian Academy of Science (MAE RAS) and registered according to legislation of the Russian Federation. In 2018, in accordance with a trilateral agreement between the MAE RAS, the Max Planck Institute of Evolutionary Anthropology and the University of Helsinki, several tooth samples from the collection were transferred to the Max Planck Institute for genetic research.

CHV

Chalmny-Varre, Murmansk, Russian Federation; 1700–1800 CE (no radiocarbon).

The cemetery is located near the abandoned village of Chalmny-Varre (before 1932 Ivanovka) on the middle flow of Ponoy River (67°10′08″, 37°35′01″). The name of the village in translation from the Sámi language means "visible forest" (or "eyes of the forest"). Until 1917 the place was used as a burial ground by a group of Ter Sámi, who were the earliest historically known inhabitants of the Ponoy River area and have traditionally occupied the easternmost region of the Kola Peninsula.[78] A family of Izhma Komi settled in Chalmny-Varre in 1917. In 1930, a group of Sámi from Kamensky Pogost also settled in the village on a permanent basis. In the 1960s, due to the plan to build a power plant on the Ponoy River, all the villagers were relocated to the village of Krasnoshchelye, located upstream of the Ponoy River. To date, the Ponoy River region and its indigenous communities have remained remote and relatively isolated due to lack of road infrastructure. In 1976 an expedition of the Institute of Ethnography of USSR Academy of Science headed by I.I. Gokhman and T.V. Lukyanchenko excavated 52 Sámi burials dated to 19th century.[79]

CHV002 - A morphologically young Sámi female 20 years old (CHV-38) Has lesions of Cribra orbitalia visible in the orbital region and enamel hypoplasia on front teeth and molars. She was infected with Parvovirus B19 Genotype 2, which we isolated from her tooth. The sample originates from the 18–19th century,[77] for phylogenetic dating the value was set to 100 years BP

The human DNA sequencing library of individual CHV002 was already published[77] and was reanalyzed for this study. Explicit permission for this study was obtained from the sample custodians, who co-authored this paper, Valery Khartanovich and Vyacheslav Moiseyev.

CRO

Costa de Ronda, Menorca, Spain; 1200–1400 CE, radiocarbon based on direct ^{14}C of one individual.

In February 2010 a driver spotted a skeleton on a slope 12 m above a road close to the natural harbour of Maó. The site was excavated the same year, and two well preserved skeletons could be recovered by excavating the exposed section. Only half of a third one could be recovered. Meaning 3 individuals were identified on the site. The type of the funerary site is an inhumation cemetery with an unknown area span, as only one part could be excavated. The site was dated using ^{14}C and the position of the bodies, both suggest that these individuals belonged to the first settlers who reached Menorca after the conquest of 1287 CE. The burials, classified as individual inhumation burials, did not follow the Islamic funerary ritual, and no grave goods were found. The anthropological observations revealed that all three skeletons were immature and had been the subject of a non-Muslim burial. They died at the age of 6 to 12, the oldest suffering from a congenital disease. We determined it as Klippel-Feil's syndrome.

CRO001 - This individual was approximately 6 years old when they died, and we isolated Parvovirus B19 Genotype 2 from its Pars petrosa. The individual is dated directly via ^{14}C to 1280–1385 cal CE, which is a mean age of 617.5 years BP.

ABF006 (Ciutadella de Menorca, s'Albufera, Menorca, Spain), CRO001 (Costa de Ronda, Menorca, Spain), TOS002 (Tossal de Manises, Alicante, Spain) where all exported under a framework agreement between Max Planck Institute for the Science of Human History, where the Department of Archaeogenetics of the Max Planck Institute for Evolutionary Anthropology was formerly housed, and the Universitat Autònoma de Barcelona, signed 2020-09-16 (no document number). Samples within this framework agreement are documented in specific sample lists mentioning the owning institutions, responsible collaboration partners and the obligation of returning samples after analysis. Analysis of aDNA is explicitly permitted within this framework.

GFW

Gross Fredenwalde, Brandenburg, Germany; 6500–5000 BCE, radiocarbon either direct or associated.

The Mesolithic burial site of Groß Fredenwalde is located about 80 km north of Berlin on a morainic hill well visible in the lowlands of the Uckermark. First Mesolithic human remains were detected in 1962 while in 2012 systematic excavation of the site started. Step by step at least 8 Mesolithic inhumation burials with 12 individuals could be documented in an area of about 5 x 5 m. Besides single burials, there are one double and one triple burials. Among the individuals (small) children are well represented by five. Red ochre was regularly used in the burial rite, and goods such as flint blades, bone daggers and animal tooth pendants were present in at least four graves. Most of the burials respect each other, and they are dated to ca. 8,000 years ago, soon after the 8.2 kyr event.

Palaeogenetic results assign them to the western hunter-gatherer population, and close relationship is confirmed for three individuals. In the centre of the site, a later burial of a male individual ca. 25 years old (feature 1/ 4) largely destroyed a child grave. The burial is about 1,000 years later (ca. 4,900 cal BC) when the exact position of the earlier burials was unknown. The bones of the male skeleton were intermingled in a pit ca. 1.6 m deep. Only the leg and foot bones were close to their anatomically correct position. This unusual situation is probably caused by the body having been placed in the pit in an almost upright position. During decomposition of the body the skeleton collapsed. No ochre was used in the rite here, but some flint blades, a small flint core used as a hammer stone and two large flint knives characterise the individual as a flint knapper and craftsman. Final sealing of the burial was performed with a hearth on top of the pit. In general, he had good health status, and his front teeth are worn, which is common for hunter-gatherers. The cause of death remains unknown. Palaeogenetic information confirms a western hunter-gatherer identity for the individual. By ca. 5,200 cal BC, colonising farmers settled in the area not far from Groß Fredenwalde. It is interesting to notice that the young male individual does not show any signs of admixture with the early farming population about 300 years after their arrival.[53,80–82]

GFW005 - This male individual contained Parvovirus B19V Genotype 1 in its Pars petrosa. The site is ^{14}C dated by multiple individuals. GFW005 has been directly dated to ca. 5200–5000 cal BC (MAMS-21437: 6137 ±22 BP), but the result is probably affected by freshwater reservoir effects. Two AMS-dates on charcoal samples originating from a hearth on top of the burial, which is directly linked, seem to be more reliable and date the individual somewhat younger to 5030–4800 cal BC (Poz-67909: 6030 ±40 BP; Poz-67910: 6010 ±40 BP),

The human DNA library sequencing of the individual GFW005 was already published[53] and was re-analyzed for this study. Explicit permission was still obtained from the sample custodians, and Thomas Terberger co-authored this paper as PI for the archaeology team.

GOZ

Gozquez, Madrid region, Spain; 500–750 CE, radiocarbon. Gózquez stands as one of the most extensively excavated early medieval villages in Spain. Archaeological excavations in 1999–2000 unearthed the complete necropolis, comprising around 400 inhumation graves, and revealed nearly 3 hectares of its settlement layout, featuring several distinct households separated by empty rectangular plots, likely gardens. Radiocarbon and stratigraphic analyses, along with well-dated pottery, glass and metallic artifacts, indicate that the site was occupied from the late 5th century to the second quarter of the 8th century CE. In addition to the individuals interred in the village cemetery, a dozen articulated bodies were discovered within three storage pits. These remains show no signs of violent death despite being discarded without particular care and commingled with the carcasses of several domestic animals. One of these bodies is the subject of this study. Prior analyses have also identified the genetic markers of bubonic plague and malaria in several of these individuals.

GOZ002 - This individual contained Parvovirus B19V Genotype 2, which was isolated from its Pars Petrosa. The site is ^{14}C dated by another individual, the date is taken to apply to GOZ002. The individual is dated 572 – 645 CE, which is sat to the median value of 1360.5 BP for phylogenetic dating.

The skeletal collection of the Early Medieval/Visigothic site of Gózquez (San Martín de la Vega) was obtained during archaeological excavations in 1998–2000 directed by Alfonso Vigil-Escalera. The studies were undertaken according to decision and under the supervision of the Dirección General de Patrimonio Histórico of the Community of Madrid and the Museo Arqueológico de la Comunidad de Madrid, where all the archaeological findings from the site are deposited. In 2018, in accordance with an agreement between the cited museum and the Max Planck Institute of Evolutionary Anthropology, several tooth samples from the collection were transferred to the Max Planck Institute for genetic research.

HAD

Hatherdene Close, Cambridgeshire, Great Britain; 400–600 CE, radiocarbon of one individual dated to 425–539 cal CE

The site was excavated from 2007 to 2016, and it is located in Cherry Hinton, Cambridgeshire. Hatherdene Close is an early Medieval cemetery that consisted of 126 inhumation graves. It dates to the early Anglo-Saxon period between the 5th and 6th centuries. The majority of graves lay to the northeast of a Roman funerary enclosure and an Iron Age square barrow, with eleven graves within the earlier features. Noteworthy about Hatherdene is the number of ‘‘stacked’’ burials where multiple individuals were buried on top of one another instead of adhering to a more usual side-by-side interment in multiple inhumation graves.

HAD011 - We isolated Parvovirus Genotype 2 out of the Pars Petrosa of this individual. The ^{14}C date median was applied as an individual date and set to 1450 BP.

HAD015 - We isolated Parvovirus Genotype 2 out of the Pars Petrosa of this individual. The ^{14}C date median of 1450 BP was applied. Skeleton 422 was an adult male found on the southeastern edge of the cemetery in his own grave accompanied by a knife and pottery.

The human DNA sequencing library of the individuals HAD011 and HAD015 were already published[83] and were reanalyzed for this study. Explicit permission for this study was still obtained from the sample custodians who co-authored this paper.

HGC

Hagios Charalambos Cave, Lasithi Crete ,Greece, 2300–1800 BCE, multiple individuals radiocarbon dated: HGC001.A: 3732±19 BP, 2200–2041 cal BCE (95% probability), (ID: MAMS-37426)
HGC002.B: 3777±19 BP, 2283-2139 cal BCE (95% probability), (ID: MAMS-37427)
HGC003.A: 3648±19 BP, 2125-1948 cal BCE (95% probability), (ID: MAMS-37428)
HGC004.A: 3716±22 BP, 2196-2034 cal BCE (95% probability), (ID: MAMS-37429)

HGC005.A: 3757±19 BP, 2276-2059 cal BCE (95% probability), (ID: MAMS-37430)
HGC006.A: 3764±19 BP, 2279-2063 cal BCE (95% probability), (ID: MAMS-37431)
HGC007.A: 3725±19 BP, 2198-2038 cal BCE (95% probability), (ID: MAMS-37432)
HGC008.A: 3795±19 BP, 2290-2146 cal BCE (95% probability), (ID: MAMS-37433)
HGC026.A: 3751±25 BP, 2280-2039 cal BCE (95% probability), (ID: MAMS-49762)

The Hagios Charalambos Cave is located on the upland Lasithi Plain in the Diktaean Mountains of eastern Crete. The cave (latitude:35.1772505, longitude:25.4410963) was discovered by chance in 1976 during the construction of a road. Dynamiting operations destroyed part of the roof of the cave and exposed its two outer chambers. There are a total of seven chambers with an abundance of human remains and artifacts. The Ephor of Antiquities of East Crete, Dr Costis Davaras, undertook rescue excavations in 1976 and 1982–1983, clearing the upper chambers. Two decades later, excavations were conducted in 2002 by Prof Davaras of the University of Athens and the Ephoreia of East Crete and this time jointly with Prof Philip Betancourt of Temple University and the American School of Classical Studies at Athens, and Eleni Stravopodi of the Hellenic Ephorate of Paleoanthropology and Speleology was added as co-director in 2003[84,85]

The cave was used as an ossuary for the secondary burial of human remains originally interred elsewhere and transported to the cave in a single short event in the Middle Minoan IIB period. The burials were commingled and mixed with grave gifts that covered a long period of time, from Late Neolithic II (4th millennium BCE) to Middle Minoan IIB (18th century BCE). They constitute the largest and best-preserved corpus of human remains from such an early period in Crete.

Both adults and children are represented. Among adults there is evidence for a range of pathologies: traumas, arthropathies, spondyloarthropathies, neoplasm, and endocrine and genetic disorders. The percentage of immature individuals is approximately 10–12% of the material; evidence of pathology reveals the participation of children in arduous tasks causing repetitive injury to their articulations. There is abundant evidence that skilful medical practitioners performed surgical procedures to treat head traumas.

Low temperatures in the cave, with minor fluctuations, afforded stable conditions ideal for the preservation of aDNA. The teeth analysed come from Room 5, an elliptical space c. 4 x 6 m, excavated in 2002 and 2003. At the time of excavation, the deposit of bones inside the room was so deep that less than a meter of space existed at the entrance from Room 4 at the south. Room 5 had no internal stratigraphy except that human skulls were on top of the deposit. The room had been prepared for the deposition of the human remains by the construction of two rubble walls—oriented north to south—one at the west near the hole leading down to Room 7 at the end of the cavern and one near the centre of the room. These walls helped retain the deposit because the floor sloped down toward the west. At its deepest, the top of the deposit was c. 1.6 m above the floor. The teeth for the aDNA analysis were collected at the centre of Room 5 several centimeters below the surface of the deposit. They were loose within the mass of bones and not associated with any specific bones or artifacts.

Forty-two well-preserved teeth were selected for aDNA analysis. After merging data from samples that belonged to the same individual, a total of 28 individuals were assembled (21 males/7 females). Radiocarbon dates obtained from the samples are compatible with some of the pottery found in Room 5.[86] They fall mainly within the Early Minoan II and III periods (second half of the third millennium BCE), before the first palaces were built at Knossos and elsewhere early in the Middle Bronze Age.[87]

HGC015 - We isolated a parvovirus B19V Genotype 1 genome out of this individual's molar. The site date is applied as a median for the individual date of 4,000 years BP.

In accordance with legislation set out by the government of the Hellenic Republic, a permit was issued in 2003 by the Ministry of Culture for the export of 75 tooth samples from the excavation to be transferred to the Max Planck Institute for genetic research. Archaeogenetic research on this material has been on-going, and it has so far led to the publication of papers concerning population origins,[88] marriage practices,[87] and evidence for *Y. pestis* and *Salmonella enterica*.[89] The archeologists and sample custodians Philip P. Betancourt, Susan C. Ferrence and Louise C. Langford co-authored this paper.

KER

Kernavė, Širvintos, Lithuania, 1401 - 1700 CE, associated radiocarbon date of the site (OxA-25454) 283±24 BP, C^{13} -19.94.

The site represents a successor to a former settlement dating from the 13th-14th centuries, located in the Neris River valley. The inhabitants of this earlier settlement were interred in the Kriveikiškiai burial ground, situated on the upper river terrace. The original site was abandoned at the end of the 14th century, likely as a consequence of one of the Teutonic crusades, during which the settlement was destroyed by fire. Subsequent climatic changes, characterized by cooler and wetter conditions, contributed to the abandonment of the lower-lying area and the establishment of a new settlement on the elevated terrace. This period also marks Kernavė's transformation into a modest post-medieval community, corresponding with the Christianization of the region and the foundation of a parish church. Archaeological excavations were conducted at the site between 1989 and 1994 by Adolfas Jankauskas, Aleksejus Luchtanas, and Gintautas Karnatka. The investigations identified three distinct phases of church construction. The first two churches were constructed of wood, while the third and final phase involved the construction of a brick church. The earliest graves, potentially dating to the early 15th century, were partially destroyed during the church's later expansion. In total, the remains of 258 individuals were exhumed. The majority of burials were oriented westward, with the deceased interred in wooden coffins. Most individuals were buried in a supine position with arms bent at the pelvis or chest; only a few had their arms extended alongside the body. The archaeological assemblage is relatively sparse, as most graves lacked accompanying grave goods. However, a limited number of burials contained items such as coins, fragments of glass, brass wallets, brass rings, pins, earrings, necklaces, and crosses or rings made of silver, brass, or iron. These artefacts enable the dating of the burials to the 15th-17th centuries.

KER001 - the individual analyzed is from grave 99 of the former churchyard, male, 30-40 years at the time of death. The skeletal remains are well-preserved with no taphonomical alterations. Pathological changes were noted on the left elbow joint that could be associated with tuberculosis. The Parvovirus B19 Genotype 2 was recovered from a rib. The date is archaeological and set to the median of 399.5 years BP.

Excavations at the Kernavė site (a UNESCO Heritage site since 2004) were undertaken between 1989 and 1994 by archaeologists Adolfas Jankauskas, Aleksejus Luchtanas, and Gintautas Karnatka. Following the excavations, the human remains were sent to Vilnius University Faculty of Medicine for anthropological analysis. Vilnius University Faculty of Medicine is responsible for the storage, analysis, and authorization of any further research related to osteological human remains (reference No. (1.13 E) 150000-TPN-22). Permission for aDNA sampling and analysis from the Kernavė site for this research has been granted.

LEU

Leubingen, Thüringen, Germany, Neolithic, Bronze Age, Iron Age, Middle Ages, Date of the feature 2088: Early Bronze Age (Únětice culture). Radiocarbon: Individual directly ^{14}C, MAMS 43536: 3554±21 BP: 1961 (82.8%) 1873, 1845 (7.8%) 1814, 1801 (4.8%) 1778 cal BC (2σ)

Leubingen is located in the Thuringian basin, a highly fertile region in the present-day German state of Thuringia (coord. 51.2062010°, 11.1834550°). The archaeological excavations of interest here were carried out on a contiguous area of 22,5 ha in 2009 and 2010 by the Thuringian State Office of Heritage Management and Archeology. The 950 x 300 m excavation area yielded 6141 archaeological features dating from the Late Neolithic ∼3650 cal BC to the Early Modern Period, of which around 500 belong to the Early Bronze Age. They document various stages of the Únětice culture, including the beginning of the classical phase, with which the construction of the well-known Leubingen Tumulus (1942±10 BC, tree-ring date) 775 m east-northeast of feature discussed in this study is associated. The preservation of the features is poor due to extensive erosion and the intensive more recent settlement of the area. Only one house from the EBA settlement could be identified. In addition to numerous EBA settlement pits, there are around 60 graves. Of these, 33 belong to a burial ground of the early to middle stage of the Únětice culture, which was fully investigated. The burial feature 2088 (individual LEU 027) discussed in this study is considerably younger than the cemetery to the north-east, but dates approximately the same as the Leubingen Tumulus. However, the dating range of the radiocarbon date is considerably larger. Whether grave 2224, which is only 15 m away but 150 years older, or the cemetery as a whole was still known when the individual in feature 2088 was buried is unclear, but not very probable. The individual LEU027 buried here is distantly genetically related to a family from the burial ground. However, it is likely that the position of the younger grave has been chosen due to its proximity to the contemporaneous settlement.[90,91]

LEU027 - This male individual was approximately 18-20-year-old at death. His grave was found spatially and temporally removed from other graves at this site. He was found to be genetically related to the individuals of the site. Only the skull is fully preserved. We recovered Parvovirus B19 Genotype 1 from his Pars Petrosa. This individual has its ^{14}C date median applied as 3819.5 years BP. Flat ''settlement grave'', ca. 26m south-west of the main burial ground. The small pit (0.65 x 0.45m in size) was rectangular and preserved up to 0.10m into the ground. There were no grave goods and the burial was poorly preserved.[90]

The Thuringian State Office for Heritage Management and Archeology is the archaeological authority of the Free State of Thuringia and is therefore responsible for all archaeological investigations in Thuringia. The TLDA hereby confirms that the human remains from Leubingen 09/100 (LEU027, 09/100-1773) for the paleogenetic studies presented here come from own excavations, which are based on the laws of the Free State of Thuringia. All permits have been obtained. The TLDA is itself involved in the work.

MIB

Mikulovice – big, Eastern Bohemia, Czech Republic, 2200 -1750 BCE, multiple individual's radiocarbon dated to the Unetice Culture, general date span. Multiple individuals directly 14C-dated between ca 2200-1750 BCE.

The site was excavated during a rescue excavation in 2006-2012 (J. Frolík, R. Sedláček). Altogether, thousands of sunken settlement features and about 100 Early Bronze Age graves (109 skeletons in 98 graves and three settlement pits) were documented in several groupings. With exception of two Proto-Únětice graves (No. 95 and 96), the graves mostly belong to the Classic and Post-Classic stages of the Únětice culture. The inhumation burials are very rich in so-called ''exotics'', especially amber artefacts (present in 28 graves), artefacts made of copper, bronze, tin, gold, seashells, animal bones and/or stones. The EBA cemetery has been completely analysed and published as part of the big international interdisciplinary project[92]

MIB039. We recovered Parvovirus B19V from the Pars Petrosa of this individual. The individual is directly ^{14}C dated, its time span is 1889 - 1751 BCE the median point is set to 3770 years BP. Grave 24 Skeleton: right-sided crouched burial, head towards the south, east-faced. Skeleton bones of skull and long bones preserved. Sex: anthropology -? (child), aDNA - F. Age: infans II (4-5). Grave goods: one vessel (flat plate) under the legs, tool made of animal bone near the vessel. Archaeological dating: Classic Únětice culture. Radiocarbon dating: CRL-19416 (3499±23) 1889-1751 cal BC 2-sigma. Published: *Ernée - Langová et al. 2020*, 60- 61, 331; Figure 221; plate 11; 42: A-B; 75. Pandora No.: MIB039. NM Prague Inv. No.: P7A 43123

MIB022 - We isolated Parvovirus B19V genotype 1 from this individual's Pars Petrosa. This individual is ^{14}C dated to 2007 - 1881 BCE, the median point of this is taken as the individual date at 3894 years BP. Grave 43 Skeleton: right-sided crouched burial, head towards the south, east-faced. Skeleton average preserved, robust. Sex: anthropology - M, aDNA - M. Age: adultus I (20-30). Grave goods: two vessels (one largel vessel in the SW corner of the grave pit, smaler cup and a larger pot sherd under the legs by the N side of the grave pit), animal bone (scapula) behind the legs by the W side of the grave pit, seashell (*Dentalium*) positioned in the place of his genitals between the pelvis bones. During the EBA seashells were commonly deposited in burials as parts of the necklaces, mostly in female graves. The positioning of the *Dentalium* seashell in the male burial in the place of his genitals is very uncommon

and rare and could have any symbolical meaning related possibly to any of his physical or psychical characteristics. . Archaeological dating: Classic Únětice culture. Radiocarbon dating: MAMS-30476 (3569±19) 2014-1826 cal BC 2-sigma. Second 14C-dating was made of animal bone (scapula, burial offering - see above): CRL-19333 (3474±37) 1896-1687 cal BC 2- sigma. Puiblished: *Ernée - Langová et al. 2020*, 65, 337; fig. 226; plate 19; 47: E; 87. Pandora No.: MIB022. NM Prague Inv. No.: P7A 43142.[92]

The human DNA sequencing libraries of the individuals MIB022 and MIB039 where already published[93] and was reanalyzed for this study. Explicit permission for this study was still obtained from the sample custodian, who co-authored the paper – Michal Ernée.

OAI

Oakington, Cambridgeshire, Great Britain, 400–600 AD, multiple radiocarbon dates available.

Oakington is historically a rural location just north of, and connected to, modern day Cambridge, in Cambridgeshire, United Kingdom. Three early Medieval burials were identified during pastureland cultivation in 1926; these remains are now lost. In 1994, the cemetery was rediscovered and 24 graves were excavated by the Cambridge County Council's Archaeological Field Unit. In 2006, 17 additional individuals were identified by CAM ARC. and 78 further graves were excavated between 2010 to 2014 as a part of a university research and teaching program. The site consists of 124 graves dating to the latter fifth and sixth centuries. The organization of the Oakington burials points to an ordering around a series of key individuals. One notable grave contained a young woman adjacent to a completely articulated cow, the site also contained two horses and is one of the few early Medieval cemeteries with extensive evidence of animal remains placed in inhumation graves Samples from Oakington were provided by the University of Central Lancashire.

OAI017 - We isolated parvovirus B19V genotype 2 from this individual tooth 26. Sample from the same grave ^{14}C dated to 426 - 541 CE, this supports the archeological date from 400 - 600 CE. The midpoint of this date applied to individual OAI017 as 1450 years BP for use in phylogenetic dating. Grave 109c is a female child aged between one and three years at death. She was found in a triple grave with two other women, an adult 109a and young adult 109b.

The human DNA sequencing library of the individual OAI017 was already published[83] and reanalyzed for this study. Explicit permission for this study was still obtained from the sample custodians, who co-authored the paper. Permission to analyze was granted by coauthor Duncan Sayer in 2017. Permission for pathogen analysis was given in 2025.

PRS

Paris Réaumur-Sébastopol, Île-de-France, France, 1290–1665 CE multiple graves radiocarbon dated.

The site was excavated in 2015 and is a part of the cemetery of the Trinité hospital in Paris. The excavation was performed ahead of works on boulevard Sébastopol. In total, more than 300 individuals were excavated from 8 mass graves which were attributed to the 14 - 18th century. The hospital was founded in the 13th century and destroyed during the French Revolution.[94]

PRS018 - The tooth 33 of this Individual yielded Parvovirus B19 Genotype 2. The individual is from a hospital cemetery, the grave is dated to late medieval early modern era. The graves where ^{14}C dated and published.[94]

The samples from PRS (Paris Réaumur-Sébastopol) where transferred directly to Johannes Krause, Director of the Max Planck Institute for Evolutionary Anthropoly on the 14th Jun 2016. The transfer was initiated by Isabelle Abadie, who was in charge of leading the archeological excavation and studies of a hospital cemetery. Their findings were published under Isabelle Abadie,[94] Société Française d'histoire urbaine.

STR

St. Rombout's cemetery, Province of Antwerp, Flanders, Belgium, 900–1800 CE, multiple radiocarbon dates available all supporting the archeological date.

The site is located in the Belgian city of Mechelen and was excavated between 2009 and 2011. The site included part of the northern cemetery of St. Rombout's parish church, and yielded the remains of 4,158 articulated individuals. The burial ground was in use between the 10th and 18th centuries.[56]

STR072 - This individual's tooth yielded a Parvovirus B19 V genome of Genotype 1. The remains were not ^{14}C dated, but were archaeologically assigned to the late phase of the cemetery, to the 17-18 c. CE.

STR140 - This adult male individual tooth yielded a Parvovirus B19V genome most likely belonging to Genotype 3. It is ^{14}C dated to 340±19 BP, 1479-1635 cal CE (2- sigma) and exhibits evidence of *P.malaria* infection. He was buried in a single-phase multiple burial together with one non-adult and three other adults.[56]

The human skeletal collection of St. Rombout's cemetery in Mechelen, Belgium was excavated by the department of Archaeology of the city of Mechelen between 2009 and 2011 (permit number from the Flemish Heritage Agency: 2009/324). Permission to use samples taken from several individuals dating between the 10th and 18th centuries AD was granted to the Max Planck Institute by the city council, who curate the remains.

SUC

Su Crucifissu Mannu, tomb 22, Sardinia, Italy, 3500–1550 BCE, multiple radiocarbon dates available.

The necropolis is located in Northwestern Sardinia, Porto Torres municipality, bordering with Sassari. One of the many reused burials surrounding a unique ceremonial site dating to the Late Neolithic-Early Copper Age, it consists in rock carved tombs composed of several rooms.[95] Excavations were conducted between 1958 and the early 1970s, with the best-documented tomb being t.16, where most human remains were attributed to the Early Bronze Age 1 based on associated material remains and a clear stratigraphy, with other phases (Monte Claro or Bell Beaker, Late to Final Copper Age) likely to be represented (Ferrarese Ceruti 1976: 191). Most of the skeletal materials from other tombs, including t.22 where individual n.101 from which sample SUC009 was removed, were also assigned to the EBA1 based on association with elements of material culture, despite no stratigraphic details

were available. The remains were partially studied by F. Germanà (1995: 129 and references therein), but unfortunately only short comments were published. Among the radiocarbon dates obtained within the context of a dating effort complementary to an archaeogenetic investigation[96] most confirmed the overall attributions. Concerning specifically t.22, one of the two individuals/ specimens yielded an early date (MAMS-38301, 5042 ± 21 BP = 5894- 5732 cal BP 2σ, Late Neolithic), the second, pertaining to sample SUC009, places it in the initial MBA (MAMS-38302, 3421 ± 20 BP = 3808-3612 cal BP 2σ), which in the Sardinian context appears in full cultural continuity with the EBA. A more comprehensive investigation of the human remains is at the planning stage and expected to bring new data on the life, ancestry and disease of these human groups.

SUC009 - This male early bronze age individual's Pars Petrosa yielded a Parvovirus B19 genome belonging to genotype 1. It was ^{14}C dated to 2200 - 1650 cal BCE.[96] This individual's date is set to the median of its dating interval to 3710 years BP.

Su Crucifissu Mannu, Sardinia. The Soprintendenza Beni Culturali, Archeologia e Paesaggio per le Provincie di Sassari e Nuoro, local branch of the Ministero dei beni e delle attivita' culturali e del turismo, Italy, provided the authorization for sampling and analysis from the site/collection of Su Crucifissu Mannu, t.16: identifier prot. 4247/ March 14th, 2017.

TOS

Tossal de Manises, Alicante, Spain, 660- 1010 CE, Radiocarbon dates of 3 samples of the site[97]

The Tossal de Manises site is located inside the broad the ancient Roman city of Lucentum, a municipality founded at the beginning of the second century BC and which has a long stratigraphic sequence that reaches the beginning of the third century CE. Although the city was abandoned for several centuries, it was occupied again in the Islamic period, when a necropolis or maqbara was installed there, from the so-called Emiral or early Islamic period (8th–10th centuries CE), the period to which the samples correspond. Excavations at the site began in the early twentieth century but it was in the nineties when the MARQ Archaeological Museum of Alicante began to work there continuously. Today, the site of Tossal de Manises is an archaeological park open to the public, which is still in the process of study and is presented as one of the most important archaeological sites in the province of Alicante.

Geographical Information: The Tossal de Manises is the site of the Roman city of Lucentum, the ancient Alicante, located at the top of an elevation (tossal) by the sea, which reaches 38 meters high, and is located 3.5 km from the center of the modern city, in the so-called neighborhood of La Albufereta. Summary of sampled materials: In the case of the Islamic maqbara register, which is the one analyzed in this study, there are hardly any archaeological materials, since although it is a funerary context, in the Islamic rite -to which these people belong-, the deposit of trousseau elements accompanying the deceased is not allowed.

TOS002 – This early Andalusian young adult female individual's permanent molar yielded a B19V genome belonging to genotype 2. This individual is ^{14}C dated to 707–976 CE, the age is set to the midpoint of this estimate at 1108.5 years BP.

ABF006 (Ciutadella de Menorca, s'Albufera, Menorca, Spain), CRO001 (Costa de Ronda, Menorca, Spain), TOS002 (Tossal de Manises, Alicante, Spain) where all exported in the framework of a framework agreement between Max Planck Institute for the Science of Human History, where the Department of Archaeogenetics of the Max Planck Institute for Evolutionary Anthropology was formerly housed, and the Universitat Autónoma de Barcelona, signed 2020-09-16 (no document number). Samples within this framework agreement are documented in specific sample lists mentioning the owning institutions, responsible collaboration partners and the obligation of returning samples after analysis. Analysis of aDNA is explicitly permitted within this framework. *Maqbara* del Tossal de Manises, Alicante, Spain. Excavations in the burial area of the archaeological site of Tossal de Manises (Alicante) were carried out in successive campaigns between 1999 and 2003 by a team of archaeologists and anthropologists from the MARQ Archaeological Museum of Alicante. The complete study of the human remains was published in 2007 (TENDERO, E. GUILABERT, A. and OLCINA, M (2007): *La maqbara del Tossal de* Manises (Alicante). Excavaciones Arqueológicas. Memorias 4. Museo Arqueológico de Alicante-Diputación de Alicante. ISBN 978-84-96979-05-5). In 2020, permission was obtained from the Regional Ministry of Culture of the Valencian Community (the competent authority in Spain) for the remains to leave the country for study.

UZZ

Grotta dell'Uzzo, Sicily, Italy, 11100 - 3950 BCE, Radiocarbon dates for multiple individuals available

The site of Grotta dell'Uzzo is located on the eastern flank of the San Vito lo Capo peninsula in NW Sicily, overlooking the Gulf of Castellammare. This large rockshelter was first excavated from 1975 to 1983 by Marcello Piperno and Sebastiano Tusa, under the remit of the Istituto Italiano di Paleontologia Umana.[98] A short excavation season was undertaken in 2004 under the direction of Sebastiano Tusa, but most of the material from the site originates from the earlier excavations and is stored at the Museo Archeologico Regionale "Antonino Salinas".[99] The different campaigns resulted in the exploration of tens of trenches, one of which, namely Trench F, preserves the original stratigraphic sequence.[98] The site is also known for its use as a burial ground during the early Mesolithic, when at least 11 inhumations took place. Interestingly, though, human remains are spread across Grotta dell'Uzzo and throughout its deposits, which suggests that more burials than those formally excavated may have existed, but also potentially from more phases than just the early Mesolithic.[53] The stratigraphic succession of Trench F covers all the known phases of the occupation at Grotta dell'Uzzo, from the late Upper Palaeolithic through the Mesolithic and the early Neolithic, when agro-pastoralism was first introduced to Sicily.[98] This makes the site noteworthy in the Mediterranean context, given that there is a dearth of late Mesolithic contexts and of sites from which the last hunter-gatherers may have interacted with pioneering farmers.[53,100] Both on stratigraphic and archaeological grounds the Mesolithic has been divided into an early and a late phase (or Mesolithic phase I and II). During phase I, Sauveterrian-like lithic industries were produced by hunter-gatherers, whose ancestors had arrived from Italy in the late Upper Palaeolithic, whilst phase II was characterized by Castelnovian-like industries, probably introduced by hunter-gatherers originating in the Balkan Peninsula who interbred with the local groups.[53] Mesolithic phase II was a phase of cultural change and mixing, but also of climatic and environmental turmoil, which coincided with the 8.2-kyr-cal-BP event.[100] This archaeological phase at Grotta dell'Uzzo (spit 14 to

spit 11) has been dated to ~8,770- 7,850 yrs cal BP and precedes the early Neolithic (~8,050-7,400 yrs cal BP), when agro-pastoralists who arrived by voyaging at sea took over NW Sicily. Individual UZZ40, which was successfully sampled and analyzed for this study, is a deciduous tooth belonging to a male infant[53] and recovered in spit 13 of Trench F. This artificial spit falls within Mesolithic phase II and a direct radiocarbon date on this specimen (MAMS-40726) has yielded a date of 7,471±26 BP (8,370-8,190 cal BP, 2σ; Supplementary Information, Data S1).[101] UZZ40 belonged to the last hunter- gatherers who populated Sicily and lived around 200 years prior to the introduction of agro-pastoralism to the central Mediterranean.

UZZ040

This Mesolithic individual's deciduous tooth yielded a Parvovirus B19 genome of Genotype 1. This individual is directly ^{14}C dated to ~8,770–7,850 yrs cal BP. For phylogenetic dating, the midpoint of this date is taken as the sample date and set to 8275 years BP.

The human DNA sequencing libraries of the individual UZZ040 where already published[101] was reanalyzed for this study. Explicit permission for this study was still obtained from the sample custodian, who co-authored the paper.

VOI

Voivodeni, Transylvania, Romania, 1700 - 1500 BCE, Multiple individual's radiocarbon dated to the Wietenberg culture span, Bronze Age and one dated to the Middle Ages.

The site of Voivodeni-*La Şcoală* was discovered by Professor Z. Bartha in 1975, during fieldwork in a local schoolyard. The first rescue excavations at the site were led by M. Petică in 1977 and 1978. The mass grave in discussion was discovered in the summer of 2008 by N. Man, prior to the construction of a new nursery school. Situated on the banks of Luț creek, Voivodeni is located on the eastern side of the Transylvanian Plain approximately 25 km from the city of Târgu Mureș. During the latest archaeological survey led by N. Man, five occupation levels were identified, from periods spanning the Bronze Age through the Early Middle Ages. The Bronze Age discoveries were represented by a few pits and a mass grave. Among the settlement objects in Trench 1, at the depth of 105 cm a feature with skeletal remains of seven individuals was discovered. Initially circular, with the depth of 74 cm, the burial pit was later cut by several features so that it appeared as an approximately 135 x 120 cm round-cornered rectangle at the time of excavation. Six individuals were interred in fetal position at a depth of approximately 140 cm with a seventh individual at 160 cm. The recovered remains included one adult male of c. 30-35 years of age, two young adult females approximately 14-15 years old, and four children between the ages of six and 13. The grave also included ceramic shards characteristic of the 3rd phase of the Wietenberg ceramic style. The first individual (the studied Skeleton no. 7.) laid in the grave was a young female positioned roughly in the middle of the pit on her right side, facing eastwards. The body was in a perfect fetal position, with curved back, bent head, with the hands bent from the elbow and the legs strongly bent and pulled up to the torso. The cranium was fragmented, the teeth were scattered in the cervical area, while the sternum was missing. The skeletal remains were highly friable. The radiocarbon dates produced from three individuals place the burial between c. 1700- 1500 BCE; however, radiocarbon analysis of VOI007 (skeleton 7) dates this individual in the Middle Ages, complicating the burial's chronology[102]

VOI007 - This medieval individual from a mass grave was previously found positive for Malaria infection. It also yielded a Parvovirus B19 Genotype 2 Genome without requiring amplification. This individual is directly ^{14}C dated to 1426-1466 CE, with a sample age of 504 years BP. It is far younger than other samples of the same site.

The human DNA sequencing library of individual VOI007 was already analyzed for Human and Pathogen (Plasmodium) aDNA and published by Michel et al.,[56] Nature and was reanalyzed for this study. Explicit permission for this study was still obtained from the sample custodian, who co-authored the paper – Rita Németh. The skeletal remains from the Bronze Age Mass Grave from Voivodeni-*La Şcoală* (Mureș County, Romania) was discovered in 2008 during archaeological excavations led by N. Man. The archaeological research was carried out by the archaeologist of the Mureș County Museum on the request of the city hall from Voievodeni, based on the authorization issued by the Ministry of Culture. All the archaeological material from the excavation is part of the Mureș County Museum's inventory. In the spring of 2018, in accordance of a bilateral agreement between Mureș County Museum from Romania and the Department Archaeogenetics of the Max Planck Institute for the Science of Human History in Jena, Germany (signed in 16.03.2018), several tooth and bone samples from all of the seven skeletons from the mass grave were sent in Jena for genomic as well as pathogenomic analysis of prehistoric human samples.

Asian archeological sites

BRE

Berel, Eastern Kazakhstan region located approximately 154 km to the east from v. Ulken Naryn, Kazakhstan

The first excavations on the Berel necropolis date back to 1998. Since then, about 90 burials have been discovered at Berel. The first finds belong to the Pazyryk culture (IV-II centuries BC) represented by typical burial mounds (kurgans) of the Saka elite. Starting from 2008, the burials that were not related to the elite mounds of the Sakas were found on Berel. These burials belong to the later Hun-Xianbei layer (dated by 2nd - 6th centuries). Approximately 70 Hun-Xianbei burials located around the big kurgans of Pazyryk culture.[103]

BRE013 - Hun-Xianbei Berel layer. Object 68/№2 was excavated in 2018 by Samashev Z.S. Object 68 is a multiple burial. The central burial in a group of three large enclosures surrounded by a ring-shaped rampart. The monument contained two burials (object 68/№1-north wall and object 68/№2 - south part). Object 68/№2 was a skeleton of young man of 18-25 years old, that buried in stone box with a slate slab ceiling. Burial without inventory. Skeleton was oriented north-east, laid in an extended position on his back. Radiocarbon: 14C BP 1821 ±21; 14C.cal (2-sigma) 131-241 AD

BRE026 - Hun-Xianbei Berel layer. Burial 13 was excavated in 2005. The individual was burned there. Nearby the remains of two horses were also discovered. The burial also contained a set of weapons characteristics of a lightly armed equestrian warrior from the Hun-Xianbei period. The presence of hepatitis B virus in bone remains of the man could be a possible reason for death.Data: The archaeological date of this sample was also the IV-III century BC, identical to BRE013.[104–107]

The human sequencing Libraries of the individuals BRE013 and BRE026 where already.[108] They were reanalyzed for this study. Explicit permission for this study was still obtained from the sample custodians, who co-authored the paper. Berel, Kazakhstan. In 2018, on the territory of SOE "Regional Historical and Local History Museum" (Ust-Kamenogorsk, East Kazakhstan Region), the scientific supervisor of State Historical and Cultural Museum-Reserve "Berel" professor Samashev Z.S. and researcher of the Center of Physical Anthropology of the Institute of Archaeology by A. Margulan (Almaty, Kazakhstan) Kitov E.P. gave the bone fragments and teeth representing human remains from several archaeological sites of Eastern Kazakhstan for the archaeogenetic study to the Director of the Institute of Genetics and Cytology (Almaty, Kazakhstan) Djansugurova L.B. and Deputy director of this Institute Bekmanov B.O. These samples included 1 fragment (Glenoid Fossa) from temporal bone (Cochlea) of a man from Berel excavation named Object 68 (№2) (Act of acceptance and transfer of skeletal remains dated September 07, 2018)

BRT

Bolgar city mausoleum, Republic of Tatarstan- Volga region, Russian Federation, dated to the 14th century CE based on Coin Artefacts

The city of Bolgar was an early settlement of the civilization of Volga-Bolgars, which existed between the 7th and 15th centuries AD. It was located approximately 130 km from modern Kazan, at the banks of the Volga River, approximately 30 km downstream from its Kama River confluence. Intermittently, bolga functioned as the capital of Volga, Bulgaria between the 10th and 15th centuries. It further was the first capital of the Golden Horde in the 13th century. The ancient Bolgar Hill fort was declared a UNESCO World Heritage Site in 2014.[109]

BRT009 - We recovered Parvovirus B19 genotype 2 from a permanent molar of this individual. The Bolgar city individual archeologically dated to the 14th century CE and set to 550 years BP, by several silver coins. The site was investigated for Y. pestis and published .[109]

The human DNA sequencing libraries from the sites BRT (Bolgar city mausoleum) and UST (Ust'-Jerusalem necropolis) were already analyzed for Human and Pathogen (Yersinia spec) aDNA and published.[109] The samples where reanalyzed for this study. Explicit permission for this study was still obtained from the sample custodian, who co-authored the paper – Maria A. Spyrou and Rezeda Tukhbatova.

JOY

Joyeong, Gyeongsangbuk-do, Republic of Korea, 400- 500 CE

JOY005 was excavated from the subsidiary chamber of tomb Joyeong CI-1, a burial structure likely constructed during the third quarter of the 5th century. The tomb represents a typical two-chambered design common within the Imdang-Joyeong burial site, with the main chamber located to the south and the subsidiary chamber to the north. Age of death was determined based on osteological and archaeological evidence. Biological sex was determined by comparing the X chromosome-to-autosome depth ratio against the Y chromosome-to-autosome depth ratio on 1240K ancestry informative SNP sites.Three human skeletons, accompanied by ample burial goods, were found in the main chamber. One individual, whose head was oriented towards the east and genetically male, was classified as the grave owner and died between the ages of 31 and 40. The remaining two deceased, who had their heads positioned westward, were classified as sacrificed individuals. The sacrificed individual positioned at the north was genetically male and died between the ages of 15 and 18. The sacrificed individual at the south was a genetically female child who died between the ages of 4 and 8. Two additional sacrificed individuals were discovered in the subsidiary tomb. The northern individual (JOY005) was genetically female, and estimated to have died between the ages of 36 and 50. The southern individual was a genetic male and estimated to have died between the ages of 41 and 60.[110–112]

JOY005 - This individual is archaeologically dated to the 400 -500 CE, and this is set to the midpoint as 1500 years BP. The individual's right-sided Pars petrosa yielded a Parvovirus B19 Genotype 1 genome.

The human skeletal materials analyzed in this study were originally recovered during an excavation of ancient tombs in the Imdang area, conducted in 1987 by the Yeungnam University Museum under permission granted by the Cultural Heritage Administration of Korea. Following the excavation, the materials have been continuously curated and housed at the Yeungnam University Museum, where a full-scale osteological analysis was carried out in 2012. Since 2019, further systematic research on these remains has been conducted as part of the Apdokguk Cultural Heritage Research and Utilization Project, funded by Gyeongsan City. The human bone data examined in the present study were analyzed through a series of research procedures, including genetic analyses, in accordance with a joint research agreement signed in 2018 between the Yeungnam University Museum, Sejong University, and the Department of Archaeogenetics at the Max Planck Institute for Evolutionary Anthropology (then at the Max Planck Institute for the Science of Human History) in Germany.

KBD

Kabardinka, Krasnodarskiy kray, Russian Federation, 2196 - 1977 BCE, all individuals where radiocarbon dated

The site Kabardinskiy 9 is a cemetery site that comprises several burial mounds dating to the Middle Bronze Age, North Caucasus culture, MBA1 and MBA2. The site is referred to as Kabardinskiy 9 and belongs to the Kurgan2 complex. The culture as revealed by the archeological evidence is the post-Catacomb horizon/Alikonovka group dated to 2200–1700/1650 BCE. The site was found to be comprised of twelve human and two animal individuals; six of the human bones were radiocarbon dated[113]

KBD002 - This individual's left Pars Petrosa yielded a Genotype 1 Parvovirus B19 genome. It is ^{14}C dated to 2188 - 2026 cal BCE, the midpoint of this dating is taken and set to 4057 years BP.

The human library of individual KBD002 was already published.[114] Explicit permission for this study was still obtained from the sample custodian, who co-authored the paper.

KED

Kedeksha, Vladimir Oblast, Russian Federation,1701 - 1900 CE, all four individuals used for genetic analysis are ^{14}C dated. Their ^{14}C dates fall in the range of 1400 - 1950 calCE

The medieval settlement site Kideksha is located on the territory of the village of the same name on the right bank of the Nerl River, 4 km east of Suzdal. Kideksha is known as a large settlement with medieval occupational layers covering an area of 16 ha. It is famous for its limestone church dedicated to Boris and Gleb, one of the earliest stone buildings in northeastern Rus', constructed in 1152. The first excavations in Kideksha were conducted in 1851 on the territory of the churchyard. Subsequent excavations and surveys revealed a settlement since the early 11th century, with expansion in the 12th–13th centuries and continuing up to modern times. Excavations conducted in 2011–2012 on the churchyard revealed 49 burials from the 18th century to the first half of the 19th century, cutting through the settlement deposits from the 16th to 17th century. Samples for genomic analysis were selected from a trench that contained disarticulated remains, including well-preserved skulls from the graves marked as Grave A (KED001), Grave B (KED002), Grave C (KED003) and Grave D (KED004). The general archaeological context indicates that the remains date to the early modern period[115]

KED002 - This individual's permanent molar yielded a Genotype 2 Parvovirus B19 genome. The individual is archeologically dated 1701 - 1900 CE and radiocarbon dated to 1661 - 1950 cal CE (MAMS35347: 188±18 BP). The date for phylogenetic dating has been set to the midpoint of this estimate to 143.5 years BP.

Sample KED002 is part of the Suzdal collection analysed for human ancient DNA by Peltola et al.[115] KED002 originates from grave B discovered in archaeological excavations in Kedeksha, Vladimir Oblast, conducted by the Russian Academy of Sciences in 2011–2021. Permission to use the sample for ancient DNA research was granted to SUGRIGE project (University of Helsinki, University of Turku, and the Max Planck Institute) by Nikolaj Makarov from Institute of Archaeology, Russian Academy of Sciences, Moscow, Russia

KHI

Khoit Tsenkher, Khovd Aimag, Mongolia, 1086 - 911 BCE, Radiocarbon date 1056 - 905 BCE

The Khoit Tsenkher (Tarvagatain Am) site (aimag Khovd) dates to the Middle/Late Bronze Age; Xiongnu; Late Medieval it is culturally associated with Late Xiongnu; Mongol and some unclassified.

KHI001 - This individual's permanent molar yielded a Parvovirus B19 Genotype 1 Genome. The individual is ^{14}C dated to 1056 - 905 BCE, the midpoint of this estimate is taken to represent the sample age at 2930.5 years BP.

Excavations at Khovd Aimag where undertaken in 1987 by Mongolian archaeologist D.Navaan (2018) during the Khovd expedition. The customs permit number associated with this sample is 12-2091008-20E00225R and the export was permitted by the Ministry of Sciences and Education of Mongolia.

KVO

Pos. Kravchenko XII, Krasnodar, Russian Federation, 2164 BCE- 720 CE

The site Pos. Kravchenko XII is archaeologically associated with the Alanic culture and dated to 400 - 700 CE.

KVO007 - This male Individual is ^{14}C dated to 667 - 766 CE, the midpoint of this is used to represent the sample age as 1233.5 years BP. This individual's permanent incisor yielded a Genotype 1 Parvovirus B19 genome.

The human skeletal remains of Poselenie Kravchenko XII (KVO), Severskiy district, Krasnodar region (Coordinates: 44.92426°, 38.49687°) were excavated by the excavation compaign 'Rosarcheolog', Rostov-na-Donu 2017, under the license granted to T. V. Cybriy. Sampled were exported in 2017 by the German Archaeological Institute, Berlin, with the permission granted to carry out genetic analyses at the Max Planck Institute for Evolutionary Anthropology, Leipzig. Human aDNA from the site was published in Ghalichi, Reinhold et al. 2024, Nature, including a short site description.

KYA

Kyang, Upper Mustang, Nepal, 762 BCE - 60 BCE, Radiocarbon dated to 636 BCE - 295 BCE

The site was first excavated by Mark Aldenderfer. Kyang is located at 3900 masl in the Manang district of Nepal on the eastern side of the Nar-Phu khola. Kyang is a collective mortuary site containing the remains of at least 23 individuals that was built within a natural crevice on a cliff face approximately 50 m above the local ground surface. Stone architecture representing walls, platforms, and a staircase providing access to the burial chamber were built into the crevice. The site was discovered in a looted state, and only a small number of wooden, bamboo, and other organic remains were found. Multiple radiocarbon dates at the site indicate it was in use from 2700-2010 BP, but most activity occurred between 2350-2150 BP. The site is roughly contemporaneous with the nearby site of Mebrak (2400-1850 BP), which is located just to the west across the Thorung La pass.

KYA003 - This individual's tooth yielded a Genotype 1 Parvovirus B19 V genome. The age of the sample is defined based on the archeological site date and the ^{14}C date of another individual of this site. The ^{14}C date places the site between 362 -204 BCE, the midpoint of this is used as the sample age and set to 2125 years BP for phylogenetic dating.

KYA008 - This individual's tooth yielded a Parvovirus B19V Genotype 1 genome. The age is set to 2125 years BP based on the 362 - 204 cal BCE ^{14}C date of another individual from the same site.

CellPress
OPEN ACCESS

Kyang, Manang, Nepal. Excavations at Kyang were authorized by the Memorandum of Understanding (MoU) between the Sky Door Foundation/USA, the University of California, Merced, and the Department of Archaeology, Government of Nepal (2011-2016). Excavations at the site were directed by Mark Aldenderfer in 2014 and were overseen by a representative of the Department of Archaeology. Approval for destructive analysis and genetic investigation of samples of human remains from the site was provided by the Department of Archaeology in 2014 as part of the permitting and export process as described in the MoU.

MEB

Mebrak, Upper Mustang, Nepal, 500 BCE - 1 CE, Radiocarbon dated indirectly

Type site for Mebrak culture, 2400-1850 BP. Mebrak is located at 3600 masl in the Upper Mustang district of Nepal in the Dzong khola, a tributary of the Kali Gandaki, near the modern village of Jharkot. The site is part of a series of artificial caves excavated into a sheer cliff face located 30 m above the ground surface. Mortuary remains at Mebrak have been recovered from Mebrak 63, which contained a communal tomb containing at least 27 individuals that was used sporadically from approximately 500 BCE to 1 CE. The tomb contained wooden bed coffins, and some individuals were naturally mummified. The preservation of organic remains within the tomb was extraordinary, and included wooden, bamboo, textile, leather, and other organic materials, as well as abundant glass and carnelian beads. Mebrak is located near Kyang, which can be reached by walking approximately 2 days east through the Thorung La pass.

MEB011 - The individual's tooth yielded a Genotype 1 Parvovirus B19 genome. The age of the individual is set to 2125 BP, the midpoint of the site date.

Mebrak, Mustang, Nepal. Excavations at Mebrak were undertaken within the framework of the Nepal-German Project on High Mountain Archaeology (Universität zu Köln,1992-1997). Sampling of the Mebrak remains was authorized by the Memorandum of Understanding (MoU) between the Sky Door Foundation/USA, the University of California, Merced, and the Department of Archaeology, Government of Nepal (2011-2016), and was overseen by DoA representatives in Kathmandu. Approval for destructive analysis and genetic investigation of samples of human remains from the site was provided by the Department of Archaeology in 2014 as part of the permitting and export process as described in the MoU

SRK

Serekty, Central part of Kazakhstan, Karagandy region, Karkaraly distyrict, near v. Nurken Karagandy, Kazakhstan

The site Serekty is one of typical monuments of the early iron age Tasmola culture (800 - 600 BCE). The Tasmolians practiced one-time, single burials under the mounds with dromos. The most famous type of burial are the round-oval octagonal stones and fences. The bridle objects (''hoards'') found in them are apparently associated with the symbolic sacrifice of a horse. The number, inventory and burials type of Serekty and other necropolises (Taldy, Bakybulak, Nurken, Karashoky, Birlik, ''37 warriers'' etc.) are archeological evidence of Saka settlements in Central Kazakhstan.[116–118]

SRK002 - The site Seryekty I, mound 11 was first excavated in 2011 by Beisenov A.Z. There were bone remains of human and sacrificial horses. The elite Saka person was buried there. But the mound showed signs of plundering. This deciduous molar yielded a Genotype 3 Parvovirus B19 genome. The sample was directly ^{14}C dated to 127 years cal BP (cal AD 1683-1936).

Serekty I, Kazakhstan. In 2019, as a part of an international collaboration for the archaeogenetic study, Director of the Institute of Archaeology by A. Margulan (Almaty, Kazakhstan) Baitanayev B.A. and researcher of the Center of Physical Anthropology Kitov E.P. gave the bone fragments and teeth representing human remains from several archaeological sites to the Head of Population Genetic Laboratory of the Institute of Genetics and Cytology (Almaty, Kazakhstan) Khussainova E.M. and researcher Musralina L.Z. These samples included two teeth of woman from Serekty I necropolis from Central Kazakhstan (Act of acceptance and transfer of skeletal remains dated May 15, 2019). Musralina L.Z transferred the samples to the Max Planck Institute to conduct the agreed upon research.

TSA

Tsagaan Chuluut, Dornod Aimag, Mongolia, 850–1650 CE

Tsagaan chuluut site is a large cemetery in eastern Mongolia consisting of more than 160 graves mostly belonging to the Late Bronze Age of Mongolia. The first excavations at the site were conducted as early as in the 1960s, mostly slab graves from the Late Bronze and Early Iron Age. During 2002-2012, an extensive archaeological excavation was conducted at the Tsagaan chuluut site comprising both the Bronze Age and medieval period of Mongolia. The grave No.164 was excavated in 2010. The burial was found badly damaged in antiquity; the skeletal remain of the deceased was found scattered in the burial pit. Numbers of iron and bronze items, including iron nails, buckle, hammer, hoe and bronze decorations, are associated with the deceased.

TSA002 - This individual's permanent molar yielded a genotype 1 Parvovirus B19 genome. Based on the site date midpoint, the sample age is set to 700 BP.

Sample TSA002 was transferred to the Max Planck Institute in 2020 for aDNA and other laboratory analysis. The customs permit number associated with this sample is 12-2091008-20E00225R and the export was permitted by the Ministry of Sciences and Education of Mongolia.

ULI

Uliastain deed denj 1, kurgan No. 2, Khovd, Mongolia, 10th -8th century BCE (kurgan No 1), 650 - 765 CE (kurgan No 2), Radiocarbon dated to 650 - 765 cal CE

Uliastain deed denj 1 is a group of two different-era burial mounds (kurgans) situated in left bank of Uliastain gol river in northern slope of Baitag Mountains between Tianshan and Mongolian Altai on the Mongolian-Chinese border. Kurgan No. 1 belongs to Early Scythian tradition with burial on ancient surface in wooden construction. Kurgan No. 2 belongs to Turkic tradition: male burial in an earthen pit with a horse. The burial had been totally robbed.

ULI002 - This sample from kurgan No. 2 is ^{14}C dated to 650 - 765 cal CE (MAMS-41128), the date has been set to the midpoint of this interval at 1243 BP (Date may be inaccurate (estimated too old) due to reservoir effect indicated by d13C value -13). This individual had a tooth 27 sampled, which yielded a Parvovirus B19 Genotype 2 genome.

ULI002 AT 675 Uliastai deed denzh, kurgan No.2. Excavations at Uliastai deed denzh in the Khovd aimag of Mongolia were undertaken in 2005 by archaeologists of the Institute of History of Mongolian Academy of Sciences and of the St.Petersburg State University (Russian Federation) (Agreement of cooperation No.193 of 14. March 2002) based on permission of Ministery of Sciences and Education of Mongolia.

USHA

Usharal-Ilibalyk, Panfilov, Kazakhstan, 14th -15th Century AD, Multiple individuals radiocarbon dated to the 15th century CE

The medieval settlement of Usharal, identified with the city of Ilibalyk, is located in the Zhetysu Region of southeastern Kazakhstan, in the Panfilov District, between the tributaries of the Ili River — the Usek and Borokhudzir. Covering an area of approximately 500 hectares, the site represents one of the largest medieval urban centers of the Ili Valley. First associated with Ilibalyk by K. M. Bajpakov in 1986, the settlement remained little studied until the 2010s, when a gravestone (kayrak) inscribed with Syriac crosses was discovered in situ, confirming the presence of a Christian community. Subsequent surveys yielded numismatic evidence, including Karakhanid and Northern Song coins, attesting to active exchange networks in the 11th-12th centuries.Systematic archaeological work has been undertaken at Usharal-Ilibalyk since 2016 under international collaboration and with the support of The Society for the Exploration of Eurasia (Switzerland). Topographical and geophysical surveys, surface collection, and targeted excavation have revealed the urban morphology of the settlement, including its citadel, shahristan, and rabad zones, as well as associated burial grounds. Stratigraphic, artefactual, and numismatic evidence indicates that the settlement flourished between the 12th and 14th centuries, when Ilibalyk functioned within the political and economic orbit of Almalyk, capital of the Chagatai Ulus. Archaeological investigations of the cemetery west of the settlement, conducted between 2018 and 2025, have documented more than 120 burials on an excavated area of 1,000 m^2. The graves are arranged in parallel rows and exhibit several construction types, including simple inhumations, ledge graves with mudbrick coverings, brick-lined chambers, and niche burials. Radiocarbon (AMS) and numismatic analysis date the burial contexts more precisely to the late 13th-early 14th centuries. The majority of burials follow the rite of the Church of the East, while recent excavations have also identified Islamic interments, indicating a multi-confessional community. Among the excavated graves, a number of female interments were furnished with high-status assemblages, including elements of the *boqtag* headdress, providing rare evidence for Mongol-period elite costume traditions in Central Asia. This diversity of funerary practices reflects the coexistence of Church of the East and Muslim groups within the multiethnic urban society of Ilibalyk. The combined archaeological, numismatic, and bioarchaeological data position Ilibalyk as a major urban and cultural center of the Chagatai Ulus, reflecting both the integration of Mongol imperial traditions and the endurance of local religious communities. The cemetery offers a unique context for exploring questions of social stratification, gendered representation, religious affiliation, and intercultural interaction in Central Asia during the 13th-14th centuries.

USHA006- The individuals indeterminate Molar yielded a low coverage parvovirus B19 GT-2 genome.

USHA007- The individual's permanent molar contained traces of parvovirus DNA likely being infected with GT-2.

USHA008 - The permanent molar of this individual yielded a low coverage GT-2 parvovirus B19 genome.

The human remains analyzed in this study originate from the medieval (13th–14th centuries) necropolis of the Ilibalyk settlement (Kazakhstan), excavated during archaeological fieldwork conducted between 2018 and 2022. All archaeological investigations were carried out in accordance with the legislation of the Republic of Kazakhstan. Archaeological Expertise LLP was responsible for the excavation, documentation, and lawful handling of the materials. The sampled material consists of 15 human teeth obtained from excavated individuals. These samples were selected and prepared for scientific analysis within the framework of ongoing research activities. All necessary permissions for the study of the human remains, including destructive sampling and genetic (ancient DNA) analysis, were obtained prior to sampling and transfer. The transfer, sampling, and analysis of the materials were conducted within the framework of a formal Memorandum of Understanding between Archaeological Expertise LLP (Kazakhstan) and the Archaeo- and Paleogenetics group at the Institute for Archaeological Sciences, University of Tübingen (Germany). All samples were transferred for analysis in accordance with this agreement and applicable regulations. An expert assessment conducted by the Central State Museum of the Republic of Kazakhstan confirmed the authenticity of the samples and their suitability for genetic analysis. All procedures were carried out in compliance with national legislation and in accordance with accepted ethical and scientific standards.

UST

Ust'-Jerusalem necropolis, Republic of Tatarstan, Volga region, Russian Federation, 1248–1389 CE, Radiocarbon date based on Individual UST103 - 1248 - 1389 cal CE.

Excavated from 1996 to 2003, the 800 m^2 area of the Ust'-Jerusalem necropolis contained 318 burials. The Ust'Jerusalem tomb within Bolgar city, a plague victim (2370), was preserved with the whole skeleton. The individual was identified as a 35–40-year-old man, with his burial not following medieval Muslim funerary customs. The site was dated to the second half of the 14th century based on several coins found during the burial's excavation. Twelve silver pieces specifically linked to this individual. The oldest coin dates

to 1362 CE. These coins have been produced and circulated between 1362 and 1370 CE under the leadership of Murad Khan and Abdullah Khan ibn Uzbeg Khan of the Golden Horde.[109]

UST154 – The permanent molar of this individual yielded a parvovirus B19 genome belonging to genotype 2. This sample was dated based on another individual's ^{14}C date from the same site.

The human DNA sequencing libraries from the sites BRT (Bolgar city mausoleum) and UST (Ust'-Jerusalem necropolis) were already analyzed for Human and Pathogen (Yersinia spec) aDNA and published.[109] The samples where reanalyzed for this study. Explicit permission for this study was still obtained from the sample custodian, who co-authored the paper – Maria A. Spyrou and Rezeda Tukhbatova.

Oceanian archeological sites

YNK

Yanuca, Viti Levu (Nadroga Navosa Province, Fiji, 1690 - 1950 cal CE, AMS mean date: 1853 CE calibrated mean

Yanuca Island (~41 ha) is located directly off the southwest coast of Viti Levu, Fiji, ~ 8 km northwest of the Sigatoka Sand Dunes National Park. Lawrence and Helen Birks first identified archaeological deposits on Yanuca from survey and test pits in 1965 and then in the edge of a road cut bulldozed for a resort development on the island in 1966, identified as site VL 16/81. The Birks excavated over 60 cubic meters of material across 8 trenches and baulks at the Yanuca Island rockshelter Site (VL 16/81) and identified a three-part sequence of ceramic 'zones' that included dentate-stamped Lapita ceramics (Zone 3) and paddle impressed ceramics (Zones 2 and 3) in the lowest cultural layers of the site (Birks & Birks, 1978; Clark & Anderson, 2000; Hunt, 1980). The Birks discovered human burials in Trench 3 located in the junction between Ceramic Zones 2 and 3 (that later may date to the Lapita period ca. 30502800 BP), and no grave cut from more recent layers was noted. The burials appear to be at least four crouched burials (facing south) placed in a line-oriented east/west, with the base of the grave over 120 cm deep (Birks & Birks, 1978; Hunt, 1980). Hunt (1980: 51) noted that a report of these human skeletal remains by Doug Sutton (then of the University of Chicago) was forthcoming, but this report appears to not have been finished.

In 1978, Terry Hunt mapped the VL 16/81 site and excavated two test pits in the eastern sector of the rock shelter, in addition to re-analyzing the cultural material from the earlier excavation by the Birks for his Master's thesis (Hunt, 1980, 1981). Hunt did not find Lapita deposits, likely because they were confined to the west area of the rock shelter where the floor to ceiling height was greatest and some deposits were possibly removed as a result of storm action or former high sea levels (Clark & Anderson, 2000; Hunt, 1980). Hunt (1980) did identify continuous cultural deposits likely from the equivalent of Birk's Zone 2 through the Historic Period. He did not record recovering any human remains from his excavation. The box that this individual was curated in at the storage facilities of the Fiji National Museum was labelled Yanuca (VL/81), the site code for the Yanuca Island Rockshelter Site.

The partial remains of an infant and adult were also located in the same box. The AMS date for the subadult indicates that this individual most likely lived during the Historic period and the bone collagen carbon and nitrogen stable isotope values from the sampled phalanx indicates a wholly terrestrial diet. Forthcoming genetic analyses confirm that this individual was a Pacific Islander and the highly terrestrial diet likely reflects the importance of horticultural foods during the Historic period in Fiji. Historic-era human remains were not recorded from the Birks or Hunt excavations and these three individuals may have been recovered from the site at a later date, or were just not detailed in the original publication (Birks & Birks, 1978) or thesis (Hunt, 1980).

YNK001 - The individual analysed for aDNA was a male child aged approximately 3 years. This individual was directly ^{14}C dated, and the calibrated mean was used for phylogenetic dating, set at 97 years cal BP. The pars petrosa yielded a Parvovirus B19 Genotype 2 genome.

The Fiji Museum issued export permit C16/1 in October 2016, authorizing the removal of samples from the Yanuca, Fiji, individual for aDNA and isotope analyses.

American archeological sites

MP2

Machu Picchu 2, Cuzco Region, Peru, contact period- all set to 1492 CE

Machu Picchu was part of a royal estate belonging to the lineage (or panaca) of the emperor Pachacuti, the ruler credited with establishing the Inca Empire (or Tahuantinsuyu). The monumental architecture at the core of Machu Picchu consists of the remains of a country palace situated within Pachacuti's royal estate. During the 1912 archaeological investigations conducted by the Yale Peruvian Scientific Expedition, George Eaton and Ellwood Erdis identified and excavated 107 burial caves on the ridges of Machu Picchu, concentrating in four clusters referred to as Cemeteries 1, 2, 3, and 4. Most of the burials were located along the edges of the palace complex. Cemetery 1 is positioned among the boulders to the northeast of the architectural core. Cemetery 2 is found on the slopes to the east, and Cemetery 3 was located along the northern slopes of Machu Picchu Mountain to the south. Additional burials have been discovered on the western terraces, referred to here as Cemetery 4. The burial caves and niches primarily contained commingled human skeletal remains of several individuals in various states of preservation, with few grave goods. Morphological assessments enabled the assignment of the human remains to 177 distinct individuals. These individuals have been studied for genomic ancestry, intentional cranial deformation, strontium 87Sr/86Sr, and other stable isotopes. For more details, refer to.[59] The skeletons examined here were part of the Bingham collection at the Peabody Museum of Natural History, and all have been returned by Yale University to the Museo Machu Picchu in Cusco, Peru, under the administration of UNSAAC .[59]

MP2004 - The tooth of this individual yielded a Parvovirus B19 genotype 2 genome.
MP2019 - The tooth of this individual yielded a Parvovirus B19 genotype 2 genome.
MP2005 - The tooth of this individual yielded a Parvovirus B19 genotype 2 genome.
MP2008 - The tooth of this individual yielded a Parvovirus B19 genotype 2 genome.

The human remains from Machu Picchu discussed in this paper are considered part of Peru's cultural heritage. The original project, led by Lars Fehren-Schmitz, Richard Burger, and Lucy Salazar, has been part of the repatriation effort envisioned by the MOU between Yale and the Universidad Nacional de San Antonio Abad del Cusco (UNSAAC) regarding the return of all Machu Picchu collections from the 1912 Yale Peruvian Scientific Expedition. This agreement included a commitment to continued research on Machu Picchu and Inca culture in general, as well as community education via displays at the Museo Machu Picchu, an institution administered by UNSAAC. The remains of all individuals from Machu Picchu are curated at this museum. Samples for analysis were exported in accordance with the Ley General del Patrimonio Cultural de la Nación (Law No. 28296) in collaboration and with the permission of the local and national Peruvian Ministry of Culture (Oficio RV026-2018-VMPCIC-MC).

SGA

San Gregorio Atlapulco, Mexico City, Mexico, Contact Period, Multiple individuals of the site Radiocarbon dated to 1410 - 1641 CE (overlay of youngest and oldest estimate)

The chronology of the archaeological site of El Japón, located in San Gregorio Atlapulco (Xochimilco, Mexico City, Mexico) corresponds to the Late Postclassic and the Contact with Europeans period.[119,120] In prehispanic times it was a seasonal activity area and became permanently settled shortly after the conquest.[121,122] The main characteristic and subsistence mode of Atlapulco was agriculture based on the chinampas system (raised beds built in shallow lakes, used for intensive agriculture).[120,122] In 1993, salvage excavations recovered almost 400 primary burials and two ossuaries from a series of ten habitational platforms surrounded by chinampa plots (Ávila, 1995). Archaeological and historic data (Nieto Chapa, 1957), along with the burial contexts, suggest that these skeletons can be dated to the years just about the time of the conquest (AD 1521) and may include individuals from some of the first post European contact generations.[121] A study of osteological markers of occupational stress on the skeletal remains of these individuals suggested that the skeletons of subadults (10-14 years-old) already showed signs of physical labour, suggesting that children began working in the chinampas at very young ages. Analyses of the health of the inhabitants of Xochimilco have revealed that pathological lesions associated with infection and malnutrition were prevalent, indicating that exploitation by the Mexica capital combined with the lacustrine environment took a heavy toll on this food-producing population.[121,123,124] These findings, together with the age-at-death distribution of the population (high percentage of juvenile and young adult skeletons) indicated a population with a high growth rate as well as high infant mortality, low life expectancy, and few individuals surviving past young adulthood .[121,125]

SGA024 - This individual was classified as a potential Tuberculosis case. Tooth and fragments from the lesion were sampled. The individual's permanent premolar yielded a Parvovirus B19 V genome belonging to Genotype 2. The individual's age is set to 1500 CE and therefore taken into consideration as 450 BP.

The samples were transferred to the Max Planck Institute with permission from the Council of Archaeology in Mexico for a scientific study on human remains including aDNA analysis. The permit numbers for the site SGA are 401.B(4)19.2015/36/1027 and 401.B(4)19.2016/36/2503.

SJN

Hospital Real de San José de los Naturales, Mexico City, Mexico, archaeologically dated to 1467 - 1616 CE, Multiple individuals ^{14}C dated

The site was excavated in 1992. Notably, genetic analysis of the cemetery population revealed almost exclusively indigenous people and some African and African descendants.

SJN003 - This individual is genetically African or of African descent. It is ^{14}C dated to 1436 - 1472 cal CE and archaeologically dated to 1441 - 1455 CE. The age of the sample is set to 1454 CE, which equals 496 BP. This individual's permanent molar yielded a Parvovirus B19 genome belonging to genotype 3.

SJN011 - This individual is ^{14}C dated to 1453 - 1625 CE, this is set to a midpoint at 411 BP. The individual's tooth 47 yielded a Parvovirus B19 genome belonging to genotype 2.

SJN013 - The individual is directly ^{14}C dated to 1414 - 1441 cal CE. The age of the sample is set to the midpoint of this interval. The age is 1427.5 CE or 522.5 years BP. The tooth 47 of this individual yielded a genotype 2 Parvovirus B19 sample.

SJN025 - This individual is ^{14}C dated to 1429 - 1454 cal CE. The age was set to the midpoint of this estimate at 1441.5 CE, which equals 508.5 BP. The individual's tooth yielded a Parvovirus B19 genome belonging to Genotype 2.

The samples were transferred to the Max Planck Institute with permission from the Council of Archaeology in Mexico for a scientific study on human remains including aDNA analysis. The permit number for the site SJN is 401.B(4)19.2015/36/1027.

METHOD DETAILS

Sampling of skeletal material and DNA extraction

The extraction of DNA was performed on tooth and bone samples (primarily pars petrosa), originally intended for human genetic analysis. About 50 mg of bone powder or pulverized dental pulp was created using a dental drill. Parvovirus DNA is expected to either show up in the bones, bone marrow or in the dental pulp, as these sides are involved in the B19V life cycle and DNA retention. The

sampling procedures were carried out in dedicated ancient DNA laboratories of the University of Tübingen and the laboratory facilities of the Max Planck Institute for Evolutionary Anthropology. The DNA extraction was performed after Dabney et al.,[126] with a rotation of 12-16 h at 37°C during an initial lysis step. One negative control was included for every 10 samples, and one positive extraction control for every extraction slot.

DNA Library generation and sequencing

From the DNA extracts, libraries were generated using single-stranded and double stranded library generation protocols, partially relying on UDG treatment. Of the 51 samples, 36 samples had double-stranded libraries constructed, and 15 samples had single-stranded libraries. The double-stranded libraries were constructed using UDG half treated libraries[127] (n = 28) and non-UDG-treated protocols[128] (n = 7). The single stranded libraries were created with modified versions of the previously published single stranded library protocol.[129,130] The details for each individual's sample and their laboratory processing history are available in Table S2.

QUANTIFICATION AND STATISTICAL ANALYSIS

Screening for Human Parvovirus B19

Initial screening was performed to evaluate the presence of B19V-originating DNA in human samples. In total, 31,364 sequencing datasets were screened using MALT [39]and HOPS[40](around 50% shotgun and 50% 1240k capture) from 21,398 libraries and 16,546 individuals. *MALT* was run using a custom reference database containing representatives of all human-infecting DNA viruses, with the following parameters: –topPercent 15 –gapOpen 1000 –maxAlignmentsPerQuery 1000 –maxAlignmentsPerRef 10. All other parameters were set to default. Resulting *RMA6* files were then processed with *Maltextract* using the –destackingOff option to summarize taxonomic assignments. Among ∼2000 libraries exhibiting matches to B19V, 106 libraries were selected for in-solution capture based on their age and region of origin as well as on the number of detected B19V reads in shotgun data to maximise both the spatiotemporal range of the sampling and the likelihood of reconstructing significant portion of the viral sequence.

Human Parvovirus B19 Capture Design

Probe sequences were designed based on three reference datasets with a 1-bp tiling, a length of 52 bp and an additional 8-bp linker sequence (CACTGCGG), as previously described.[131] Low-complexity and duplicated probes were removed. The first reference dataset consisted of 180 human parvovirus B19 sequences resulting in 57955 unique probes replicated 15 times. The second reference dataset consisted of 6 animal erythrovirus sequences resulting in 29046 unique probes replicated 3 times. The third reference dataset consisted of 2 human parvovirus B19 ITR sequences resulting in 6 unique probes replicated 1500 times. The complete set of probes was ordered on an Agilent SureSelect DNA Capture Array and turned into an in-solution DNA capture library.[131–133]

Capture data processing with the nfcore/eager pipeline

The sequencing data was processed using nf-core/eager version 2.4.7 with the parameters specified in the config file provided here. More specifically, adapter sequences were removed from the raw reads using AdapterRemoval (v2.3.2) with the option to preserve 5p and minquality 30. Processed reads were then aligned to the reference genomes for GTS 1 (M13178.1,), 2(AY044266.2), and 3(AJ249437.1), respectively. Using bwaaln (v0.7.17-r1188) with parameters -n 0.01 and -l 9999. A mapping quality filtering step was applied using samtools (v1.12) -q 37. To remove PCR duplicates, Picard Mark Duplicates was used. The unique quality filtered reads were used to run genotyping using GATK Unified Genotypes (v3.5), using the output mode 'EMIT_ALL_SITES'. Coverage statistics for each sample were generated using Qualimap (v1.14). For the P6 promoter region we added one additional mapping step, using only the promoter sequence as a reference we mapped again using the same parameters except applying the bwaaln parameter -n 0.00001 and set the mapping quality threshold to zero. In a second step we aligned the recovered P6 sequences and the recovered whole sequences, the resulting consensus sequence between the high coverage high quality parameter mapped whole sequence and the less stringendlty mapped p6 sequence were used for analysis including the P6 region.

Genotyping, sequence recovery and alignment curation

The initial Full coding sequence alignment was produced by combining modern and published ancient sequences with full coding sequences generated from mapping to the genotype with the highest sequence identity. We classified all ancient genomes based on their similarity to modern B19V references belonging to genotypes 1, 2 and 3 (GenBank accession numbers: M13178.1, AY044266.2 and AJ249437.1, respectively). The percentage pairwise identity match between the dataset at hand and each reference sequence was used to identify the genotype of the sample. The MultiVCFAnalyzer (version 0.85.2; https://github.com/alexherbig/MultiVCFAnalyzer) was employed to generate consensus sequences from the VCF files produced by *nf-core/eager*, in the form of full coding sequence alignments Positions were called when at least 2-fold covered with a minimum genotyping quality of 30. All Alignment components: modern, ancient published, new ancient GT-1, GT-2 and GT-3 were composed into one fasta file and aligned via Mafft (version 7.467). Mafft was set to auto detection of the datatype, the gap extend penalty was set to 0.123, the gap opening penalty was set to 1.53. The direction of the nucleotide sequences was set to not be adjusted and as the output format fasta was chosen.

This new created alignment fasta was used as the input for the full coding sequence phylogenetic analysis, and for the recombination analysis. The full coding sequence alignment was used to identify recombinant regions and separated into split alignments

containing the hybrid strains (GT-2) separated by their parental sequence parts alongside the full coding sequence of the non-hybrid genotypes GT-1 and GT-3. These alignments were created using RDP5 for recombinant region detection and alignment export. RDP5 Beta 5.83 was run using the default settings and exported recombination separated alignments. All alignments used in phylogenetic dating analysis had the low coverage samples removed. The resulting alignment had a sequence length of 4601 nucleotides and contained the full NS and VP genes as well es the subunits of both ORFs in full.

Recombination analysis

Recombination analysis was performed using seven algorithms built into RDP5.[41] The embedded algorithms are RDP,[134] GENECONV,[135] BootScan,[136] MaxChi,[137] chimaera,[138] SiScan,[139] and 3Seq.[140] The analysis used all available ancient sequences and all listed modern sequences. The analysis was run two additional times, once only with high coverage ancient sequences and once with "artificial ancestors" included, meaning consensus sequences of the two clades of the GT-1 parental clade were included to see whether these consensus sequences fill the sequential requirements of the recombination parents better than any of the authentic detected sequences. Since the sample ABF006 was not able to be securely identified as a GT-2 or a GT-3 sample by the % sequence identity-based method, the recombination analysis was used to identify the genotype of ABF006. The sample was found to be GT-3 by recombination analysis. ABF006 contained no evidence of the recombination event and was phylogenetically identified to be more similar to modern GT-3 than to GT-2. The recombination analysis was then re-run on an Alignment containing ABF006 mapped to GT-3. The samples with masked recombinant regions were directly exported from RDP5using the "save distributed alignment" option. The resulting alignments contained the GT-1 and GT-3 sequences in full and the GT-2 sequences split and filled with Ns. The Alignment GT-3 originating GT-2 contains all nucleotides of the GT-2 sequences expect the positions1881-3351, which were replaced by N. The GT-1 originating Alignments contained only N masked positions expect the positions 1881–3351.

Phylogenetic Analysis

Phylogenetic reconstruction was performed on each of the three alignments (the full alignment and the two recombination-free alignments). Both the dataset with all sequences and the subset containing only the samples qualifying for phylogenetic dating where analyzed. Substitution trees were generated *via* maximum likelihood (ML) using RAxML version 8.2.12. The low coverage GT-2 virus sequences USHA006 and USHA008 were manually masked for the GT-3 originating GT-2 and the GT-1 originating GT-2 alignments.

Phylogenetic dating Analysis

A Bayesian phylogenetic analysis was performed to reconstruct a timetree and estimate the age of the Parvovirus B19V diversity (i.e. the time to the most common ancestor; tMRCA) as well as that of the modernly defined genotypes. Genomes we retained for phylogenetic dating analysis only if $\geq$ 50% of their coding sequence was covered at $\geq$ 3X depth. The alignment was produced by mafft aligning all sequences. Tipdates were obtained by setting the date, in BP to the value of the calibrated mean or the midpoint of the archeological date estimate. To assess whether our dataset contained sufficient temporal signal for phylogenetic dating, root-to-tip regression was performed on 3 different trees. 1) Maximum likelihood tree of the GT-1 originating GT-2 sequences and the full GT-1 and GT-3 sequences, 2) Maximum likelihood tree of the GT-3 originating GT-2 sequences and the full GT-1 and GT-3 sequences, 3) Maximum likelihood tree of the full coding sequence alignment. The regression was performed in TempEST (version 1.5.3)[141] with the best-fitting root parameter enabled. Furthermore, we performed a date randomization analysis using BEAST2 version 2.7.7[142] For all model setups described hereafter, tip dates were randomized 10 times using a custom python script and runs were otherwise kept identical to the random relaxed lognormal run set ups presented in the main text of the paper. The 95%HPD intervals of the tree height's posterior distributions were then compared between runs with randomized or authentic dates. The dates of all samples were permuted using a custom written python script relying on the library's pandas, numpy and random. The ages of each leaf were randomly reassigned to other leaves 10 times resulting in 10 datasets with an identical number of dates attributed to different samples. The randomized dates have been used as tip dates for the date permutation testing of the temporal signal within the original data. In all cases, their results were indicative of significant temporal signal as none of the estimates obtained from randomized dates overlapped with that obtained with the authentic dates.

Nested sampling[143–147] was then run to select the best-fitting model clock model on both hybridisation removed alignments. Three clock models were tested: a strict clock, an uncorrelated lognormal (UCLN) relaxed clock with and without enforced monophyly of the genotypes 1 and 3 with their respective masked genotype 2 descendants.[148] The nested sampling was run with a chain length of 20000, a particle counts of 35 and a sub chain length of 18000, all on a single threat. The marginal likelihood favored the relaxed clock which was therefore shown in the main text.

For both models, tip dates were set to years before present (BP), based on reported sampling date for modern genomes and mean calibrated radiocarbon date or midrange of contextual dating for ancient genomes. Site model averaging was performed using the *bModelTest* package.[149] A Coalescent Bayesian Skyline tree prior was used with all hyperpriors left to default .[150] For the strict clock, we used an initial value of 1.0E-5 subst./site/year and a uniform prior between 1e–9 subst./site/year and 1e-3 subst./site/year for the clock rate (based on previous estimates by Mühlemann et al.,[8] Guzman solis et al.[35]). For the relaxed clock, we used the default gamma prior for the mean clock rate, using an initial value of 1.0E-5 subst./site/year and lower and upper bounds of 1e-9 subst./site/year and 1e-3 subst./site/year, respectively. In addition, as the relaxed clock model would result in unexpected tree topologies, a third model was compared in which the relaxed clock was used while constraining the monophyly of modernly defined genotypes

(including the inclusion of GT-2 within GT-1 or GT-3 for the corresponding recombination-free alignments), consistently with prior knowledge and the results of other phylogenetic analyses, including the ML tree estimation and strict-clock phylogenetic dating performed here.

For all model setups, the MCMC was run with 240,000,000 iterations, and a sampling frequency of 2,000. Runs converged fully, all ESS parameters reaching >200. The resulting tree files were down-sampled using LogCombiner version 2.7.7 with a down-sampling frequency of 5000. The final Maximum Clade Credibility trees were created using the down-sampled files and TreeAnnotator version 1.6.2 a burnin of 10. The XML files of the runs and commands used to process the runs are available.